Unclassified

SECURITY CLASSIFICATION OF THIS PAGE

REPORT DOCUMENTATION PAGE

Form Approved OMB No. 0704-0188

1a. REPORT SECURITY CLASSIFICATION Unclassified	1b RESTRICTIVE MARKINGS
2a. SECURITY CLASSIFICATION AUTHORITY	3 DISTRIBUTION/AVAILABILITY OF REPORT Approved for public release; distribution unlimited.
2b. DECLASSIFICATION/DOWNGRADING SCHEDULE	
4. PERFORMING ORGANIZATION REPORT NUMBER(S)	5. MONITORING ORGANIZATION REPORT NUMBER(S) Technical Report REMR-GT-6
6a. NAME OF PERFORMING ORGANIZATION Department of Civil Engineering 6b. OFFICE SYMBOL (If applicable)	7a. NAME OF MONITORING ORGANIZATION USAEWES Geotechnical Laboratory
6c. ADDRESS (City, State, and ZIP Code) Virginia Military Institute Lexington, VA 24450	7b. ADDRESS (City, State, and ZIP Code) PO Box 631 Vicksburg, MS 39181-0631
8a. NAME OF FUNDING/SPONSORING ORGANIZATION US Army Corps of Engineers 8b. OFFICE SYMBOL (If applicable)	9. PROCUREMENT INSTRUMENT IDENTIFICATION NUMBER Contract No. DACW39-86-K-0006
8c. ADDRESS (City, State, and ZIP Code) Washington, DC 20314-1000	10. SOURCE OF FUNDING NUMBERS PROGRAM ELEMENT NO. / PROJECT NO. / TASK NO. / WORK UNIT ACCESSION NO. WU I-32315

11. TITLE (Include Security Classification)
GEOTECHNICAL APPLICATIONS OF THE SELF POTENTIAL (SP) METHOD; Report 2, The Use of Self Potential to Detect Ground-Water Flow in Karst

12. PERSONAL AUTHOR(S)
Erchul, Ronald A. and Slifer, Dennis W.

13a. TYPE OF REPORT	13b. TIME COVERED	14. DATE OF REPORT (Year, Month, Day)	15. PAGE COUNT
Report 2 of a series	FROM Jun 86 TO Jul 87	May 1989	122

16. SUPPLEMENTARY NOTATION
See reverse

17. COSATI CODES			18. SUBJECT TERMS (Continue on reverse if necessary and identify by block number)
FIELD	GROUP	SUB-GROUP	See reverse

19. ABSTRACT (Continue on reverse if necessary and identify by block number)

Self potential (SP) is a geophysical method that measures naturally occurring voltage in the earth. Negative anomalies arise from electrokinetic, or streaming potential, effects resulting from the flow of groundwater. ~~In this study~~ SP was monitored at sites in karst terrain in Virginia. ~~The~~ results were evaluated for effectiveness in detecting and mapping ground-water flow paths and flow rates. The ability of SP to distinguish between shallow flow in soil and regolith and deeper flow through bedrock conduits was examined. It was demonstrated that soil temperature, ~~soil~~ moisture, and precipitation are major variables influencing SP data. An automated data collection system was ~~devised~~ and used for: ~~two tasks:~~ ~~1)~~ ~~(a)~~ long-term monitoring of SP changes and environmental variables, and ~~(b)~~ measuring SP changes induced by the rapid artificial recharge of water into a sinkhole. ~~The~~ SP results were ~~evaluated by~~ compared with geological observations, electrical resistivity and electromagnetic terrain conductivity surveys, streamflow measurements, and speleological

(Continued)

20. DISTRIBUTION/AVAILABILITY OF ABSTRACT	21 ABSTRACT SECURITY CLASSIFICATION
☒ UNCLASSIFIED/UNLIMITED ☐ SAME AS RPT ☐ DTIC USERS	Unclassified
22a. NAME OF RESPONSIBLE INDIVIDUAL	22b TELEPHONE (Include Area Code) / 22c OFFICE SYMBOL

DD Form 1473, JUN 86 *Previous editions are obsolete.* SECURITY CLASSIFICATION OF THIS PAGE

Unclassified

16. SUPPLEMENTARY NOTATION (Continued).

A report of the Geotechnical problem area of the Repair, Evaluation, Maintenance and Rehabilitation (REMR) Research Program. This report is available from the National Technical Information Service, 5285 Port Royal Road, Springfield, VA 22161.

18. SUBJECT TERMS (Continued).

Electrodes	Self potential	Surface drainage
Flow path	Sinkhole	
Geophysical technique	Subsurface drainage	

19. ABSTRACT (Continued).

surveys. Results indicate that SP can effectively locate and track shallow (less than 20 m) ground-water flow paths in karst terrain. A relationship was observed between SP and changes in flow rate where the flow was through porous material, but SP could not be directly related to flow through solutional channels and conduits. However, the presence of conduits may be indicated by SP anomalies where surface soil moisture is drawn into fractures that supply water to conduits at greater depths. The influence of geologic structures on ground-water flow must be considered in interpreting SP results in karst. Further refinement of the SP technique is promising for applications to environmental and geotechnical problems.

PREFACE

The work described herein was performed by Dr. Ronald A. Erchul during the period from June 1986 to July 1987 under a contract with the Virginia Military Institute (VMI), Lexington, VA. The work was authorized by the US Army Engineer Waterways Experiment Station (WES), Vicksburg, MS, under Contract No. DACW39-86-K-0006. The work was funded by the Repair, Evaluation, Maintenance, and Rehabilitation (REMR) Research Project "Geophysical Techniques for Assessment of Existing Structural Foundations," Work Unit No. WU I-32315. This is the second of two reports in a series of three.

The field work was performed during the period from July 1986 to May 1987 by Messrs. Dennis W. Slifer, Robert Thren, Steven Richards, and Cadets D. R. Gibbings and R. W. Marsh, VMI. The data analysis phase of the investigation was performed by Mr. Dennis W. Slifer and Cadets D. R. Gibbings and R. W. Marsh. This report was written by Dr. Robert A. Erchul and Mr. Dennis W. Slifer. Principal Investigators for the REMR research project are Dr. Dwain K. Butler and Mr. Jose L. Llopis, Earthquake Engineering and Geophysics Division, Geotechnical Laboratory, WES. Mr. Benjamin I. Kelley, Headquarters, US Army Corps of Engineers, was Technical Monitor for this work. The report was edited by Ms. Joyce H. Walker, Information Products Division, Information Technology Laboratory, WES.

Acting Commander and Director of WES during preparation of this report was LTC Jack R. Stephens, EN. Dr. Robert W. Whalin is Technical Director.

CONTENTS

CONVERSION FACTORS, NON-SI TO SI (METRIC)
UNITS OF MEASUREMENT

Non-SI units of measurement used in this report can be converted to SI (metric) units as follows:

Multiply	By	To Obtain
degrees (angle)	0.01745329	radians
Fahrenheit degrees	5/9	Celsius degrees or Kelvins*
feet	0.3048	metres
gallons	3.785412	cubic decimetres
inches	25.4	millimetres
miles (US Statute)	1.609347	kilometres
millimbus per foot	3.28	millimbus per metre
ohm-foot	0.3048	ohm-metres
pounds (force) seconds per square foot	14.88164	poise
pounds (force) per square foot	47.88026	pascals

* To obtain Celsius (C) temperature readings from Fahrenheit (F) readings, use the following formula: C = (5/9) (F - 32). To obtain Kelvin (K) readings, use: K = (5/9) (F - 32) + 273.15.

The Use of Self Potential to Detect Groundwater Flow in Karst

PART I: INTRODUCTION

Background

1. Report 1 in this series (Erchul 1987) presented a preliminary proof-of-concept field evaluation of a technique for mapping subsurface water flow into/from sinkholes and between sinkholes. The evaluation used a novel scheme consisting of (a) circumferential self potential (SP) electrode arrays to detect flow into or from sinkholes and then of (b) rectangular SP electrode arrays to track or map flow paths "cross country" between sinkholes. Results of the proof-of-concept field evaluation were positive and indicated that the concept might lead to a simple, inexpensive procedure for mapping subsurface water flow paths in karst areas. This current report (Report 2) extends the preliminary work to investigate:

a. Environmental effects (temperature, rain, vegetation, etc.) on SP measurements with metal electrodes.

b. Relationships between flow quantity and SP magnitudes.

c. Limitations of method.

Review

2. Karst regions, areas of soluble carbonate bedrock, have unique hydrological characteristics. Environmental and engineering problems result from the solutional removal of bedrock--a process that produces sinkholes, preferential subsurface drainage, and random soil depths. Water supply and quality, drainage, flooding, and land use problems are different from those in nonkarst areas. Karst terrain comprises approximately twenty percent of the land area of the United States and is extensive worldwide (Quinlan and Ewers 1986). Although this research was conducted in the karst of the Valley and Ridge Province of the Appalachian region, the results should be applicable to most other karst regions and perhaps nonkarst areas as well.

3. There is always a need for more information about subsurface conditions and processes in the earth. The SP technique promises to be an effective method for producing such information. Although it is one of the least understood geophysical methods, recent research and applications indicate that because of a close relationship between SP and hydrogeologic parameters, SP may become a valuable and standard technique in hydrogeology (Ernston and Scherer 1986).

4. SP is an electrical geophysical technique that measures naturally occurring voltage fields in the earth's surface. SP is one of the oldest geophysical methods, first used by Robert Fox in the copper mines of Cornwall, England in 1830. As a prospecting tool for sulphide ores and graphite deposits, SP has been widely used by geologists around the world. Likewise, SP logs are commonly made from boreholes and wells to record changes in permeability, pore fluid, and lithology.

5. In recent years, the SP technique has received increased study for a variety of novel geotechnical applications. Geothermal exploration using SP has been successfully demonstrated in many locations (Anderson and Johnson 1976; Corwin and Hoover 1978). SP has also been used to detect and track underground coal mine fires (Rodriguez 1984; Corwin and Hoover 1978). Electromagnetic anomalies induced by water diffusion prior to earthquakes have been studied by Fitterman (1978) and Ishido (1981). SP monitoring techniques in this application may eventually produce a useful predictive tool. Soviet scientists (Ogilvy, Ayed, and Bogoslovsky 1969; Bogoslovsky and Ogilvy 1972) were among the first to experiment with SP methods in applied hydrological and geotechnical uses. They found that SP was able to detect leakages at dams, reservoirs, and drainage structures, and it is this application that has potential for REMR applications. Another useful application is evaluating ground-water patterns relating to landslide processes.

6. In the United States, the application of SP to geotechnical problems has been studied by the US Army Corps of Engineers at some of its dam sites. Cooper, Koester and Franklin (1982) conducted an SP survey at Gathright Dam in Virginia. Other studies include Clearwater Dam in Missouri (Koester, Butler, Cooper, and Llopis 1984), Mill Creek Dam in Washington (Butler, Wahl, and Sharp 1984), Medford Cave and Manatee Springs in Florida (Cooper 1983), and Beaver Dam in Arkansas (Llopis and Butler 1988). Other agencies (US Bureau of Reclamation) and consulting firms are beginning to use SP

methods for seepage analysis and to define hazardous areas in landslide masses (Markiewiez and Randall 1984).

7. Many of the studies conducted by the Corps of Engineers are of particular interest because of their locations in karst terrain. Impoundments in karst areas have always been plagued by leakage problems because of the presence of caves, sinkholes, erratic and heterogeneous ground-water patterns, and other solutional features which contribute to unpredictable subsurface conditions. It is not necessary to stop all leakage, but it is necessary to control it to the extent that there is no danger of piping or uplift-induced failure. To control leakage from an existing water resources structure or its foundation, one has first to find the seepage path or paths.

8. Karst terrain is especially vulnerable to ground-water contamination. Researchers have used other geophysical techniques (electrical resistivity, seismic refraction, gravimetry, terrain conductivity, ground probing radar, etc.) in studying subsurface features of karst, but SP is attractive as a cost-effective method for initial investigations of an area. This is due in part to the use of simple metal electrodes which was pioneered on Corps of Engineers projects; this adaptation makes the technique relatively fast and easy to execute. This simplification of the technique combined with the apparent environmental and engineering applications in sensitive karst areas are the basis for the present study. As a simple, fast, and inexpensive method, SP should be valuable for augmenting other geophysical and geotechnical subsurface explorative methods. It seems especially well suited for monitoring changes over relatively long periods of time. In addition to its utility for helping to solve site-specific geotechnical problems, SP research in karst areas may contribute to advances in theoretical concepts about ground-water movement, storage, and recharge processes.

9. The purpose of this research is to evaluate the SP technique (as developed by the Corps of Engineers) by applying it to a monitoring program at a variety of karst features within a study area in west central Virginia. The SP results are evaluated by comparison with site observations, geological studies, results from other geophysical methods, stream flow measurements, cave surveys, artificial water injections (recharge) into sinkholes, dye tracing, and monitoring of soil temperature, precipitation, ground-water conductivity, and other environmental parameters that may affect SP. In addition, a computerized data collection system is developed for field use. This system

greatly increases the capabilities and effectiveness of monitoring both short-term hydrologic recharge events as well as long-term and seasonal changes at the study sites.

Theory of Streaming Potential

10. As used in geophysics, SP refers to a phenomenon that originates from several different mechanisms. Electrochemical SP effects are caused by differences in solution concentrations and oxidation states of earth materials. This is the basis for the earth cell or galvanic (battery) cell explanation commonly used in connection with SP anomalies generated by metallic ore bodies. The electrokinetic (or electrofiltration) mechanism, on the other hand, generates potentials by the flow of water or heat through a porous medium. SP originating from this source is known as streaming potential and is of primary interest in ground-water investigations and the present study.

11. Electrical effects resulting from the application of man-made currents to the earth are not included in the definition of SP, hence the term "spontaneous." Telluric currents (electromagnetically induced earth currents) are also excluded from a consideration of SP effects. This is not to say that cultural or telluric signals can be ignored in SP work; in some situations they can produce noise which must be recognized and filtered out. Another possible source for signal noise in SP work may derive from "bioelectric currents" from vegetation (Nourbehecht 1963). Presumably, this effect can be recognized as obvious differences in background between wooded and open terrain when conducting traverses across such boundaries. Electrode polarization effects can also influence SP results. Electrodes and techniques of use have been debated in the literature. The relatively recent trend toward using metal electrodes (as opposed to porous ceramic nonpolarizing electrodes) is still somewhat controversial. More detail on this topic is given later in this study.

12. Interpretation of the results from the present study is based on the detection of negative anomalies in the potential field which are assumed to be primarily due to streaming potential effects. Therefore, an increasing SP value is one that is becoming more negative; whereas, decreasing SP value is one that is becoming less negative (or more positive). Ogilvy (1967) states that the most significant results are obtained in karst regions where

considerable quantities of water are lost in sinkholes. He recommended tracing shallow near-horizontal ground-water flows using radial configurations of electrodes and reported that streaming potentials are a maximum in the direction of flow.

13. Cooper, Koesoer, and Franklin (1982) reported that the electrochemical and telluric contribution to SP are relatively minor and that one may assume that values measured relative to a local reference in a similar geologic condition are due to the electrokinetic contribution or streaming potential. Likewise, Corwin and Hoover (1978) have demonstrated that, for models of similar geometry, SP anomalies generated by electrokinetic coupling are larger in amplitude than those generated by other mechanisms. Nourbehecht (1963) determined that streaming potential mechanisms are capable of producing anomalies of "several hundred millivolts." These figures are consistent with the anomalies commonly measured in the present study (as great as -500 mv). Streaming potentials may produce very large anomalies on the surface. According to Corry (1985), areas with large amplitude streaming potentials are characterized by high rainfall and steep topography. An extreme example is the -2,693-mv anomaly found on Agadak Volcano in Alaska (Corwin and Hoover 1978) and the -1,600-mv anomaly associated with Kilauea Volcano in Hawaii.

14. The streaming potentials produced by the motion of ground water under a pressure gradient through a porous media result from the preferential adsorption of ions. This process was first recognized in 1809 in its inverse form--electro-osmosis, where the application of an electric potential across a wet soil causes a net flow of water to the cathode (Mitchell 1976). In natural systems, streaming potentials occur because of the electric double layer of ions associated with the interface between the mineral grains and the pore fluid (ground water). Unsatisfied bonds at the surface of mineral grains adsorb ions from solution; positive ions are attracted to the surface, negative ions are repulsed. The direction of flow, or streaming, is therefore characterized by a net increase of negative ions in the solution (Figure 1). The phenomenon was explained and quantified by Helmholtz in 1879 and has been further refined by the work of others--especially soil physicists and colloidal chemists.

15. According to the Helmholtz equation,

$$V = \frac{\rho \varepsilon \xi}{4\pi\mu} \Delta P$$

where

V = the measured stream potential (stat volts)

ρ = fluid resistivity $\left(\text{stat ohm-ft or } \frac{\text{stat volt-sec-ft}}{\text{stat coulomb}}\right)$

ε = fluid dielectric constant $\left(\frac{\text{stat coulomb}}{\text{stat volt-ft}}\right)$

ξ = voltage across the Helmholtz double layer (stat volts)

μ = viscosity of pore fluid $\left(\frac{\text{lb-sec}}{\text{ft}^2}\right)$

ΔP = pressure drop along flow path $\left(\frac{\text{lbf}}{\text{ft}^2}\right)$

16. For a given set of materials properties, the only variables in the above equation are V and ΔP ; V is proportional to ΔP and $V/\Delta P$ is a constant (Cooper, Koester, and Franklin 1982). $V/\Delta P$ is known as the electrokinetic coupling coefficient, but it is difficult to calculate because little is known about the behavior of ρ , ξ , and μ in the pores of rocks and soil (Corwin and Hoover 1978). For laminar flow through porous media, the quantities V and ΔP are related through Darcy's law to permeability, hydraulic gradient, and flow. Sand-sized sediment produces the greatest streaming potential (i.e., large negative values). Streaming potential values drop (become more positive) for media of lower permeabilities (silts and clays) and for flow through coarse rubble in open fissures (Ogilvy, Ayed, and Bogoslovsky 1969). If turbulent fluid flow takes place in channels and fractures, it is thought that less intense streaming potentials are caused than would arise from an equal quantity of water flowing through a porous media under laminar conditions.

17. Understanding the relationship between SP and ground-water flow through fractures and channels is critical to a successful application of the technique in areas of consolidated bedrock. This is especially true for karst, where flow regimes can range from diffuse fracture flows to open solutional conduits. Often, in karst, the solutionally enlarged channels are wholly or partially filled with secondary material which can consist of particle sizes ranging from clay to gravels. Karst channels can also be either air filled, water filled, or a combination of air, water, and sediments. Such complexity requires careful consideration in interpreting SP results over these areas.

18. The literature is scant regarding streaming potentials produced in fracture or conduit flow conditions. Laboratory experiments have been conducted by Ahmad (1964) and Bogoslovsky and Ogilvy (1972) to study streaming potentials in channel flow models. Both studies affirm the proportional relationship between SP and ΔP , or hydraulic head (the driving force behind the fluid movement). Otherwise, they found that SP fields in fissured media differ from those in unconsolidated porous media. For instance, at similar pressures (ΔP) the SP values produced in fissures 2 to 6 mm in width are several orders of magnitude smaller than those produced in media-grained sand (Bogoslovsky and Ogilvy 1972). SP values were found to decrease with the opening of fissures, i.e., larger fissures (6 mm) produce SP values approaching zero or positive values while smaller fissures (2 mm) produce SP values that are more negative. However, the presence of sand fill in the fissures considerably increased the SP over values obtained for empty fissures. A filling of 40 percent sand produced the maximum SP; whereas, introducing a clay fraction to the fill resulted in a decrease in the SP. Ahmad (1964) concluded that the geometry of flow was relatively unimportant in its effect on SP in fissured flow and that SP decreases as salinity of the electrolyte (pore fluid) increases.

19. Ogilvy, Ayed, and Bogoslovsky (1969) reported that clay-filled fissures with low permeabilities are characterized by low SP values. As supporting evidence for this, they cited the relatively high positive values of SP associated with clay layers in borehole geophysical logs. They also claimed that salinization also leads to a decrease in SP values. Warriner and Taylor (1986) conducted laboratory experiments in an attempt to model streaming potential mechanisms and parameters. They also found that the presence of clay in or near the flow path degrades SP magnitudes, and also mentioned the positive SP values for shale layers in well logs as confirmation. In their experiments, all measured streaming potentials were negative.

20. The dependency between SP values and ΔP has been further demonstrated at various Corps of Engineers reservoirs. Perturbations to the water flow regimes were created by changing the level of the reservoir pool. These changes in hydraulic head correlated to SP fluctuations at electrodes located over seepage zones, indicating that flow rate affects SP (Warriner and Taylor 1982).

21. Some insight into depth resolution and the ability of SP to detect water-filled conduits was gained in an SP survey over Manatee Springs in Florida (Cooper 1983). Manatee Springs is a large water-filled solution conduit and was detected by SP at a depth of 90 ft.* Florida's karst often has high diffuse permeability and may also contain appreciable amounts of sand; this may explain the significant streaming potential anomalies encountered at this test site. Further evidence of SP depth capability was demonstrated by a Corps of Engineers survey at Waterbury Dam in Vermont, where there was a good correlation of negative anomalies with man-made outlet works conduits at a depth of 120 ft below the embankment on which the surveys were conducted.

22. It is important to refine the SP technique and our interpretation of its results to distinguish between different types of ground-water flow regimes. Most basic would be differentation between filtration flow (seepage) through soil and unconsolidated sediments and concentrated flow in fractures or channels. Within karst terrain this amounts to detecting shallow recharge ground water percolating through soil and regolith, water confined to solutionally developed channels in the epikarst and moving laterally or vertically, and deeper flow through solution conduits in either vadose or phreatic conditions. This variety of conditions entails a multitude of variables which could affect SP generation and interpretation, such as:

a. Local relief, which could influence hydraulic gradients.
b. Lithology (insolubles would affect permeability of fill).
c. Variations in water and soil chemistry.
d. Bedrock structure and deformation.
e. Degree of karstification, extent of subsurface drainage.
f. Depth to "water table" or major conduits.
g. Climatic and seasonal parameters.

---

* A table of factors for converting non-SI to SI (metric) units of measurement is presented on page 3.

PART II: DESCRIPTION OF STUDY AREA

Sites

23. In this research, SP was studied by means of observations and data from a number of sites in Rockbridge County, VA--within the Valley and Ridge Province. All of the sites are underlain by Ordovician limestones and dolomites. Karst topography is well developed locally; numerous sinkholes, caves, karren, and sinking streams are present. Elevation is about 360 m above sea level.

24. Nine sites were selected for study. Six sites are sinkholes (one contains a cave entrance), two sites are sinking streams, and one site is at an intermittent stream bed. Figure 2 shows the location of Rockbridge County and several of the study sites. The sites were chosen to represent a range of karst features (collapse sinks, subsidence sinks, sinkholes with known cave passages under them, sinkholes above springs, fault-related sinkholes and sinking streams, and a failed sinkhole pond). All are examples of ground-water recharge points, and, as such, should exhibit high streaming potential values.

Harris and Hunter sinkholes

25. Two of the sites (Harris and Hunter sinkholes) were monitored in 1985; for all the other sites, study began in July 1986. Unfortunately, the commencement of this research in 1986 coincided with a prolonged and severe drought that caused record low water levels throughout the area. The natural oscillations in water levels and flow volumes that were anticipated in the design of this research did not occur until the spring of 1987. The Harris and Hunter sinkholes are located in open pasture land on Kiger Hill and are developed in the Beekmantown Formation on an anticlinal fold. The Harris sinkhole collapsed during heavy rain in August 1984 and now displays a blind shaft at its bottom. The Hunter sinkhole is a more shallow subsidence feature and is located 180 m up-gradient from the Harris site.

Moore sinkholes

26. The Moore sinkhole site is also in open pasture land about 1 mile west of Lexington. It is underlain by the Lincolnshire limestone which displays numerous large sinkholes in the immediate area. The Moore sinkhole "A" was developed into a farm pond in the 1970's and apparently held water

(surface runoff) successfully for several years until leakage failure occurred around 1980. It has been dry since then, although there is currently another pond holding water 90 m away (which is not a sinkhole). The Moore sinkhole A is aligned with other adjacent sinkholes in a northeasterly bearing (along strike). A small transverse fault (striking E-W) is exposed one-half mile east of the site. Two other sinkholes (Moore "B" and "C") are located downgradient from and close to sinkhole A. These three sinkholes form a related complex and were monitored for SP, electrical resistivity (ER), and electromagnetic conductivity (EM) data beginning in December 1986 to determine the nature of their relationship and to look for any hydrologic connections implied by the data.

McHenry sinkholes and cave

27. The McHenry site contains two sinkholes (A and B) and a cave named Whose Hole. This area is located at the base of Little Camp Mountain (local relief is 450 m) in the Lincolnshire limestone. The structure here is complex, consisting of a series of small, compressed folds and minor faulting. Whose Hole Cave contains a permanent stream which flows northeast, along strike, for 0.4 km to discharge at a spring immediately below sinkhole B. Sinkhole B is developed in the trough of a small syncline and contains a relatively recently collapsed blind shaft (although no connection can be made here into the cave passage that is presumed to underlie it). A fluorescent dye trace established the hydrologic connection between the cave stream and the spring at sinkhole B. Sinkhole A at the McHenry site is located between the cave and sinkhole B. It is a shallow but well defined feature and contains good exposures of bedrock that suggest that a fault cuts through this sinkhole. An intermittent stream course is adjacent to the sinkhole entrance of Whose Hole Cave and trends easterly to join the stream that flows from the spring discharge of the cave. A long-term electrode monitoring station has been installed across this normally dry streambed at a point 270 m east of the cave entrance. All of the McHenry sites are in pasture land except for the cave site which is wooded.

Spring Branch sinking stream

28. One of the sinking stream sites is located on Spring Branch about 1.6 km east of the McHenry site. The Spring Branch site is also developed in the Lincolnshire limestone. This is technically a loosing stream in that normally only a portion of the flow in Spring Branch is lost underground here

through a series of four or five enlarged joints in the bed and bank of the stream. However, between July 1986 and January 1987, the entire flow of Spring Branch was lost underground because of the low flow levels resulting from drought. A thrust fault runs parallel to Spring Branch and has been suggested as a plausible cause of the watershed piracy that has been observed in the area (Johnson 1980 and MacMillan 1980). It is likely that the Spring Branch site is related to this fault and that the water lost from Spring Branch is diverted to another watershed (South Buffalo Creek).

Ford site's sinking stream

29. The Ford site is another example of a sinking stream; overflow from a spring is lost into solutional fissures in a rocky streambed 1 km west of Lexington. This site is underlain by Lincolnshire limestone as well. The extreme surface rockiness and numerous sinkholes nearby suggest a high degree of solutional weathering has taken place here. During very heavy precipitation some of the water continues beyond the normal point of loss for about 45 m to the entrance of a small cave passage where it is finally lost to underground channels.

Research Methodology

30. An array of electrodes was installed at each site and monitored for SP over a period of months. A double ring concentric configuration was used for sinkholes and a rectilinear grid pattern was used at sinking stream sites and as a tracking array between sinkholes. Electrodes were numbered with reference to the compass so that spatial patterns of anomalies could be related to other directional features (such as geologic structure, stream flow directions, etc.). A reference electrode was located at least 25 m distant from the test electrodes in a direction up-surface elevation gradient from the array. Some sites received two or more reference electrodes (for instance, in the center of a sinkhole) as a check on the results.

31. SP values were read for each site at approximately weekly intervals, with special attention following precipitation events. Although SP values for electrodes varied considerably over time, the relationship between electrodes remained constant (i.e., the strongly negative anomalies were always in the same location). The locations of consistently anomalous electrodes were presumed to represent areas of concentrated ground-water flow

(maximum streaming potential). SP readings were taken with a high impedance digital voltmeter by connecting wire leads between the reference electrode (always common, or ground, for polarity convention) and each test electrode. SP values ranged between +400 and -500 mv and were steady while reading (fluctuating only one or two mv).

32. Other types of data were collected to confirm interpretation of SP anomalies as areas of increased ground-water flow. Electrical resistivity (both Wenner and Lee arrays) and electromagnetic conductivity surveys were conducted at the Moore and cave sites to provide an alternate geophysical interpretation of parameters such as anisotropy and permeability. Precipitation (from rain gages) and soil temperature data (by thermometer and thermocouple probes) were recorded for each site. Fluctuations in stream levels were determined by constructing weirs above sinking stream sites and from a float/electrical resistance device in the cave stream. In addition, visual observation of surface runoff patterns along with geological study of nearby outcrops provided clues for interpreting subsurface conditions and related SP effects.

33. The electrodes used were copper-clad steel rods, 2 cm in diameter and 60 cm in length, and were driven into the ground about 50 cm. This type of electrode was successfully used to detect SP anomalies over zones of leakage in dams by the Corps of Engineers (results were confirmed by both drilling and other geophysical methods). This is a departure from the traditional technique of using nonpolarizing (NP) SP electrodes. NP electrodes are commonly employed in mineral and geothermal surveys and in corrosion control applications. NP electrodes consist of a copper rod immersed in a saturated solution of copper sulphate with a porous ceramic tip that allows ionic diffusion and electrical contact between the soil and electrolyte. The purpose of this design is to eliminate the effects of local polarization (concentration cells) that may occur on metallic electrode surfaces.

34. Although the use of metal electrodes does introduce some local polarization effects into SP data, it appears that they are effective in long-term monitoring of streaming potential and that polarization effects are minimal and tend to be averaged out. The NP electrodes would be preferable for instant readings of one-time surveys over large areas and for applications where anomalies are small and accuracy requirements are great. For use in small areas of uniform geologic setting, metal electrodes are apparently

adequate for long-term monitoring of large-scale anomalies and systematic changes in SP. A process of equilibrium occurs for metal electrodes after being placed in the ground; the time required for this may vary from 1 day to 1 week. SP values become relatively stable when this equilibrium of polarization effects takes place. The polarization equilibrium process for several test site electrodes is recorded in Figure 3. Adequate time should be allowed before reading SP values after initial electrode placement. Electrodes are then left in place for as long as needed. Polarization effects are further minimized because the high internal resistance of the metres that are used allows practically no current flow to occur. The use of a bimetallic electrode (copper-clad steel) may be advantageous in that the exposed steel tip acts as a sacrificial anode, thereby reducing corrosion and polarization effects on the copper sheath. The advantages of metal electrodes over the NP electrodes are their low cost, ease of placement and use, and durability. NP electrodes were used to verify the results obtained from metal electrodes at some of the sites in this research. The actual SP values were different, but in most cases there was general agreement of relative values between electrode locations (lowest values were in the same places, etc.).

35. In addition to the manual collection of data with voltmeters, an automated data collection system was devised and implemented. This system consisted of a portable battery powered computer, an analog/digital signal converter interface and temperature/soil moisture sensors. The entire system was housed in a weatherproof case and could be left in the field and programmed to gather data at any desired frequency. The metal electrodes were wired directly to the signal inputs of the interface. The automated data collection (ADC) system was used for two tasks--to monitor the effects of environmental variables on SP over time and to monitor SP changes induced by the artificial recharge (dumping) of water into a sinkhole. The long-term monitoring of electrode behavior was conducted at the intermittent streambed site east of the cave on the McHenry site. The water dumping experiment took place at the Moore sinkhole A near Lexington. An example of the ADC record from the long-term monitoring is shown in Table 1, and from the water dumping test in Table 2.

36. Two water dump tests were conducted--4 and 18 October 1986. For both tests 15,900 ℓ of water were discharged into the center of the sinkhole from four trucks over a period of several minutes. SP measurements were taken

before, during, and after the dumping, both by voltmeter and by the ADC system. The purpose of this test was to look for SP response to the flow of a known amount of water into the sinkhole system, with the hope that SP changes could be related to flow rate in a soil-regolith recharge setting.

37. Other experiments aimed at understanding SP changes relative to ground-water flow were conducted at Whose Hole Cave on the McHenry site. The cave was accurately surveyed, and electrodes were placed on the surface at locations that could be related to underlying cave features. A weir was constructed across the cave stream and a flow measuring device was installed and wired to the surface so that stream level changes could be conveniently monitored. This device consisted of a float attached to a potentiometer; changes in float height could then be detected as a linear change of resistance and calibrated in relation to water levels at the weir.

38. An array of electrodes was installed on the surface in rows perpendicular to the cave stream passage at a point directly above the weir location. The vertical distance from the center of this array to the cave stream was calculated to be 25 m. In addition, a ring of electrodes was placed around the sinkhole entrance to the cave so that SP data could be related to underlying cave features at depths ranging from 10 to 20 m. An initial ring of 12 electrodes was used from September to December, 1986, after which the standard double ring of 32 electrodes was installed in the sinkhole. In December 1986 an EM conductivity survey was conducted at this sinkhole using intercoil spacings of 10 m.

39. For all the sites, the SP data show considerable variability as seen in the standard deviations of individual electrode readings. Although the relative values between electrodes remain fairly constant, it is difficult to interpret meaningful trends from masses of variable numbers. Others have attempted to gain better resolution in their data by determining and removing a mean regional SP value (Cooper 1983). The mean regional SP is determined by averaging all the SP values for a given reading and subtracting this value from each individual value for that date.

40. The present research suggests that the time varying influence of temperature and moisture introduces systematic shifts in the SP data. This influence can mask or exaggerate the streaming potential values. An effort was made to filter the data by using ranks to preserve the ability of the data to document negative anomalies and variability while removing the seemingly

erratic swings in the raw data. Negative readings are shown as low rankings and positive readings are shown as high rankings (Erchul 1987). The major advantage is the removal of systematic changes in the data. The major disadvantage is the insensitivity to factors which exaggerate scale. A more negative reading due to increased ground-water flow is not visible in the ranked data until one reading passes another. A comparison of the spatial patterns of SP anomalies calculated by both averaging and ranking shows that no significant difference is obtained. This suggests that the use of averaging may be adequate for plotting SP values to infer flow paths and that systematic data changes of whatever source are cancelled by averaging. Further refinements in quantifying SP data for use in flow rate studies, however, will probably necessitate development of additional statistical treatment.

PART III: RESULTS AND DISCUSSION

Evaluating and Comparing SP Results

41. This research set out to examine several basic questions by evaluating and comparing SP results from various sites having different characteristics. Of primary concern are the following issues:

a. How effective is SP in detecting flow paths in karst features?

b. Are detected anomalies characterized by percolation and seepage flow or by fracture-conduit flow?

c. Can SP results be related to flow rates?

d. What is the relationship between SP variations and environmental variables?

42. At every site significant SP anomalies have been measured. These anomalies differ by as much as an order of magnitude from the SP values of the surrounding electrodes, and their locations remain fixed within the electrode array space. The magnitudes vary with time, but the relative values between electrodes remain fairly consistent. At the Harris and Hunter sinkholes, anomalies were linked and used to infer flow paths within and between the two sinkholes over a distance of 180 m (Erchul 1987). The plotted SP values were calculated by averaging all readings for each date and also by ranking the data (lowest reading electrode for a given date equal to one, etc.). For purposes of plotting the values to infer flow paths, the spatial relationships produced by these two methods of calculation do not differ significantly (i.e., the anomalies do not change relative to each other, and connecting them creates the same flow paths). At the Harris and Hunter site, the flow paths are aligned with the geologic strike of the underlying bedrock (N 50° E) and with joint or fracture orientations perpendicular to the strike. An electrical resistivity survey showed anisotropy in the form of an ellipse oriented in the strike direction, also. In addition, nearby caves (there are five within 1.5 km of the site) are predominately strike controlled in their passage development (Figure 4). It is reasonable to assume that the flow paths inferred by the SP data at the Harris and Hunter site represent strike and offset joint control that has created areas of preferential water movement. Figure 5 shows electrode arrays and inferred flow paths at the Harris and Hunter sinkholes (Erchul 1987).

Spring Branch site results

43. The Spring Branch site was selected because it is a sinking stream and appears to be related to a fault that may divert ground water out of the watershed. A grid array of electrodes spaced on 7.5-m centers was placed on the hillside above the point of stream loss (swallet). A weir was constructed above the swallet to measure fluctuations in flow. An experiment was conducted with two reference electrodes at this site. The results are shown in Figure 6 and indicate excellent agreement between SP values for all electrodes. Data were collected weekly for about 3 months and used to calculate average SP values. Figure 7 shows the Spring Branch site with the electrode array and an SP (mv) contour map. Anomalous areas are identifiable as concentrations of contours (areas of maximum SP gradient). The bedrock here strikes northeast and dips 15° SE. The stream sinks into a solutionally enlarged joint striking SE (direction of dip) which coincides with the orientation of the zone of maximum SP gradient. The contours indicate preferential water movement in this southeasterly direction and also to the east. From examination of outcrops exposed along the streambed, a set of joints has been measured striking N 85° E. The two linear trends displayed on the SP contour map and marked B-B and C-C are interpreted as ground-water flow paths based on observation of outcrop features (dip and joint strikes being the dominant structural controls). No physical evidence of faulting is displayed at the site, but the geologic map (Spencer 1968) indicates a low angle thrust fault in the vicinity, dipping east. MacMillan (1980) and Johnson (1980) have identified this fault and this portion of Spring Branch as the most likely source of watershed loss into the adjacent watershed to the east. The SP data appear to confirm this interpretation by indicating a major anomalous zone below the swallet. This could be the point where the fault captures the water lost from Spring Branch.

44. Since the water from Spring Branch is lost into solutional channels, this site should provide some indication of SP ability to detect channelized flow. Averages were calculated for the western half of the electrode array (upstream of the swallet) and for the eastern half (downstream of the swallet). The results are shown in Figure 8, along with a record of stream flow and precipitation. The SP values for the eastern half of the array are more negative than the western half, indicating that those electrodes downgradient of the swallet may be measuring increased streaming potential because

of channelized flow below them. The entire array is located on a uniformly north sloping hillside with no obvious differences between the two halves. It can also be seen from Figure 8 that SP becomes more negative in response to either precipitation (soil moisture) and/or streamflow. Figure 9 depicts evidence for SP generation because of the nonchannelized flow at Spring Branch for those electrodes nearest the streambed. The SP data for the two dates shown indicate a negative shift of about 200 mv at electrodes Nos. 31, 4a, and 5a during a period of increased streamflow. These electrodes are only about 5 m from the bed of the stream. On 10 October the streambed below the swallet was dry (all the flow was going into the swallet) but on 2 November the added flow caused the swallet to overflow and this additional water was absorbed into the sediments of the streambed for a distance of 25 m below the swallet. This seepage flow through the streambed sediments probably caused an increased streaming potential that is represented by the negative shift in those streamside electrodes as depicted in Figure 9. A similar negative SP response was measured at an electrode of the long-term monitoring site whenever the normally dry streambed would carry water following heavy rains.

Ford site results

45. The Ford site is a sinking stream also, although no faulting is known to occur here. Overflow from a spring development for livestock, along with intermittent surface water runoff, is lost into solutional openings at the head of a small steep-sided valley. Flood flow produces more water than can be taken by the swallet and the excess is carried 25 m beyond to the entrance of a small cave (a single conduit 7 m in length). Figure 10 shows a map of the Ford site with electrode array and SP values plotted as millivolt contours. Data for this site does not seem to depict a linear flow path. The greatest anomaly is on a line connecting the swallet and overflow cave, and this line coincides with the direction of strike (northeast). Streamflow (from a weir above the swallet), soil temperature, and average SP for the array are recorded, for the period June - November, along with SP for electrode No. 9 (the greatest anomaly) in Figure 11. There is no obvious correlation here between streamflow and SP. Soil temperature has a direct effect on array average SP at times (the month of August, especially), but at other times this relationship seems less direct, probably the result of precipitation events interacting with temperature change. The response of the anomalous electrode No. 9 differs from the response of the array average,

indicating that No. 9 reacts differently to environmental changes or to other unknown factor(s) that may influence this anomalous zone but not the surrounding electrodes. It may be that the anomaly at electrode No. 9 represents a site where ground water is descending vertically rather than flowing laterally. Vertical shafts are not unusual in karst aquifers and are a principal element in the epikarst model (subcutaneous zone) of Williams (1983) and White (1977). It is reasonable to assume the existence of vertical ground-water movement at the Ford site because:

a. The base level (Maury River) is 40 m lower than the Ford site.

b. There are no known major springs or resurgences between the swallet and the Maury River (a distance of 2.4 km).

c. The lithology of the site, and terrain between the site and the Maury River, is soluble carbonates with no perching beds or aquicludes.

46. An examination of the SP data collected at both of the sinking stream sites (Tables 3 and 4) shows an interesting seasonal trend which is not evident at any of the other study sites. At both the Spring Branch and Ford sites the SP values trend from largely negative in the summer and fall (July to November) to almost entirely positive for the period December through April. The period July to November corresponds to the severe drought which began to cease with the return of significant rainfall in December. The only other site to show a pronounced reaction to the drought was the sinkhole entrance to Whose Hole Cave, but here the SP response was exactly opposite (positive during the drought and negative in response to returning normal rain and ground-water flow). The fact that the sinking stream sites show this apparently unique reaction may indicate that conduit flow is playing a role in SP values here, but we do not have an explanation for this phenomenon at this time. It is difficult to say why the transition from a severe drought to normal "wetter" weather would cause such wholesale systematic shifts in SP from negative to positive values.

McHenry site results

47. The McHenry site contains two sinkholes, a cave with a stream in it, a spring (resurgence of the cave stream), and a typical dry karst (intermittent) surface stream course. All of these features are within 0.4 km of each other in an area of complex geologic structure (Figure 12). The McHenry sinkholes A and B were monitored for SP changes from July to November

(Tables 5 and 6). Figure 12 shows the spatial relationship between the two sinkholes and the spring. Sinkhole A is located about 15 m higher than sinkhole B, in a direction generally up-dip (to the southeast). The spring emerges from the base of a steep slope about 10 m lower than sinkhole B. The flow of ground water can be assumed to be from A to B to the spring. SP data for sinkhole A is shown as millivolt contours in Figure 13. The strongly anomalous zone in the southeast quadrant corresponds to a fault that is exposed in bedrock ledges outcropping here. The linear trend of these contoured anomalies is oriented to the northwest in the direction of sinkhole B. In Figure 14, the fault-related anomalous zone in sinkhole A is shown to have an equal effect on both the inner and outer rings of electrodes implying that at least some flow is lateral (towards sinkhole B and the spring). The millivolt contour map for sinkhole B (Figure 15) exhibits two main anomalous zones. The anomaly in the southeast quadrant probably represents the flow path of water coming from the direction of sinkhole A. The largest anomalous zone, in the northeast quadrant, represents the outflow of water from sinkhole B toward the spring. This assumption is supported by observation of outcrops; the spring emerges from the trough of a small synclinal fold. Ground water in the vicinity of sinkhole B would therefore flow down-dip on either limb of the syncline and would have to exit along the axis of the synclinal trough. The SP results from McHenry sinkholes A and B exhibit especially strong anomalous zones that demonstrate a linear pattern of connections. The fortuitous exposure of outcrops in the vicinity helps to confirm these interpretations of flow paths.

48. During the course of monitoring these sinkholes, the phenomena of short-term anomalies were observed at both sinkholes. In both cases, the events occurred between mid-August and mid-October. Figure 16 shows an SP increase of 500 mv for two electrodes at sinkhole A (these two electrodes were unique in this behavior at A). At sinkhole B only one electrode (No. 21) exhibited a similar SP increase over this time period. These phenomena have not been observed at any of the other sites during this research. It is possible that these dramatic but short-term events were related to the conditions of extreme drought that prevailed at the time. The Palmer Index for the end of September showed all regions of the state in severe drought, according to the *Virginia Water News* (Vol 17, No. 10, p 6). Precipitation at the McHenry site totalled only 13.7 cm between 21 July and 13 October. Figure 17

depicts SP changes at sinkhole A. The short-term anomalies at electrodes Nos. 26 and 29 can be seen in the west and southwest quadrant from 17 and 23 September. On 14 October there was 1.3 cm of rain, which eliminated these two anomalies. On 19 October, after drying out, these two electrodes again became negative, but not to the extremes reached previously. These short-term anomalies occur in outer ring electrodes and apparently are not reflected by corresponding changes in the inner ring of electrodes. They probably represent vertical flow or seepage of soil moisture into fractures. To sustain base flow of ground water at the spring (its output was relatively unaffected by the drought), water that is tightly held in fractures and soil pores is pulled downward into conduits and channels as the more accessible storage water is exhausted from the ground. This supply of ground water, that is otherwise tightly held in storage by capillary forces, would likely generate high streaming potentials when flowing through very small fractures (or sediment-filled fissures). Perhaps the reason this effect was observed at the McHenry sinkholes is because they are close to base level discharge (the spring); whereas, all the other sites are areas of ground-water recharge. During extreme drought, areas near a spring may be subjected to conditions that make extraordinary demands on ground water held in storage, and this could create ephemeral anomalies that reflect temporary areas of preferential flow.

Whose Hole Cave results

49. At Whose Hole Cave three different arrays of electrodes were emplaced. A ring of 12 electrodes was placed in the sinkhole containing the cave entrance (Table 7), and three rows of ten electrodes were placed directly above that portion of the cave containing the stream (Table 8). An array of 32 electrodes (two concentric rings of 16 each) was emplaced in December 1986 (Table 9). Figure 18 is a map showing the 360 m of passage that have been surveyed and the relationship of the electrode arrays to the underlying cave passages. Passages are strike controlled and trend to the northeast toward the McHenry sinkholes A and B. The stream inside the cave has been dyed to establish its connection to the spring at sinkhole B. A weir and water level measuring device (float attached to a potentiometer) provided streamflow data for the cave stream. Streamflow could not be related to SP changes at the array of electrodes over the stream passage. This may be due to the depth of 25 m or to the relatively small stream (flows ranging from 0.002 m/sec to 0.01 m/sec) or to the lack of sand-sized sediment in the fill within the cave

(mostly clay and gravels). A profile of average SP for the array over the stream passage is shown in Figure 19. One might expect an anomalously negative area directly above the cave. In this case the reverse is observed--the positive SP values being over the cave. The two negative anomalies seen on either side of the array are unexpected. The anomaly at electrodes Nos. 2 and 3 may be the result of the intersection of a joint or fault plane with the surface here. Such a plane would allow preferential movement of water that would generate high SP values. As can be seen in Figure 19, this plane is exposed as a wall in the cave passage. The cave contains numerous tube-like features that incline at similar angles and which serve as conduits for descending trickles of water. The anomaly at electrodes Nos. 7 and 8 cannot be explained. Perhaps another joint or fault that is unknown intersects the surface here. The implications of this data are that SP results in karst areas of structural complexity must be interpreted very critically with regard to underlying structure. The effect of inclined planes on preferential water movement may mean that the location of SP anomalies is offset from underlying cavities or features of interest. This research suggests that SP results over Whose Hole Cave are related to soil water percolating downward into planes of greater permeability and preferential flow rather than to the flow of the vadose cave stream. This result is consistent with SP theory as expressed in the literature.

50. SP results from the sinkhole entrance to the cave can be related to underlying cave features. Plan views of this portion of the cave with the associated electrode arrays are given in Figures 20 and 21. For Figure 20, with an array of 12 electrodes, the anomalous electrodes are Nos. 1, 2, 3, 9, and 12, while all other electrodes have positive SP values. The anomalous electrodes are located above cave passages where ground water seeps through sediment fill (silty clay and gravel deposits) or above steeply inclined narrow fissures which channel downward percolating soil water into the cave. These vertical fissures and tubes are relatively high in the cave and extend upward in proximity to the surface (especially electrode Nos. 1 and 3). The values for electrodes Nos. 9 and 12 are probably explained by the fact that the passage between them contains a pool of water during wet weather that is created by a natural "dam" of sediments and breakdown. Water in the pool percolates slowly through the permeable material in the dam, moving from the vicinity of electrode No. 9 toward electrode No. 12. This direction of

flow can be observed in the cave but is also confirmed by the consistently greater SP values at electrode No. 12 than at electrode No. 9. During dry weather there is little or no water feeding into this area and the pool disappears. Water percolating through this dam of sediment would probably generate large streaming potentials. The series of SP contour maps shown in Figures 22, 23, and 24 all indicate major anomalous zones within the northeast quadrant of the array. Also, the contour map of EM conductivity (Figure 25) shows the northeast quadrant as the principal EM anomaly. The cave passages under this area are high, narrow fissures that are close to the ground surface serve as zones of preferential ground-water movement. When the EM conductivity survey was conducted in December 1986, soil moisture content was fairly high. It is probable that the soil near the tops of these fissure passages (and the soil and sediment filling the fracture systems feeding these fissures) was saturated to a greater extent than the surrounding soil. Therefore, this zone of greater saturation would be more conductive and would produce the conductivity anomaly seen in Figure 25. Similarly, the percolation of water in this area would generate anomalous streaming potentials also.

51. A temporal effect on SP can be seen in Figure 26. SP values for the 12 electrodes around the entrance sinkhole are profiled for each reading date, from September through November. The desiccating effects of drought are reflected as a gradual shift of SP values from negative to positive. The middle of October showed all positive values (the anomalous spikes have even been lost) which correspond to maximum drought conditions. In late October, as some rain began to return and vegetation became dormant, moisture was recharged to the ground, and the SP profiles began to shift back toward negative (with the anomalous peaks returning). In early November, conditions of increasing seepage were observed in the cave around electrodes Nos. 3 and 9. The data presented in Figure 26 appear to portray a direct relationship between drought-induced desiccation effects, the return of more moisture, and SP values. Although electrodes Nos. 7 and 8 were located over cave passage, they had a consistent positive value. This was probably because their passages were relatively deeper than those areas beneath the anomalous electrodes (about 20 m as opposed to 5 m). Also, even though there is water flowing near electrodes Nos. 7 and 8, it is a relatively small quantity and the flow is over bare rock and travertine deposits (a condition that would not be likely to generate appreciable streaming potentials). At this site then, the SP

anomalies are in areas where ground water percolates through a sediment dam or plug and around high vertical fissures and tubes that approach the surface and serve as channels to concentrate the entry and downward seepage of moisture from the soil and epikarst into the cave passages below. Passages about 15 to 20 m deep with water flowing over rock or travertine do not appear as SP anomalies.

Time Varying Effects on SP Results

52. The time varying effects of soil temperature and precipitation on SP values have been observed at all the study sites. It is difficult to characterize the exact response of a given site or electrode to these changing stimuli as the reactions sometimes appear contradictory or erratic because of an interactive effect of these variables. There may be other factors influencing SP values as well, further complicating the detection of cause and effect. Such factors would include physical and chemical properties of soil, depth to bedrock, relief, vegetation, aspect of the site, and seasonal climatic changes. The fluctuations imposed by these factors constitute signal noise that can mask or exaggerate the streaming potential effects that are being sought. Not only do the various sites respond differently to changing environmental factors, but individual electrodes within a given array can respond differently, as seen in Figure 27. Here the mixed reactions of four electrodes to 3.4 cm of rain are shown. It may be that such behavior is attributable to the extreme drought conditions that existed during the study period, and that during periods of more normal soil moisture the SP responses are more predictable.

53. Soil moisture is a critical parameter to consider, along with precipitation, as it can be related to soil saturation conditions and the lag times between precipitation events and SP values. Soil moisture data also compensate for the effects of vegetation types and activity on infiltration of precipitation. In general, increased soil moisture causes an SP increase (values become more negative), presumably resulting from a greater streaming potential as the water percolates through the soil and regolith. Figure 28 illustrates this reaction for two test electrodes. A sharp increase in soil moisture produced an SP change of grater than 100 mv in the negative direction, but this occurred about 18 hr after the rain began. It can also be seen

that the SP returns to its former value very gradually over a period of days. However, depending on the degree of saturation, some precipitation events may produce relatively minor SP changes or may even result in a positive change of value.

54. The time varying influence of temperature also changes SP values. Thermocouple probes that produce a digital reading on a voltmeter have been used to measure soil temperature at a depth of about 15 cm. The tip of the electrodes are deep enough to be at a constant or slowly changing temperature; whereas, the exposed and near-surface area is subject to fluctuations of up to 10° C. A diurnal cycle in the SP values has been observed that corresponds to the warming and cooling effect of the surface soil. This effect is more pronounced when soil moisture is at low levels, as can be seen in Figure 28. Similarly, greater daily temperature extremes produce a larger SP cyclic change. If the exposed portion of the electrode is warmed by the sun, particularly on cold mornings, a large SP change can result from the thermocouple effect. Such changes are systematic and affect the SP values relatively uniformly for a site. An SP change of 50 mv has been observed for frosty mornings followed by sunny days that produced a surface soil temperature range of 4° C and an air temperature range of 16° C. Temperature effects on SP are not yet fully understood, as evidenced by the observation that at some sites SP increases as temperature increases, and at other sites SP decreases as temperature increases. More work needs to be done to understand the complex interaction between temperature, moisture, SP, and other factors which may be site specific.

55. Until such effects can be isolated and predictably quantified, using SP results based on averages of many readings may be the only practical approach for describing the general response of a site to variables. To understand the nature of individual electrode responses to processes affecting it, long-term accurate monitoring is required. At the long-term monitoring site, data were collected from 1 August 1986 to 8 October 1986 using voltmeters and thermometers (Tables 10, 11, 12, and 13). Data at this site were collected automatically by the ADC system from 8 October 1986 to 11 May 1987 (Tables 14-19). The automatic data collection system described previously has great potential for such application. Temperature and moisture sensors can be placed in the ground and data can be sampled at rates adequate for detecting subtle changes. The data presented in Figures 28 and 29 were recorded with

the ADC at the electrode monitoring site (dry stream bed below Whose Hole Cave). From Figure 28, the data show soil moisture responding to diurnal temperature cycles, but the SP record does not show a similar response when moisture levels are high. Also, when soil moisture is high, the SP changes, as a result of additional precipitation, are lessened by a factor of about two (60-mv change on 5 November as opposed to 140-mv change on 25 October) compared with dry soil conditions.

56. During the eight month period that the ADC system was used to measure SP at the five electrodes of the long-term monitoring site, electrode No. 5 was the only electrode that was always negative. The location of electrode No. 5 did not seem to be any different from the other electrodes except that the soil there appeared to have more clay. Consequently, soil samples were taken by coring beside each of the five electrodes, and a particle-sized distribution was determined by sieve and hydrometer analysis. The resulting gradation curves are shown in Figure 30 and it can be seen that the soil at electrode No. 5 does indeed contain appreciably more clay than the other electrodes. The coarsest material is the gravelly soil from the streambed at electrode No. 3 (which was positive when dry and negative when the intermittent stream flowed). The relationship between high clay content and negative SP, as shown by electrode No. 5, is of interest because this seems to contradict the SP literature, which reports positive charges associated with clay and negative streaming potentials associated with sand-sized particles. Although this is only one data point represented here, it seems to be supported by subjective observations in the field. While pulling electrodes from the ground at various sites, many electrodes that had been consistently anomalous (negative) were very difficult to extract because of their being in a sticky, plastic clay. It may be that the greatest negative anomalies in karst terrain are not a result of streaming potentials in sand-sized material but, instead, are from ionic charges or membrane activity in clay minerals. The mineralogy of carbonate residual soils could have a drastically different SP effect than that of soils derived from siliceous lithologies, and would therefore impose different criteria for interpreting ground-water flow regimes from SP data. Also, the surficial aspect of a short electrode stuck into a high clay content soil ought to be considered. If the clay overlaid a sandy subsoil or permeable regolith through which ground water was flowing, it could be possible that the ionic charges associated with the clay could mask or amplify

any streaming potential charges produced at a greater depth. The vertical aspect of SP phenomena is an area that needs to be explored, along with the other factors previously mentioned.

Sinkhole Artificial Recharge Investigations

57. Since the Moore sinkhole A was an unsuccessful pond site, it presumably contains one or more leakages and would therefore be an ideal place to conduct an experiment in detecting flow paths and rates. An array of 32 electrodes (two concentric rings with diameter of 15 and 45 m) was installed. SP data were collected by voltmeter (Table 20). Two separate tests were then conducted. For each test, water trucks discharged a total of 15,900 ℓ into the sinkhole over a period of 4 to 5 min. SP was monitored before, during, and after the discharge, both by the ADC system and manually by voltmeters.

58. Both the water-dumping tests were successful in demonstrating that a negative SP shift occurred in response to the water draining through the sinkhole and that the greatest SP anomaly occurred around the same electrode (No. 3) on both occasions. Although moisture and temperature conditions differed for the two tests, the No. 3 electrode produced a strong anomaly in SP both times, as shown in Figure 31. Since electrode No. 3 is located on the inner ring of electrodes, one could expect the opposite electrode in the outer ring (No. 19) to also show a peak if the flow is outward in a lateral plane. Since this is not the case, it appears that the water was descending vertically in the vicinity of No. 3, and was not reaching the outer ring of electrodes.

59. For the first test on 4 October 1986, the ground was extremely dry from drought conditions (the preceding 2 months had received only 8 cm of rain, with no rain at all for the month before the test). Diurnal temperature swings were not great at that time. The discharged water ponded in the bottom of the sinkhole to a depth of about 10 cm and took 70 min to be absorbed. This represents a percolation rate of roughly 227 ℓ/min over an area of about 177 m^2. The induced SP changes are shown as a polar plot in Figure 32. Electrode No. 3 experienced an SP change of about 200 mv and goes off the scale compared with the relatively smaller changes of the other electrodes (ranging from 0 to 32 mv). The time required to reach the maximum change varied from 2 to 24 hr for the various electrodes.

60. During the first test, the water was dumped in the northeast quadrant of the sinkhole and during the discharge process water flowed over electrodes Nos. 1, 2, and 3. Their response was immediate, as can be seen by the charts in Figure 33. This illustrates the initial response to wetting which occurs in a matter of seconds. The sudden sharp negative increase followed by a sharp positive shift is probably the "moto-electric" effect that is described by Ogilvy, Ayed, and Bogoslovsky (1969). This effect arises when a metallic electrode is washed by the streaming potential fluid (water, in this case), which causes a negative SP shift, the magnitude of which is a function of the metal. Copper is given a value of -26 mv, which is about the same value as the recovery period (positive shift) seen for electrode No. 3. Likewise, electrode No. 2 went from an initial value of -8 mv to one of +25 mv (a total of 33 mv change due to moto-electric effect) before settling into a steady negative increase.

61. The second test was conducted 2 weeks later on 18 October 1986. The soil was more moist than during the first test, since 1.8 cm of rain had fallen 4 days before. Temperature extremes were much greater because of heavy frost followed by clear sunny days. Figure 34 illustrates the temperature ranges of 16° C for air and 4° C for surface soil. The corresponding plots of SP values show a pronounced diurnal cycle because of the influence of temperature. This effect produced a change in SP of more than 50 mv in a systematic fashion that served to mask the subtle SP changes that may have been induced by the water discharge, with the exception of electrode No. 3. Preferential water movement at electrode No. 3 was again implied by the anomalous SP change of 94 mv, nearly twice the value of all the other electrodes. A polar plot of the change in SP for the second test is nearly circular with the exception of a peak at No. 3. For the second test, the water was discharged from the northwest side of the sinkhole so that electrode No. 3 would not be directly wetted as occurred during the first test. Data were collected by the ADC system for a day following the test, and, as seen in Figure 34, it discloses the presence of the diurnal temperature cycle influencing the SP values in a nearly identical manner for both days. The anomalous behavior of electrode No. 3 to the water discharge tests is also evident from the SP record shown in Figure 35. Both tests produced significant negative shifts at No. 3, but only produced a relatively minor negative shift for the array average SP.

62. During the second test it took 165 min for the 15,900 ℓ of water to percolate down into the soil, a rate of 95 ℓ/min for the same area as in test 1. This slower rate was presumably because of the greater moisture content of the soil during the second test. Although flow rates for the second test are less than half the value during the first test, it is difficult to equate the figures to SP changes because of the large systematic influence of temperature that masked most of the SP data. However, it is interesting to note the correspondence between SP change of electrode No. 3 and the flow rate estimates--a ratio of about 2:1 in both cases:

	Flow Rates (ℓ/min)	ΔSP (mv) No. 3
Test 1	227	194
Test 2	95	94

63. From Figure 32 it can be seen that the location of electrode No. 3 is in the northeastern quadrant of the sinkhole. This is on the down-gradient side of the sinkhole, and it is reasonable to assume that water is probably leaving the sinkhole in this direction, which corresponds to the strike of the underlying beds. Figure 32 is a polar plot of azimuthal electrical resistivity data on several dates, showing an ellipse oriented to the northeast also. This data suggests that resistivity of the subsurface material is greater along the direction of strike than it is at right angles to the strike. A possible explanation for this phenomenon may be that proportionally more fissures or conduits are developed in the strike direction (most cave passages in the area are strike oriented), and these are mainly empty so that the collective volume of air-filled spaces increases the resistivity. If this model is correct, the resistivity along the northeast axis should decrease as more water enters and fills these channels (water being more conductive than air, of course). This response does take place for the two dates plotted. The 18 October data were collected several hours after the water was discharged into the sinkhole. The data for 24 October, nearly a week (with no rain) later, show that resistivity has increased along the northeast axis of the ellipse, suggesting that some water has drained out of the fissures and fractures.

64. Following the two water discharge tests in the Moore sinkhole A, the investigation at this site was expanded to include two other sinkholes

(B and C) which are in close proximity (Table 21). The general vicinity is a complex of sinkholes, and it was hoped that water draining out of sinkhole A (the highest in elevation of the three) would be detectable as a flow path leading to either or both of the sinkholes B and C. In addition to SP measurements, an EM conductivity survey was made at the three sinkholes and the results are shown in Figures 36-39. Sinkholes A and C appear to be more closely related to one another in terms of conductivity anomalies. As seen in Figure 39, the anomalous zones of A and C are also related to topographic expression as well, being clustered at the point where surface water flow would enter sinkhole A and seep downward in the center of the sinkhole, then again where surface water would first concentrate in the western limb of sinkhole C and flow subterraneously out of C to the northeast toward another large sinkhole. This northeasterly flow direction out of C also corresponds to the geologic strike. At sinkhole B the conductivity anomaly is located in the northwest quadrant where a small (2 m) sinkhole occurs on the edge of B. This anomaly also aligns on the northeast (strike) direction from the nearby pond. Based on the conductivity data, one could interpret a ground-water drainage or flow path entering sinkhole A on the west, descending in the center of the sinkhole and moving eastward to sinkhole C. In sinkhole C the flow then appears to be directed along strike toward the next sinkhole adjacent to the northeast. The locational relationships of the three Moore sinkholes are seen in Figure 40.

65. The SP data from the Moore sinkhole appear to be compatible with the interpretation based on EM conductivity. Figures 41, 42, and 43 show SP contours at sinkholes A, B, and C, respectively. These SP data were collected in early January 1987, a few days after the EM conductivity survey was made in later December 1986. The SP anomalies largely agree with the conductivity anomalies so that the same interpretation of a flow path from A to C seem reasonable. In sinkhole B (Figure 42) a very obvious SP anomaly occurs above the small 2-m sinkhole in the same location as the EM conductivity anomaly of Figure 37. Since Moore sinkhole A has been monitored for SP for several months before sinkholes B and C were studied, these data are shown in Figure 44. The SP anomalies are slightly different for this time period (which occurred during the drought), but they still tend to suggest a flow direction from west to east and toward sinkhole C. All of this data show a relationship between SP and EM conductivity, and it also suggests a ground-water flow connection

between sinkholes A and C. What it does not help explain is the anomalous SP response of electrode No. 3 in sinkhole A during the two water discharge tests. This electrode, in the northeast quadrant of sinkhole A, does not appear anomalous in any of the other SP or EM conductivity data. Perhaps a combination of the drought conditions that prevailed in October 1986 and the fact that flow was artificially induced offer some explanation for the response of electrode No. 3 at that time. More water discharge tests, excavating sinkhole A to bedrock, or penetrometer tests around electrode No. 3 may be the only way to ascertain what is really happening. Despite this contradiction, the bulk of the data from the Moore site suggests that SP anomalies around sinkholes can be used to infer flow paths, and that EM conductivity seems to confirm this. These inferred flow paths are probably shallow--within a 20-m depth, as the EM data at 10 and 20 m agree with the interpretation, but the 40-m survey appears rather amorphous in this regard.

66. Other results from the long-term monitoring of SP electrodes and environmental variables are shown in Figures 45-56 and in Tables 13-22. Initially these data were collected manually (Tables 13, 14, 15) from 1 August 1986 through 8 October 1986, after which the automated data collection (ADC) system was employed until termination on 11 May 1987. The graphs shown in Figures 45-56 were generated by computer (Lotus program) using the digital data collected automatically and do not reflect the time period 1 August - 8 October. Of the five SP electrodes that were monitored, No. 5 was always negative, No. 4 was always positive, No. 2 began positive but after November it changed to negative for the remaining monitored time period, and No. 1 varied between negative and positive values over the entire time period. Electrode No. 3 (Figure 47) was positive as long as the intermittent streambed in which it was located remained dry, but when the stream flowed temporarily after heavy rainfall the SP values became negative, as seen in the sharp peaks in Figure 52. Presumably, these anomalous SP values are a result of streaming potentials generated by the flow of water through the sediments of the stream bed. Figure 55 shows standard deviation of electrode No. 3 and the greatest values here are because of the extreme changes in SP (within a 24-hr period) as a result of this streaming potential.

67. The five electrodes at the long-term monitoring site were monitored at sampling rates of one-half hour to 4 hr, and these data have been averaged over 24 hr to produce the data in Tables 13-22 and Figures 45-56. Changes in

standard deviation shown are thus relative to SP variations within a 24-hr period. Standard deviation and SP change are proportional as seen in Figure 54. All of the five electrodes show similar SP responses initially (October), but the first significant rainfall to occur after implanting the electrodes (1.35 in. on 25 October) caused a major negative shift in all of them, after which their SP variations were dissimilar. Throughout the 8-month period, episodes of major rainfall produced marked negative SP responses in all five electrodes.

68. The effect of soil moisture (Figure 51) on SP response is less obvious than that of rainfall. Soil moisture was monitored electronically (the scale in Figure 51 is in relative "digital" units where high values represent higher moisture content) from a gypsum block sensor buried at 20-cm depth in the soil. The pattern of soil moisture in Figure 51 is similar to that of soil temperature (Figure 50), but this may be from a thermal effect transmitted from wires exposed to atmospheric temperature changes. There are undoutably lag times between rainfall and soil moisture/SP effects, but these are not immediately obvious in the data. The extreme fluctuation of soil moisture data shown in the beginning of Figure 51 is because of artificial effects produced by dumping water on the sensor to test its performance.

69. Soil temperature seems to play a more direct role in affecting SP than does soil moisture. Taken alone, soil temperature seems to be inversely proportional to SP (at this site), as seen in Figure 53. In this figure the SP record for electrode No. 2 has been inverted and compared with the soil temperature record. They agree favorably over most of the time period, but the pattern is reversed under extremely wet conditions as seen in late March through April. This implies that soil temperature effects are masked or reversed when soil moisture reaches a threshold level. This emphasizes the complex interactive nature of environmental variables on SP. Extreme conditions in the environmental variables will override the other factors and dominate or reverse SP responses.

PART IV: SUMMARY AND CONCLUSIONS

70. Spontaneous potential has been monitored at a variety of karst features for a period of 5-9 months. Significant SP anomalies were measured at all sites, and are assumed to be due primarily to streaming potentials created by ground-water flow. The magnitude of SP anomalies and SP changes is related to ground-water flow rates along with a host of other factors which make interpretation difficult. Direction of flow is indicated by concentration of SP gradients. Flow paths are inferred by SP data at all of the sites and seem especially well defined at the Moore, Spring Branch, McHenry, and Harris sites. Geologic studies along with electrical resistivity and EM conductivity surveys support the interpretation of flow paths at these sites.

71. The detected SP anomalies at these sites appear to be due primarily to water seepage and percolation through porous material rather than conduit or fracture flow. There is some evidence from Spring Branch for a general systematic registering of conduit flow from the electrode array, but individual electrodes could not be related to changing flow regimes. The stream in Whose Hole Cave could not be detected by the electrodes overhead. SP probably provides indirect evidence for conduit flow by indicating anomalies produced by the seepage of water from soil and regolith into small fractures that supply water to nearby conduits. It seems possible that SP can distinguish between lateral and vertical flow, as seen at the Ford and Moore sites. SP was able to detect underlying cave passages at Whose Hole Cave if they were relatively shallow (5-10 m) and if they contained water seeping through sediment fill or else intercepted water seepage from the soil and regolith storage.

72. On the basis of water discharge tests at Moore sinkhole there seems to be promise of relating flow rates to flow-induced SP changes. At the sites where conduit flow is known to exist (Spring Branch, Fords, Whose Hole Cave), it has not been possible to correlate stream flow with SP.

73. The relationship between SP and environmental variables is complex and not well understood. Soil temperature, soil moisture, and precipitation are the primary factors that have been examined, although this research implies that the influence of soil properties such as clay content or mineralogy may also be a dominant factor in SP, at least in karst areas. The interactive nature of these influences, and perhaps others, requires accurate

long-term monitoring to isolate and characterize them. If causal relationships and systematic variations can be identified and quantified, it would allow more precision in interpreting and applying SP results. ADC systems employing computers and remote sensors are a means of gathering sufficient data to attack the problems presented by environmental variables. Such a system was implemented in the course of this research and has functioned successfully. Refinements of this system will allow useful applications to long-term seepage/flow monitoring. Of theoretical benefit, the nature of recharge and storage processes in karst aquifers could be better explained with the monitoring capabilities inherent in an ADC system. Some practical applications are geotechnical in nature; for example, foundation studies and stabilization techniques can be monitored and supplemented, well pump tests can indicate aquifer characteristics from SP effects, and long-term SP monitoring can indicate development or increase of anomalous seepage from water retention structures. Possible environmental applications may exist in areas of saltwater intrusion and contamination plumes of high conductivity emanating from waste sites.

74. In summary, the SP technique is an effective method for detecting and mapping shallow flow paths in soil, regolith, and rock around most karst features. Its utility in detecting deep flow through conduits is not resolved in the current study. SP can possibly be related to flow rates if the flow is primarily through porous material. Computer technology promises to further develop the SP method for successful applications to hydrogeologic problems in karst areas and is addressed in Reports 3 and 4 in this series.

BIBLIOGRAPHY

Agarwal, N. P. 1984. "Quantitative Interpretation of Self-Potential Anomalies," Proceedings, 54th Society of Exploration Geophysicists Meeting, Atlanta, GA.

Ahmad, M. 1964. "Laboratory Study of Streaming Potential," Geophysical Prospecting, Vol 12, pp 49-64.

Anderson, L. A. and Johnson, G. R. 1976. "Application of the SP Method to Geothermal Exploration in Long Valley, California," Journal Geophysical Research, Vol 81, No. 8, pp 1527-1532.

Becker, A. and Telford, W. M. 1964. "Spontaneous Polarization Studies," Geophysical Prospecting, Vol 8, pp 174-188.

Black, W. E. and Corwin, R. F. 1984. "Application of Self-Potential Measurements to the Delineation of Ground-Water Seepage in Earth-Fill Embankments," Proceedings, 54th Society of Exploration Geophysicists Meeting, Atlanta, GA.

Bogoslovsky, V. A. and Ogilvy, A. A. 1973. "Deformations of Natural Electric Fields Near Drainage Structures," Geophysical Prospecting, Vol 21, pp 716-723.

_____, 1972. "The Study of Streaming Potentials on Fissured Media Models," Geophysical Prospecting, Vol 20, pp 109-117.

_____, 1970. "Natural Potential Anomalies as a Quantitative Index of the Rate of Seepage from Water Reservoirs," Geophysical Prospecting, Vol 18, No. 2, pp 261-268.

Brieden, H. J. et al. 1979. "Investigation of Intermediate Electrical Fields-An Effective Method for Cave Detection," Neve Bergbavtech, Vol 9, No. 5, pp 247-253.

Burr, S. V. 1982. "A Guide to Prospecting by the Self-Potential Method, Ontario," Geological Survey Miscellaneous Paper 99.

Butler, D. K. 1984. "Geophysical Methods for Seepage Detection, Mapping, and Monitoring," Proceedings, 54th Society of Exploration Geophysicists Meeting, Atlanta, GA.

Butler, D. K., Wahl, R. E., and Sharp, M. K. 1984. "Geophysical Seepage Detection Studies at Mill Creek Dam," Miscellaneous Paper GL-84-16, US Army Engineer Waterways Experiment Station, Vicksburg, MS.

Cooper, S. S. 1983. "Cavity Detection and Delineation Research: Report 3, Acoustic Resonance and Self-Potential Applications: Medford Cave and Manatee Springs Sites, Florida," Technical Report GL-83-1, US Army Engineer Waterways Experiment Station, Vicksburg, MS.

Cooper, S. S., Koester, J. P., and Franklin, A. G. 1982. "Geophysical Investigation at Gathright Dam," Miscellaneous Paper GL-82-2, US Army Engineer Waterways Experiment Station, Vicksburg, MS.

Cooper, S. S. and Bieganousky, W. A. 1978. "Geophysical Survey of Cavernous Areas, Patoka Dam Indiana," Miscellaneous Paper 5-78-1, US Army Engineer Waterways Experiment Station, Vicksburg, MS.

Cooper, S. S. and Koester, J. P. 1984. "Detection and Delineation of Subsurface Seepage Using the Spontaneous-Potential Method," Proceedings, 54th Society of Exploration Geophysicists Meeting, Atlanta, GA.

Corry, C. E. 1985. "Spontaneous Polarization Associated with Porphyry Sulfide Mineralization," Geophysics, Vol 50, No. 6, pp 1020-1034.

Corwin, R. F. 1984. "The Self-Potential Method and Its Engineering Applications: An Overview," Proceedings, 54th Society of Exploration Geophysicists Meeting, Atlanta, GA.

Corwin, R. G. and Hoover, D. B. 1978. "The Self-Potential Method in Geothermal Exploration," Geophysics, Vol 44, pp 226-245.

Dzhashi, G. G. and Abramishvile, T. D. 1975. "Change of Electrode Potentials at the Boundary of the Electronic Conductor and the Surrounding Materials," Soobshcheniya Akad. Nauk Gruzinskoy SSR, Vol 80, pp 589-592 (Eng. Sum.)

Erchul, R. A. 1987. "Geotechnical Application of Self Potential (SP) Methods: Report 1, The Use of Self Potential in the Detection of Sub-Surface Flow Patterns Around Sinkholes," Technical Report REMR-GT-6, US Army Engineer Waterways Experiment Station, Vicksburg, MS.

_____. 1986. "The Evaluation of Spontaneous Potential in the Detection of Sinkhole Drainage Patterns," Letter Report, US Army Engineer Waterways Experiment Station, Vicksburg, MS.

Erchul, R. A. and Butler, D. K. 1986. "The Use of Spontaneous Potential in the Detection of Subterraneous Flow Patterns In and Around Sinkholes," Proceedings, Environmental Problems in Karst Terrains Conference, Bowling Green, KY.

Erchul, R. A. and Slifer, D. W. 1987. "The Use of Spontaneous Potential in the Detection of Groundwater Flow Patterns and Float Rate in Karst Areas," Proceedings, Second Multidisciplinary Conference on Sinkholes and Environmental Impacts of Karst, Orlando, FL.

Erchul, R. A. 1974. "Ocean Engineering Applications of Electrical Resistivity Techniques," Proceedings, Offshore Technology Conference, Dallas, TX.

Ernston, K. and Scherer, H. U. 1986. "Self-Potential Variations with Time and Their Relation to Hydrogeologic and Meteorological Parameters," Geophysics, Vol 51, No. 10, pp 1967-1977.

Fitterman, D. V. 1979. "Calculations of Self-Potential Anomalies Near Vertical Contacts," Geophysics, Vol 44, No. 2, pp 195-205.

_____. 1978. "Electrokinetic and Magnetic Anomalies Associated with Dilatant Regions in a Layered Earth," Journal Geophysical Research, Vol 83, No. B12, pp 5923-5928.

Gondouin, M. and Scala, C. 1958. "Streaming Potential and the SP Log," Journal of Petroleum Technology.

Gunn, J. 1981. "Hydrologic Processes in Karst Depressions," Zeitschrist suer Goemorphlogie, Vol 25, pp 313-331.

Holsinger, J. R. 1975. "Descriptions of Virginia Caves," Virginia Division of Mineral Resources, Bulletin No. 85, p 450.

Johnson, S. 1980. "Hydrology of North Buffalo Creek," unpublished BS thesis, Washington and Lee University.

Kilty, K. T. 1984. "On the Origin and Interpretation of Self-Potential Anomalies," Geophysical Prospecting, Vol 32, No. 1, pp 51-62.

Koestler, J. P., Bulter, D. K., Cooper, S. S., and Llopis, J. L. 1984. "Geophysical Investigations in Support of Clearwater Dam Comprehensive Seepage Analysis," Miscellaneous Paper GL-84-3, US Army Engineer Waterways Experiment Station, Vicksburg, MS.

Lachaud, J. C. 1983. "Role of Geophysical Electrical Method Applied to Prospection of Ground Water in Fissured Media," L'Eau et l' Industrie, Vol 71, pp 37-40.

Llopis, J. L., and Butler, D. K. 1988. "Geophysical Invesitgation in Support of Beaver Dam Comprehensive Seepage Investigation," Technical Report GL-88-6, US Army Engineer Waterways Experiment Station, Vicksburg, MS.

MacMillan, K. J. 1980. "Hydrologic Study of the South Buffalo Creek Watershed," unpublished BS thesis, Washington and Lee University.

Marusiak, I. and Tezky, A. 1977. "Selective and Controlled Self-Potential Methods," Sb. Geol. Ved., Rada VG, No. 14, pp 119-137. (Russian, Eng. Summ.)

Markiewiez, R. D. and Randall, J. A. 1984. "The Use of Self-Potential Surveys in Geotechnical Investigations," Proceedings, 54th Society of Exploration Geophysicists Meeting, Atlanta, GA.

Meiser, P. 1962. "A Method for Quantitative Interpretation of Self-Potential Measurement," Geophysical Prospecting, Vol 10, pp 203-218.

Mitchel, J. K. 1976. Fundamentals of Soil Behavior, Wiley, New York.

Nayak, P. N. 1981. "Electromechanical Potential in Surveys for Sulphides," Geoexploration, Vol 18, No. 4, pp 311-320.

Nourbehecht, B. 1963. "Irreversible Thermodynamic Effects in Inhologeneous Media and Their Application in Geoelectric Problems," Ph.D. thesis, Massachusetts Institute of Technology, Cambridge, MA.

Ogilvy, A. A. 1967. "Studies of Underground Water Movement," Geological Survey of Canada, Report No. 26, pp 540-543.

Ogilvy, A. A., Ayed, M. A., and Bogoslovsky, V. A. 1969. "Geophysical Studies of Water Leakages from Reservoirs," Geophysical Prospecting, Vol 27, No. 1, pp 36-62.

Paul, M. K. 1965. "Direct Interpretation of SP Anomalies Caused by Inclined Sheets of Indefinite Horizontal Extension," Geophysics, Vol 30, pp 418-423.

Quinlan, J. F. and Ewers, R. O. 1986. "Practical Karst Hydrogeology with Emphasis on Groundwater Monitoring," Groundwater Monitoring Review, Winter.

Randall, J. A. 1983. "Natural Potential in the Search for Water," Geophysical Laboratory Publication, Guanajuato School of Mines, Mexico.

Rodriques, B. D. 1984. "A Self-Potential Investigation of a Coal Mine Fire," Proceedings, 54th Society of Exploration Geophysicists Meeting, Atlanta, GA.

Roy, A. 1968. "Bedrock Depth From Surface Potential Measurements," Geophysical Prospecting, Vol 16, pp 447-453.

Roy, A. and Chowdhyry, D. K. 1959. "Interpretation of SP Data for Tabular Bodies," Journal Science and Engineer Research, Vol 3, pp 35-54.

Sill, W. R. 1982. "Self-Potential Effects Due to Hydrothermal Convection-Velocity Crosscoupling," US DOE/ID/2079-68.

_____. 1983. "Self-Potential Modeling from Primary Flows," Geophysics, Vol 48, No. 1, pp 76-86.

Slifer, D. W. 1986. "Evaluation of Spontaneous Potential for Monitoring Groundwater Movement in Karst Terrain," unpublished MS thesis, Virginia Polytechnic Institute, Blackburg, VA.

Spencer, E. W. 1968. "Geology of the Natural Bridge Quadrangle, Virginia," Virginia Division of Mineral Resources, Report of Investigation, Vol 3, p 55.

Telford, W. F., Geldart, L. P., Sheriff, R. E., and Keys, D. A. 1976. Applied Geophysics, Cambridge University Press, New York.

Warriner, J. B. and Taylor, P. A. 1982. "Modeling of Electrokinesis," Miscellaneous Paper GL-82-13, US Army Engineer Waterways Experiment Station, Vicksburg, MS.

White, W. B. 1977. "Conceptual Models for Karst Aquifer-Revisited, Hydrologic Problems in Karst Regions," Western Kentucky University, Bowling Green, pp 76-187.

Williams, P. W. 1983. "The Role of the Subcutaneous Zone in Karst Hydrology," Journal Hydrology, Vol 61, pp 45-67.

Zohdy, A. A., Anderon, L. A., and Muffler, J. P. 1973. "Resistivity, Self-Potential, and Induced-Polarization Surveys of a Vapor Dominated Geothermal System," Geophysics, Vol 38, No. 6, pp 1130-1144.

Zohdy, A. A., Eaton, G. P., and Mabey, D. R. 1974. "Application of Surface Geophysics to Ground Water Investigations," Techniques of Water-Resources Investigations of the US Geological Survey, Chapter D1, US Geological Survey, Washington, DC.

Table 1

Data from ADC System for SP Electrode Monitoring Site, November 4-6, 1986 (Data used to construct Figure 28; SP Values in Millivolts for Electrodes Nos. 1-5)

Time	No. 1	No. 2	No. 3	No. 4	No. 5	Temp °C	Soil Moisture Relative Units (Digital)	
18.1397	118	-76	228	228	-169	13	242	
19.1397	121	-76	231	230	-167	13	242	
20.1397	117	-80	229	228	-170	13	241	
21.1397	120	-78	232	231	-167	13	241	
22.1397	122	-78	233	232	-167	13	241	
23.1397	122	-79	233	232	-166	13	241	Rain begins
.139722	120	-78	231	230	-167	13	241	
1.13972	118	-74	225	225	-165	15	241	
2.13972	91	-78	197	197	-184	14	252	SP becomes more negative
3.13972	94	-94	200	202	-189	14	251	
4.13972	94	-96	202	203	-193	14	250	
5.13972	97	-105	203	203	-196	14	249	
6.13972	99	-110	203	203	-201	13	248	
7.13972	104	-113	207	207	-203	13	246	
8.13972	106	-115	207	207	-207	13	244	
9.13972	107	-115	207	207	-210	13	242	
10.1397	107	-117	207	208	-212	12	241	
11.1397	108	-119	208	209	-213	12	240	
12.1397	108	-122	208	211	-214	13	239	
13.1397	107	-120	204	208	-217	13	239	
14.1397	96	-119	192	197	-225	12	240	
15.1397	111	-120	187	195	-221	12	241	
16.1397	97	-125	187	196	-220	12	240	
17.1397	94	-131	189	199	-220	12	240	
18.1397	96	-134	195	205	-218	12	239	
19.1397	101	-137	199	208	-217	12	238	Rain ends (1.2")
20.1397	101	-135	200	209	-220	12	238	
21.1397	98	-136	202	211	-224	12	237	
22.1397	99	-136	204	213	-225	12	236	
23.1397	98	-134	205	214	-225	12	236	
.139722	99	-135	207	216	-225	12	236	
1.13972	98	-134	209	218	-223	12	235	
2.13972	103	-130	215	223	-212	12	235	SP becomes more positive
3.13972	101	-132	215	223	-206	12	235	
4.13972	103	-130	216	224	-202	12	235	
5.13972	101	-131	218	226	-199	12	235	
6.13972	103	-130	220	228	-197	12	235	
7.13972	104	-129	221	228	-195	12	235	
8.13972	101	-129	222	229	-191	12	234	
9.13972	104	-123	222	229	-186	12	233	
10.1397	104	-117	221	228	-183	12	232	
11.1397	102	-117	220	226	-186	12	233	
12.1397	100	-117	220	226	-187	13	235	
13.1397	97	-118	216	222	-191	13	237	
14.1397	98	-117	219	225	-190	14	239	

Table 2

ADC Data of SP and Soil Temperature at Moore Sinkhole During Water Dump Test on October 4, 1986 (Data used to develop Figures 31 and 32)

	Electrode Number											
Time	No. 1	No. 3	No. 7	No. 12	No. 18	No. 20	No. 21	No. 22	No. 23	No. 25	No. 29	Temp(F)
moores STARTING AT: 86/10/04 12:56:42												
12:56:47	-278	-69	-17	-347	92	9	-196	-180	14	-102	-254	85
13:01:46	-278	-68	-17	-347	92	9	-197	-180	15	-101	-254	87
13:06:46	-278	-68	-17	-347	92	9	-197	-180	15	-101	-254	89
13:11:46	-279	-69	-16	-347	92	9	-198	-180	15	-101	-253	89
13:16:46	-278	-69	-17	-347	93	9	-197	-180	15	-101	-254	91
13:21:46	-279	-70	-17	-348	93	8	-197	-180	15	-101	-253	93
13:26:46	-279	-69	-17	-348	93	9	-197	-181	15	-101	-254	92
13:31:46	-278	-71	-18	-348	93	9	-198	-181	15	-101	-254	92
13:36:46	-278	-70	-16	-348	93	9	-197	-179	15	-101	-254	90
13:41:46	-279	-72	-18	-348	93	8	-197	-180	15	-101	-253	89
13:46:46	-279	-72	-17	-348	93	9	-198	-180	15	-101	-254	88
13:51:46	-279	-71	-17	-348	93	8	-197	-181	15	-102	-254	89
13:56:46	-278	-72	-17	-348	93	9	-197	-181	15	-102	-254	88
14:01:46	-279	-73	-17	-347	93	8	-196	-181	15	-101	-253	89
14:06:46	-278	-73	-18	-347	94	9	-197	-181	15	-101	-252	90
14:11:46	-278	-73	-18	-347	94	9	-196	-181	15	-101	-252	88
14:16:46	-278	-73	-17	-347	94	9	-197	-181	15	-102	-253	97
14:21:46	-280	-74	-18	-348	94	8	-197	-181	15	-103	-252	92
14:26:46	-280	-74	-17	-349	94	8	-197	-181	16	-102	-252	97
14:31:46	-280	-75	-18	-350	94	8	-197	-181	16	-102	-253	98
14:36:46	-280	-75	-17	-349	94	8	-197	-180	16	-102	-252	91
14:41:46	-280	-76	-18	-349	95	9	-196	-180	16	-101	-252	94
14:46:46	-279	-74	-16	-349	94	8	-196	-180	16	-102	-252	94
14:51:46	-279	-75	-17	-349	94	8	-197	-180	16	-102	-252	95
14:56:46	-280	-77	-18	-349	95	8	-197	-181	16	-102	-252	94
15:01:46	-280	-77	-18	-349	95	8	-196	-181	15	-102	-252	92
15:06:46	-279	-77	-17	-348	95	8	-195	-181	15	-103	-253	91
15:11:46	-279	-78	-18	-348	94	8	-195	-180	15	-102	-253	90

Table 3

SP Values (millivolts) at the Spring Branch Sinking Stream Site

(Data collected by voltmeter between July 1986 and April 1987)

SPRING BRANCH SITE

DATE	7/22	7/24	7/27	7/29	8/3	8/9	8/19	8/28	9/5	9/17	9/23	10/2	10/10	10/17	11/2	11/6	11/29	12/24	12/25	1/20	3/2	4/30
TIME	1000	1830	1100	1800	0900	1530	1630	1300	1630	1700	1700	1800	1400	1700								
SOIL TEMP (C)	16	33	25	33	24	26	22	21	18	14	19	21	17	12	11	11	8	4	0	1	2	12
FLOW (cfs)						.099	.324	.201	.282	.132	.132	.072	.072	.132	.24	.24	.324	3.98	1.57	.75	3.92	
ELECTRODE #																						
1	98	74	67	80	80	65	50	190	201	303	381	343										
2	22	22	25	39	28	-3	4	169	164	271	324	271										
3	41	19	20	21	-7	-4	0	146	161	209	259	185	109	163	38	83	280	270	305	386	450	489
4	22	10	9	20	-13	25	8	35	91	89	95	-98	-168	-121	-74	38	194	110	151	215	300	369
4a					-56	-21	-21	134	163	225	281	207	160	188	58	82	271	240	279	351	417	455
5	-34	-26	-30	-52	-172	-58	-93	73	116	86	108	-16	-114	-99	-15	10	173	158	188	262	314	362
5a					-60	2	-5	153	191	248	303	231	193	193	89	138	245	215	237	348	413	485
6	-252	-256	-273	-309	-385	-288	-338	-145	-105	-98	-55	-182	-307	-307	-192	-177	-35	0	15	60	121	155
7	-129	-125	-140	-156	-228	-150	-163	-6	59	88	137	50	-10	-10	-32	22	151	164	70	226	307	299
8	-92	-93	-113	-125	-191	-125	-149	-3	41	58	101	6	-75	-75	-117	-50	89	102	99	144	228	242
9	-1	-4	10	19	-12	24	-6	163	185	230	268	212										
10	51	42	32	48	32	40	19	163	187	257	317	247										
11	-55	-43	-56	-65	-114	-42	-53	99	141	154	207	122										
12	0	-2	0	4	-31	-1	-27	126	158	210	277	207										
13	-101	-92	-97	-87	-102	-34	-41	104	139	69	104	-41	-22	114	61	122	217	165	205	271	327	385
14	-148	-148	-171	-198	-284	-230	-269	-114	-34	-94	-73	-194	-268	-233	-216	-58	68	65	80	143	235	314
15	-207	-197	-207	-235	-311	-210	-262	-61	17	6	48	-99	-196	-163	-109	-57	106	108	110	176	211	270
16	-375	-360	-380	-424	-465	-361	-355	-120	-7	-110	-73	-134	-114	15	-91	71	204	161	198	274	321	355
17	-244	-246	-276	-309	-405	-333	-349	-155	-46	-150	-119	-222	-304	-267	-298	-85	5	54	67	83	170	153
18	-208	-238	-291	-314	-397	-359	-377	-248	-179	-183	-153	-259	-333	-292	-351	-201	-96	-5	-48	22	45	-19
19	-137	-121	-141	-163	-272	-225	-249	-115	-57	-122	-84	-182										
20	-73	-71	-86	-99	-158	-103	-199	23	68	72	112	-83										
21	-186	-180	-203	-215	-292	-171	-209	2	90	96	135	0										
22	-82	-85	-106	-133	-202	-134	-150	8	66	60	92	-60										
23	-204	-190	-212	-234	-342	-243	-265	-52	31	12	43	-95	-207	-160	-150	-7	130	83	125	249	342	345
24	-166	-157	-184	-222	-328	-230	-290	-92	-12	-56	-38	-199	-265	-218	-207	-116	29	51	41	92	155	205
25	-339	-324	-337	-378	-458	-398	-379	-207	-99	-146	-122	-235	-318	-269	-289	-147	-13	44	40	85	155	164
26					-308	-219	-299	-28	32	7	15	-140	-237	-199	-196	-35	98	95	127	172	237	246
27					-375	-313	-374	-67	-13	-37	-39	-204	-250	-219	-265	-174	-55	-65	-50	16	68	75
28					-419	-357	-401	-190	-77	-137	-142	-265	-326	-274	-260	-128	-20	-5	5	43	112	131
29					-194	-147	-150	-16	26	34	74	-15	-73	-34	-76	-64	101	111	150	263	333	310
30					-226	-98	-88	78	118	90	113	8	-74	-5	37	6161	164	174	205	272	321	373
31					11	-5	-21	102	121	250	320	278	249	237	45	49	251	265	298	371	424	495
32													33	68	50	91	253	-65	-15	139	312	473
33													-45	-13	-15	-8	138	125	133	211	267	352
34													-33	-12	-14	2	115	75	105	166	218	290
35													-24	-3	-22	-13	75	38	63	89	128	190
36													33	56	9	62	160	118	148	198	256	296
37													-94	-77	-70	-53	25	35	44	68	110	120
38													-226	-219	-118	-111	-29	-33	-42	23	73	117
39													18	59	33	46	161	130	153	213	270	320
40													-65	-24	-19	0	127	102	124	177	238	240
41'													35	75	47	83	228	181	208	282	329	375

Table 4

SP Values (millivolts) at the Ford Sinking Stream Site for July 1986 to May 1987

DATE	7/21	7/23	7/25	7/28	7/30	8/5	8/7	8/21	8/25	8/27	8/30	9/2	9/8	9/19	9/24	10/2	10/8	10/14	10/24	10/27	11/6	12/15	1/14	1/19	3/4	5/7
TIME	1500	1900	0800	1630	1520	0940	1530	1630	1500	1400	1200	1300	1300	1300	1200	1300	1300	1230	1500							
SOIL TEMP			25			20	24	19	24	22	14	15	16	16	18	21	16	17	17	14	12	3	3	3	3	8
FLOW (cfs)							.015	.023	.035	.035	.039	.046	.046	.053	.088	.07	.07	.07	.088	.088	.088	.107	.107	.15	.2	
ELECTRODE #																										
1	-150	-80	-52	-111	-71	-21	-22	-160	-72	-64	-71	-87	-102	-53	-64	-57	-28	-46	-3	-166	-245	242	272	223	287	304
2	43	42	58	40	-67	42	53	3	39	48	36	-10	-23	-11	-18	-11	1	-16	25	-38	-50	408	419	359	469	444
3	-16	-23	7	9	37	84	92	12	59	73	59	-2	-4	8	8	15	33	-6	47	-17	-88	91	95	12	73	91
4	-186	-164	-101	-109	-55	72	76	-133	0	20	43	-73	-50	5	2	2	24	-125	24	-59	-57	374	370	322	414	418
5	-284	-275	-284	-269	-265	-261	-240	-156	-154	-97	25	-4	-6	-15	-19	-20	-5	-4	23	-25	-174	46	30	16	83	93
6	106	94	107	102	84	145	132	15	60	77	65	11	-2	17	13	22	35	7	51	-30	-38	320	360	337	457	456
7	-301	-310	-309	368	-344	-272	-240	-270	-295	-278	-279	-183	-297	-230	-236	-265	-181	-37	41	-21	-39	70	120	84	164	187
8	-104	-102	-100	-118	-230	-142	-94	-167	-165	-151	-130	-72	-200	-46	-20	-10	8	-8	38	-70	-225	115	115	164	136	94
9	-114	-125	-135	-149	-227	-277	-270	-255	-248	-246	-275	-257	-266	-322	-323	-330	-284	-200	-206	-179	-255	140	156	126	184	312
10	25	47	41	11	-154	-217	-149	-113	-43	-18	1	-60	-121	-65	-59	3	12	-9	14	-100	-151	225	212	209	294	414
11	-189	-172	-160	-182	-196	-101	-57	28	66	73	63	13	4	-1	-2	2	26	23	53	-5	-141	32	14	14	94	72
12	-97	-111	-96	46	77	147	141	12	61	76	71	5	-2	15	13	25	53	13	71	-10	-96	288	287	240	274	220
13	87	93	83	82	75	103	88	8	47	42	34	-10	-14	-39	-61	-75	-62	-33	-6	-39	-67	332	375	331	410	452

Table 5

SP Values (millivolts) at McHenry Sinkhole A from July 1986 to April 1987

DATE	7/22	7/24	7/27	7/29	8/3	8/6	8/19	9/17	9/23	10/9	10/14	10/15	10/24	10/26	11/2	11/6	11/27	12/19	12/25	1/14	3/5	4/29
TIME	0900	1900	1000	1830	0800	1930	0600	1820	1800	1700	0930	1500	0930	1700								
SOIL TEMP (C)	15	32	26	29	24	24	21	22	22	17	16	14	14	11	13	11	8	2	11	1	2	9
ELECTRODE #																						
1	25	9	38	4	18	16	16	7	4	-2	43	44	10	26	18	11	-109	-343	-248	-253	-209	-274
2	29	11	35	-2	7	32	10	-54	-63	-82	-5	-8	-46	9	8	10	-5	-167	-105	-120	-74	-84
3	50	28	50	16	33	35	24	23	21	5	41	49	13	23	14	16	13	-118	-91	-139	-166	-138
4	48	28	50	15	36	69	27	17	20	19	58	58	23	28	26	19	-130	-329	-306	-386	-426	-401
5	70	48	67	35	54	62	48	27	29	21	60	67	21	41	34	22	-33	-81	-46	-124	-177	-214
6	-177	-197	-201	-269	-313	-215	-281	-233	-317	-417	-323	-370	-431	-293	-326	-354	-405	-389	-307	-397	-395	-325
7	-90	-94	-80	-128	-150	-85	-138	-131	-161	-227	-141	-182	-233	-110	-112	-31	-62	-109	-75	-162	-272	-249
8	-106	-96	-88	-135	-141	-43	-14	-59	-82	-342	-224	-287	-350	-128	-141	-85	-347	-417	-352	-433	-450	-431
9	22	17	39	-2	5	41	26	2	-2	-38	20	13	-28	15	16	11	-102	-229	-228	-273	-299	-297
10	-160	-143	149	-207	-235	-108	-135	-325	-332	-385	-310	-338	-388	-178	-282	-229	-423	-444	-375	-451	-472	-465
11	20	8	32	-6	-1	19	12	-1	-4	-37	13	13	-30	-1	6	0	-254	-322	-242	-344	-396	-396
12	15	3	30	0	18	32	16	8	7	-16	33	35	-9	19	15	12	-259	-426	-349	-430	-446	-401
13	26	13	38	4	27	41	37	19	22	13	38	53	15	37	26	20	-120	-203	-167	-210	-241	-286
14	17	6	25	-7	18	21	15	0	0	-8	25	27	0	17	14	10	-55	-100	-66	-125	-176	-203
15	-5	-10	9	-29	-53	6	-6	-16	-25	-85	-4	-7	-72	-1	2	-108	-303	-316	-220	-292	-262	-189
16	15	1	23	-4	20	14	17	6	6	-1	29	31	6	19	13	2	-172	-353	278	-377	-355	-362
17	7	-5	15	-19	-11	-29	-48	-170	-260	-50	-10	-12	-46	-76	-70	-80	-50	2	48	9	11	14
18	38	12	42	10	44	43	20	24	32	35	59	76	30	38	46	25	-240	-304	-252	-313	-256	-186
19	-112	-84	-65	-125	-212	-9	-1	-8	-6	-10	1	7	-5	0	10	4	1	3	43	-1	-138	-115
20	66	38	57	25	60	79	36	3	6	11	38	48	5	22	15	1	-239	-420	-356	-437	-451	-437
21	52	36	55	24	38	84	40	9	12	5	57	57	13	56	43	27	0	-58	-38	-115	-213	-244
22	70	38	56	29	45	72	41	-184	-230	-342	-246	-292	-363	-189	-236	-371	-440	-413	-344	-405	-422	-330
23	48	22	50	17	29	50	36	-211	-226	-258	-81	-70	-108	-28	-18	-33	-17	-3	35	0	9	29
24	3	4	22	-9	-13	13	5	-137	-158	-240	-143	-176	-214	-102	-78	-144	-366	-329	-262	-341	-345	-244
25	-13	-10	13	-23	-64	-6	-19	-10	-12	-58	-1	-4	-46	7	12	10	-142	-372	-308	-414	-452	-474
26	15	2	23	-10	-10	17	3	-413	-418	-355	-161	-183	-254	-130	-269	-334	-370	-376	-286	-388	-392	-363
27	-17	7	14	-14	-4	29	21	-48	4	-45	0	-5	-34	-38	-50	-53	-96	-117	-71	-118	-165	-95
28	34	14	35	0	30	48	24	8	10	-2	31	40	4	15	11	6	-245	-347	-302	-378	-434	-481
29	-9	-9	12	-19	-6	11	11	-519	-528	-214	-55	-41	-24	-8	5	-118	-402	-409	-365	-416	-383	-277
30	4	3	21	-10	4	16	9	-44	-24	-26	-2	-2	-21	0	9	10	-53	-112	-65	-223	-312	-390
31	-60	-174	-301	-353	-233	272	-87	-204	-29	-20	-10	-2	-32	-8	-8	-34	-207	-332	-249	-324	-333	-325
32	-342	-404	-390	-489	-466	-287	-294	-460	-435	-192	-27	-18	-34	-13	-68	-235	-354	-400	-249	-437	-490	-447

Table 6

SP Values (millivolts) at the McHenry Sinkhole B for July 1986 to April 1987

	McHenry Sinkhole B														
DATE	7/22	7/24	7/27	7/29	8/3	8/6	8/19	9/17	9/23	10/15	11/30	12/25	1/13	3/5	4/30
TIME	0900	1915	1030	1830	0830	2000	1800	1830	1800	1600					
SOIL TEMP (C)	15	27	23	27	23	22	21	18	21	16	7	4	1	1	15
ELECTRODE #															
1	-50	-4	18	-9	10	5	4	0	-9	-5	18	59	23	17	26
2	-336	-403	-397	-456	-305	-143	-253	-176	-114	-29	-273	-189	-250	-230	-152
3	1	0	25	-11	6	10	2	7	-3	22	-203	-168	-240	-248	-254
4	17	11	33	-3	12	29	12	4	-1	11	-84	-56	-111	-112	-66
5	-17	-22	0	-33	-20	-50	-21	-23	-34	-18	-79	-53	-58	-53	-39
6	-1	2	22	-10	4	21	10	2	-8	1	18	63	19	21	27
7	0	3	28	-4	14	22	17	-92	-134	-58	-3	7	7	10	13
8	3	8	33	4	27	22	20	-115	-120	28	13	56	15	16	28
9	0	0	23	-15	6	16	4	12	5	-6	26	72	29	29	38
10	0	-4	15	-9	8	5	2	0	-11	-10	12	65	17	16	19
11	-306	-286	-265	-241	-311	-15	-240	-272	-134	-11	-19	-24	-178	-121	-84
13	7	8	29	-5	8	20	10	16	7	8	28	64	28	23	34
14	-21	-20	5	-31	-15	-6	-2	3	-5	-13	-37	-72	-126	-128	-95
15	-218	-236	-305	-380	-367	-217	-287	-318	-427	-417	-446	-421	-495	-522	-498
16	-98	-38	10	-44	-20	13	9	7	0	12	23	72	26	23	24
17	16	12	34	-5	7	32	14	2	-6	10	14	56	15	10	9
18	8	6	26	-5	20	13	8	-1	-12	5	-1	-11	-62	-116	-116
19	18	5	29	-5	16	17	15	2	-6	15	15	57	17	12	24
20	-196	-150	-115	-126	-146	-42	8	-7	-19	-10	8	48	10	4	4
21	12	13	32	-5	5	-7	4	-401	-223	7	9	50	5	-220	-363
22	0	6	29	0	18	7	12	-8	-20	-20	13	59	9	14	-5
23	3	-2	208	-8	19	-49	-3	4	0	10	19	69	23	24	32
24	-44	-16	8	-14	15	18	14	25	18	43	-278	-343	-397	-432	-274

Table 7

SP Values (in millivolts) for 12 Electrode Array at Cave Sink

for September to December 1986

DATE	9/12	9/18	9/27	10/3	10/9	10/14	10/15	10/24	10/26	11/2	11/6	11/27	12/10
TIME	1500	1400	1300	1500	1400	0800	1500	0900	1500	1400	0800		
SOIL TEMP (C)	16	13	18	19	16	16	13	13		13	11	8	8
FLOW (cfs)					.03	.05	.11	.32	.37	.25	.25	.15	.15
ELECTRODE #													
1	-242	-182	-54	0	45	128	185	276	184	-54	-188	-240	-231
2	-169	-80	187	261	244	235	282	304	190	162	-148	-207	-200
3	-351	-304	-289	-286	-231	171	234	292	202	173	-67	-305	-306
4	111	176	215	220	178	160	200	223	108	74	91	151	143
5	180	253	291	298	262	250	289	316	111	95	94	210	235
6	215	342	395	402	380	302	363	420	231	173	161	210	241
7	249	355	398	408	381	332	390	424	263	210	206	271	293
8	180	284	326	336	307	259	297	343	216	168	173	267	301
9	-249	-197	178	275	275	262	311	322	213	167	-110	-174	-161
10	158	265	306	302	265	230	272	295	162	136	115	165	187
11	114	220	260	265	229	217	266	279	192	162	167	183	202
12	-358	-277	-185	-25	-62	42	-34	-28	-77	-210	-170	-178	-151

Table 8

SP Values (Millivolts) at Three Rows of Electrodes Over Cave Stream for August 1986 to March 1987

	DATE	8/26	8/28	8/31	9/7	9/12	9/18	9/27	10/3	10/9	10/14	10/15	10/24	10/26	10/28	11/6	11/27	12/21	12/25	1/13	2/5	3/3
	TIME	1200	1500	1500	1500	1500	1400		1500	1500	0830	1500	0900	1500	1000	0800						
	SOIL TEMP	16	17	14	15	17	14	17	19	17	14	13	13	12	12	11	9	3	4	3	1	6
	FLOW (CFS)										.05	.11	.32	.37	.32	.23	.15	.17	.89	.25	.47	1.11
	ELECTRODE #																					
ROW 1	0															-51	-128	-135	-122	-134	-154	-170
	1	-161	-149	-138	-126	-84	-71	-63	-60	-63	-56	-51	-42	-25	-15	-3	17	65	48	67	94	100
	2	-204	-226	-251	-224	-264	-323	-376	-402	-422	-389	-404	-417	-278	-299	-325	-341	-287	-280	-257	-255	-251
	3	-336	-317	-299	-348	-302	-229	-322	-334	-343	-321	-338	-331	-259	-178	-349	-450	-409	-422	-388	-406	-406
	4	-198	-120	-90	-72	-95	-101	-109	-122	-141	-132	-133	-138	-88	-70	-198	-336	-275	-270	-249	-255	-268
	5	-94	-117	-138	-104	-131	-146	-151	-165	-184	-158	-168	-175	-115	-111	-180	-335	-282	-292	-234	-264	-257
	6	-155	-132	-133	-152	-106	-76	-90	-95	-106	-88	-88	-92	-46	-40	-95	-250	-173	-208	-153	-149	-168
	C	-190	-145	-119	-137	-121	-79	-76	-77	-93	-83	-86	-97	-63	-59	-133	-273	-231	-262	-241	-235	-232
	7	-71	-87	-104	-75	-105	-113	-114	-125	-144	-149	-136	-129	-163	-161	-188	-239	-214	-230	-204	-215	-207
	8	-112	-139	-171	-139	-169	-177	-145	-163	-187	-180	-181	-191	-119	-121	-228	-314	-276	-283	-259	-241	-248
	9	-86	-92	-61	-39	-44	-48	-39	-46	-62	-50	-55	-64	-35	-28	-128	-331	-279	-296	-236	-277	-276
	10																					
ROW 2	0															-39	-99	-68	-77	-42	-33	-21
	1	-234	-267	-233	-339	-242	-228	-185	-234	-268	-201	-226	-256	-279	-286	-380	-381	-295	-345	-292	-288	-286
	2	-162	-218	-235	-184	-195	-229	-240	-240	-240	-154	-163	-143	-152	-146	-239	-327	-281	-259	-232	-242	-228
	3	-174	-231	-245	-220	-266	-295	-244	-284	-298	-272	-275	-269	-149	-167	-179	-341	-305	-293	-275	-283	-297
	4	-209	-214	-212	-145	-186	-148	-107	-123	-140	-125	-137	-132	-114	-123	-218	-338	-271	-282	-244	-252	-254
	5	-86	-124	-162	-86	-125	-166	-186	-202	-240	-188	-217	-241	-105	-93	-161	-253	-243	-231	-246	-238	-237
	6	-275	-302	-285	-215	-227	-240	-222	-231	-217	-184	-188	-184	-175	-211	-330	-328	-280	-288	-275	-296	-319
	C	-108	-150	-180	-137	-132	-122	-129	-141	-162	-145	-151	-158	-167	-186	-184	-260	-238	-264	-226	-218	-204
	7	-72	-91	-90	-212	-103	-87	-84	-94	-107	-102	-99	-94	-120	-120	-190	-290	-163	-244	-128	-227	-212
	8	-293	-327	-320	-351	-323	-321	-267	-298	-298	-281	-300	-323	-292	-321	-407	-449	-422	-391	-404	-372	-300
	9	-333	-329	-292	-423	-311	-276	-276	-291	-327	-308	-329	-335	-342	-352	-403	-441	-384	-380	-353	-372	-335
	10															-220	-373	-330	-380	-305	-320	-336
ROW 3	0															-113	-256	-230	-240	-213	-204	-217
	1	-242	-266	-267	-251	-270	-250	-63	-60	-320	-296	-320	-317	-407	-306	-407	-406	-351	-348	-340	-353	-340
	2	-103	-129	-144	-83	-125	-82	-376	-402	-107	-100	-102	-106	-112	-82	-149	-250	-231	-238	-221	-202	-220
	3	-103	-103	-106	-59	-90	-100	-322	-334	-134	-125	-129	-136	-78	-79	-108	-164	-120	-130	-114	-104	-127
	4	-254	-254	-230	-270	-232	-106	-109	-122	-80	-92	-87	-79	-140	-151	-204	-322	-257	-268	-241	-340	-230
	5	-208	-171	-142	-210	-156	-128	-151	-165	-127	-127	-131	-135	-121	-124	-300	-330	-262	-305	-228	-281	-227
	6	-161	-154	-137	-118	-149	-99	-90	-95	-139	-129	-133	-142	-49	-49	-96	-215	-218	-213	-203	-210	-196
	C	-160	-105	-120	-87	-115	-96	-76	-77	-54	-62	-53	-50	-36	-35	-101	-250	-235	-242	-232	-233	-233
	7	-209	-183	-165	-222	-171	-168	-114	-125	-197	-170	-179	-185	-260	-233	-363	-373	-284	-315	-258	-270	-280
	8	-389	-357	-322	-397	-355	-334	-145	-163	-370	-334	-364	-374	-408	-398	-452	-484	-465	-448	-435	-434	-381
	9	-41	-48	-52	-70	-41	-31	-39	-46	-40	-42	-41	-41	-44	-39	-35	-214	-249	-250	-236	-205	-213
	10																					

Table 9

SP Values (millivolts) for the 32 Electrode Array at Cave Sink

(Data collected by voltmeter between December 1986 and April 1987)

DATE	12/21	12/25	1/13	2/5	3/3	4/28
SOIL TEMP (C)	2	14	4	2	6	9
FLOW (cfs)	.17	.86	.25	.5	.9	
ELECTRODE #						
1	-15	66	-5	30	46	-2
2	-200	-168	-289	-292	-294	-277
3	-122	-155	-123	-152	-174	-182
4	-175	-139	-235	-265	-247	-318
5	-156	-128	-233	-230	-240	-266
6	-325	-302	-338	-313	-268	-297
7	55	100	50	57	50	219
8	-265	-181	-250	-266	-252	-298
9	118	201	127	90	63	99
10	197	255	290	321	336	341
11	-74	-14	-85	-82	-133	-177
12	170	177	103	114	112	49
13	217	234	177	160	185	169
14	204	229	157	161	189	204
15	121	121	27	38	41	36
16	-70	-60	-99	-98	-113	-97
17	110	137	100	130	122	100
18	-10	-17	-86	-44	-45	-120
19	-300	-277	-303	-294	-292	-274
20	-240	-166	-183	-194	-167	-188
21	-280	-247	-321	-304	-259	-264
22	63	118	15	44	94	328
23	81	134	171	256	245	297
24	-32	-11	-23	-42	-10	-46
25	173	203	199	217	233	229
26	90	149	175	200	203	214
27	35	84	50	15	35	21
28	150	191	216	230	266	298
29	275	320	311	324	337	337
30	226	254	258	276	284	276
31	194	149	7	62	68	62
32	198	198	163	91	85	68

Table 10

SP Values in Millivolts for Long-Term Monitoring

Array of Electrodes

		ELECTRODES					SOIL TEMP	RAINFALL
DATE	TIME	#1	#2	#3	#4	#5	6"	
1 AUG	1100	251	121	233	187	214	23	
	1200	269	120	269	210	192	24	
	1300	290	129	302	235	172	24	
	1400	304	140	323	252	171	24	
	1500	313	150	338	264	167	24	
	1700	327	167	358	284	169	24	
	1800	331	171	368	295	164	25	
	1900	334	176	376	300	162	24	
	2000	334	184	378	302	159	24	
	2300	314	182	375	292	127	23	
2 AUG	0700	316	198	399	314	101	21	
	0800	328	209	408	328	108	21	
	1000	343	224	433	349	115	23	
	1200	349	233	442	358	117	24	
	1400	355	243	444	368	120	24	
	1600	364	260	454	383	124	24	
	1800	367	267	456	389	122	24	
	2000	369	273	460	393	121	24	
3 AUG	0700	341	263	446	386	85	21	
	0900	340	262	448	387	85	22	
	1100	353	275	464	404	92	23	
	1300	361	285	471	416	102	24	
	1500	365	287	472	419	101	25	
	1700	366	292	478	422	102	25	
	1900	367	293	457	424	100	25	
	2100	343	280	446	402	82	23	
4 AUG	0600	320	259	436	391	49	21	
	0800	337	272	457	411	62	21	
	1000	348	280	470	425	74	22	
	1500	358	289	473	435	81	23	
	1700	359	289	473	437	80	23	
	1900	358	289	474	436	78	23	
	2100	352	288	465	433	73	23	
5 AUG	0600	324	264	447	415	43	22	
	0800	333	271	457	426	52	22	
	1700	356	290	480	450	72	23	
	2200	345	287	466	442	66	23	
6 AUG	0600	326	269	450	432	41	22	
	1700	60	55	119	127	4	23	.8" @1500
	1900	65	61	115	133	-6	23	
	2100	66	50	112	140	-20	22	
	2300	67	69	112	145	-25	22	
7 AUG	0600	66	72	119	156	-26	21	
	0800	65	71	120	155	-27	21	
	2000	74	80	147	164	-14	23	
8 AUG	0700	66	76	163	171	-31	23	
	1000	67	77	166	173	-29	22	
	1300	69	78	168	174	-24	23	
	1800	73	82	173	179	-16	23	

Table 11

SP Values in Millivolts for Long-Term Monitoring

Array of Electrodes

DATE	TIME	ELECTRODES #1	#2	#3	#4	#5	SOIL TEMP 6"	RAINFALL
9 AUG	0800	67	75	177	182	-40	21	
	1000	69	75	179	184	-35	21	
	1200	77	83	188	192	-20	23	
	2000	82	88	194	198	-19	24	
10 AUG	0800	81	88	202	205	-33	22	
	1300	91	96	211	214	-12	25	
	2000	93	98	211	215	-17	24	0.1"
	1900	102	109	230	233	-14	24	
12 AUG	0800	104	112	239	241	-23	22	
	1900	128	136	265	268	1	23	
13 AUG	0700	122	132	263	266	-16	21	
	1900	147	157	291	293	7	22	
14 AUG	0800	143	154	291	292	-3	21	
18 AUG	1600	141	166	276	289	4	23	.5"(18 AUG)
20 AUG	1500	-34	-41	70	58	-263	21	.6"(19 AUG)
	1800	-18	-41	63	42	-260	21	1.1"(20 AUG)
	2000	-12	-47	65	44	-257	21	.4"
21 AUG	0800	30	-84	66	8	-262	21	.2"
	1800	51	-96	82	-2	-254	22	
22 AUG	0800	77	-132	87	-43	-259	21	
	1800	85	-121	98	-36	-242	24	
23 AUG	0800	79	-132	114	-32	-210	21	
	1800	81	-109	118	-8	-193	25	
24 AUG	0900	75	-120	126	25	-167	19	
	1800	83	-100	134	43	-171	22	
25 AUG	0700	67	-123	135	61	-156	21	
	1800	80	-85	139	93	-142	24	
26 AUG	0800	63	-109	140	100	-131	20	
	1800	75	-81	144	114	-129	23	
27 AUG	0700	65	-92	150	120	-123	22	
	1900	66	-65	149	127	-109	24	
28 AUG	0800	60	-57	150	131	-98	20	.1" @0600
	1800	71	-31	154	141	-103	19	
29 AUG	0800	59	-16	157	143	-97	13	
	1800	79	18	160	153	-78	17	
30 AUG	0800	64	22	159	150	-87	13	
	1800	79	39	160	157	-73	17	
31 AUG	0800	67	36	159	153	-76	15	
	2000	75	45	159	157	-66	18	
1 SEP	0800	68	44	159	155	-77	17	.2"
	1200	68	43	157	154	-74	18	
	1600	69	44	156	153	-60	18	
	1800	70	44	155	153	-67	17	.1"
2 SEP	0800	61	38	144	147	-167	17	.4"
	1800	78	33	156	155	-202	18	

Table 12

SP Values in Millivolts for Long-Term Monitoring

Array of Electrodes

		ELECTRODES					SOIL TEMP	RAINFALL
DATE	TIME	#1	#2	#3	#4	#5	6"	
3 SEP	0800	108	34	180	176	-205	18	.2"
	1800	130	26	197	191	-204	18	
4 SEP	0700	133	11	202	197	-208	18	.1"
	1800	146	0	213	206	-208	19	
5 SEP	0800	149	-49	217	210	-212	18	.2"
	2100	164	-78	231	219	-178	19	
6 SEP	0900	167	-87	238	228	-198	18	
	2000	172	-77	238	229	-182	19	
7 SEP	0800	158	-85	230	228	-179	17	
	1800	161	-65	228	227	-150	19	
8 SEP	0800	157	-30	230	232	-133	18	
	1800	164	-3	230	235	-114	18	
9 SEP	0800	146	-26	223	229	-105	16	
	1900	147	1	217	225	-101	17	
10 SEP	0700	143	1	222	229	-92	16	
	1800	142	27	220	229	-76	18	
11 SEP	0800	129	21	222	230	-76	18	
	1800	134	39	221	229	-71	19	
12 SEP	0800	126	44	222	230	-75	19	
	1800	131	57	223	231	-76	19	
13 SEP	0900	119	63	222	230	-64	18	
	1800	127	76	220	228	-51	19	
14 SEP	0800	115	78	221	228	-61	16	
	1700	127	88	221	230	-45	18	
15 SEP	0700	113	82	216	224	-61	17	
	1800	119	89	217	226	-52	19	
16 SEP	0800	114	86	217	225	-59	18	
	1800	119	91	216	225	-41	19	
17 SEP	0700	110	87	217	225	-60	15	
18 SEP	0800	118	91	221	231	-51	15	
	1800	126	97	222	232	-34	17	
19 SEP	0800	120	92	221	229	-50	17	
	1900	123	92	218	227	-44	18	
20 SEP	0900	123	93	222	230	-52	17	
21 SEP	0800	121	92	221	230	-61	17	
22 SEP	0700	127	98	225	234	-59	18	
23 SEP	0800	131	100	228	239	-62	18	
	2000	139	106	234	234	-54	20	
24 SEP	0700	139	108	239	238	-58	19	
	1900	121	87	217	215	-76	20	
25 SEP	1900	126	89	218	216	-76	21	
26 SEP	2000	127	88	218	217	-78	21	
27 SEP	1400	129	90	221	222	-80	21	
28 SEP	1400	134	90	225	225	-80	21	
30 SEP	0800	126	88	226	231	-114	19	
1 OCT	1100	141	97	236	242	-105	21	
2 OCT	1700	145	94	233	239	-109	21	
3 OCT	1200	144	94	236	243	-112	19	
6 OCT	0800	139	87	235	242	-128	18	
7 OCT	0800	134	85	233	243	-129	16	
8 OCT	0900	132	88	234	247	-129	18	
	1800	147	95	241	253	-110	18	

Table 13

Record of Precipitation from Rain Gage at Long-Term SP Electrode Monitoring Station

DATE	INCHES	NOTES
7-21-86	.5	
7-22-86	.1	
7-23-86	.4	
7-26-86	.25	
8-06-86	.8	
8-17-86	.5	
8-19-86	.6	
8-20-86	1.1	
8-21-86	.2	
8-28-86	.1	
9-01-86	.2	
9-02-86	.5	
9-03-86	.2	
9-04-86	.1	
9-05-86	.2	
10-13-86	.25	
10-14-86	.25	
10-25-86	1.35	
11-01-86	.5	
11-05-86	1.2	
11-07-86	.4	
11-11-86	.1	
11-18-86	.25	
11-20-86	.32	
11-26-86	.8	
12-02-86	1.5	
12-09-86	.3	
12-11-86	.9	
12-18-86	.4	
12-24-86	2.4	
01-01-87	.4	as snow
01-15-87	.15	
01-19-87	1.5	
01-30-87	[illegible]	snow melt
01-31-87	1	snow melt
02-12-87	.1	
02-28-87	2	
03-08-87	.45	
03-16-87	.5	as snow
03-19-87	.4	
03-27-87	.3	
03-30-87	1.2	
03-31-87	.6	
04-03-87	.5	as snow
04-15-87	2.5	
04-16-87	2.9	
04-17-87	1.4	
04-24-87	3.6	
05-04-87	1.1	

Table 14

Record of SP, Soil Temperature, Soil Moisture, and Standard Deviation at Long-Term Monitoring Site for October to November 1986 (Data reduced to 24-hr average from ADC record)

Date	#1 (sp)	#2 (sp)	#3 (sp)	#4 (sp)	#5 (sp)	Soil Temp	Soil Mois	#1 (std)	#2 (std)	#3 (std)	#4 (std)	#5 (std)	ST (std)	SM (std)
10/8	142	93	238	251	-116			6	3	3	3	6		
10/9	139	94	241	253	-114			6	3	4	4	7		
10/10	139	97	246	257	-111	16		5	4	4	4	5	1	
10/11	144	103	253	266	-103	14		6	5	5	6	6	1	
10/12	154	113	266	278	-88	15		6	5	6	6	6	1	
10/13	146	115	256	273	-71	16		6	4	12	7	6	1	
10/14	133	107	234	257	-65	17		4	3	2	3	6	1	
10/15	135	108	244	265	-75	14	305	6	5	5	5	5	1	42
10/16	145	117	260	281	-68	12	141	8	6	6	6	7	1	78
10/17	150	122	269	291	-61	12	74	10	8	6	8	9	1	24
10/20	123	95	255	278	-85	12	386	3	4	6	5	5	1	8
10/21	144	115	280	304	-63	10	298	13	10	10	11	12	2	32
10/22	156	127	294	315	-48	13	233	10	8	8	10	11	2	11
10/23	159	131	303	319	-45	14	185	12	9	9	10	11	2	12
10/24	159	134	315	321	-44	14	141	10	8	8	9	9	1	10
10/25	129	114	285	288	-54	16	166	20	14	27	24	6	1	55
10/26	57	-1	168	173	-170	13	229	8	32	17	21	36	1	6
10/27	67	-24	1[illegible]	166	-196	14	227	3	2	2	2	3	1	4
10/28	73	-25	177	174	-189	14	230	2	3	2	2	3	1	2
10/29	76	-20	187	185	-178	12	221	3	5	2	2	5	1	3
10/30	77	-11	191	190	-166	12	216	2	3	2	1	3	1	3
11/1	78	-4	197	197	-150	12	205	4	2	8	7	5	0	8
11/2	83	-41	189	190	-176	13	231	11	18	10	10	6	1	5
11/3	104	-77	215	215	-176	14	235	3	2	4	4	2	2	1
11/4	117	-76	230	229	-168	12	236	3	5	2	2	2	1	4
11/5	102	-115	203	207	-208	13	242	7	19	10	8	17	1	5
11/6	99	-126	220	226	-194	13	238	3	6	5	4	12	1	4
11/7	77	-125	217	224	-186	13	241	15	7	15	11	9	0	2
11/8	69	-127	224	235	-201	14	242	3	5	7	6	10	1	5
11/9	65	-115	241	252	-176	14	251	4	3	4	4	4	1	3
11/10	69	-94	258	270	-149	12	248	7	6	2	2	7	1	2
11/11	61	-88	251	262	-151	12	244	6	6	6	9	10	2	1
11/12	58	-91	248	261	-157	*	244	1	1	1	2	1	*	1
11/13	64	-81	261	275	-144	9	240	5	6	5	5	6	1	3
11/14	74	-49	270	286	-117	6	226	8	10	4	4	5	0	3
11/15	75	-39	260	277	-112	6	223	3	3	8	8	6	1	2
11/16	75	-46	257	272	-119	6	231	4	2	3	2	1	0	3
11/17	75	-50	260	275	-119	9	238	6	5	3	3	4	1	4
11/18	63	-57	254	268	-124	9	242	21	10	24	23	21	1	2
11/19	53	-76	242	262	-155	9	236	11	5	10	11	8	1	2
11/20	46	-69	238	261	-146	8	231	21	16	27	24	14	1	2
11/21	49	-62	235	269	-161	7	228	7	8	10	9	4	0	1
11/22	68	-40	253	283	-143	6	228	10	8	3	3	7	1	2
11/23	69	-34	257	286	-126	6	231	4	4	4	4	3	1	3
11/24	67	-42	252	280	-132	8	242	5	5	2	2	2	1	4
11/25	60	-45	254	281	-128	8	245	7	5	5	5	4	1	3
11/26	5	-95	189	225	-181	11	242	18	18	21	19	18	1	4
11/27	18	-80	232	267	-160	10	240	9	6	10	8	3	1	3
11/28	29	-61	254	284	-156	9	240	10	6	2	2	6	1	2
11/29	38	-47	263	292	-140	9	240	12	6	2	2	5	1	2
11/30	34	-45	261	289	-126	8	239	11	5	3	3	3	0	2

Table 15

Record of SP, Soil Temperature, Soil Moisture, and Standard Deviation at Long-Term Monitoring Site for December 1986 (Data reduced to 24-hr average from ADC record)

Date	#1 (sp)	#2 (sp)	#3 (sp)	#4 (sp)	#5 (sp)	Soil Temp	Soil Mois	#1 (std)	#2 (std)	#3 (std)	#4 (std)	#5 (std)	ST (std)	SM (std)
12/1	34	-39	262	286	-115	7	237	3	3	1	1	5	1	2
12/2	-19	-78	175	213	-171	7	223	21	19	26	21	20	1	6
12/3	-10	-61	215	255	-169	8	223	5	8	18	15	5	0	2
12/4	9	-36	237	265	-131	5	219	12	14	65	76	55	0	3
12/5	28	-18	265	292	-122	4	215	14	7	2	3	4	0	1
12/6	31	-13	263	287	-114	3	212	16	6	2	3	16	0	2
12/7	37	-10	261	282	-101	3	212	11	4	3	3	9	0	2
12/8	40	-15	260	279	-97	5	220	2	3	2	2	3	1	4
12/9	5	-59	210	233	-137	8	230	27	31	37	34	28	1	2
12/10	-11	-76	220	250	-158	9	238	2	4	15	13	5	0	2
12/11	-31	-82	205	236	-175	8	233	15	16	25	22	14	0	4
12/12	-17	-48	248	277	-159	6	227	5	6	9	7	2	1	1
12/13	0	-26	269	293	-140	4	220	13	7	3	2	7	1	4
12/14	10	-14	275	292	-126	3	212	16	3	5	7	12	0	2
12/15	25	-7	267	281	-108	3	210	12	6	3	4	7	0	2
12/16	22	-11	266	276	-105	4	215	7	3	3	3	6	1	3
12/17	19	-20	262	269	-105	5	223	4	4	4	5	3	1	2
12/18	-22	-77	202	215	-152	7	225	16	20	24	25	21	1	1
12/19	12	-41	253	265	-134	5	220	14	7	5	4	3	1	2
12/20	21	-32	263	270	-134	4	220	12	4	2	2	2	0	2
12/21	14	-24	268	271	-131	3	218	7	4	2	2	5	0	2
12/22	15	-8	276	277	-122	2	213	12	5	2	2	7	0	2
12/23	17	-1	280	277	-87	2	211	10	3	3	3	29	0	2
12/24	6	-37	45	188	-135	4	209	20	28	161	51	40	1	2
12/25	9	-50	-28	205	-138	4	213	5	4	168	9	5	1	4
12/26	18	-37	244	242	-124	4	216	14	7	17	5	3	0	2
12/27	19	-32	274	251	-125	4	215	5	2	2	1	4	1	1
12/28	25	-29	283	254	-131	4	217	12	4	2	2	3	0	2
12/29	17	-20	297	262	-124	3	215	15	7	3	3	5	0	2
12/30	18	-16	301	262	-117	3	213	9	3	2	2	4	0	1
12/31	21	-15	302	260	-118	3	214	13	5	1	1	3	0	2

Table 16

Record of SP, Soil Temperature, Soil Moisture, and Standard Deviation at Long-Term Monitoring Site for January 1987 (Data reduced to 24-hr average from ADC record)

Date	#1 (sp)	#2 (sp)	#3 (sp)	#4 (sp)	#5 (sp)	Soil Temp	Soil Mois	#1 (std)	#2 (std)	#3 (std)	#4 (std)	#5 (std)	ST (std)	SM (std)
1/1	17	-18	301	257	-111	3	213	5	1	1	1	3	0	0
1/2	25	-17	300	255	-112	3	215	1	1	0	1	1	0	1
1/3	23	-18	299	254	-111	3	216	4	2	2	2	3	0	1
1/4	19	-21	302	257	-111	3	215	12	3	3	3	3	0	2
1/5	14	-22	308	261	-104	2	214	14	5	3	2	4	0	2
1/6	6	-19	314	265	-81	2	211	6	6	3	3	10	0	2
1/7	-31	-55	278	229	-112	3	212	32	36	37	36	44	1	2
1/8	-27	-50	284	236	-136	3	216	10	8	8	8	3	0	2
1/9	-9	-28	306	256	-129	2	215	11	6	4	4	4	0	2
1/10	1	-29	299	252	-115	3	214	6	4	3	4	6	1	2
1/11	-16	-29	307	254	-144	3	218	2	2	3	3	4	0	1
1/12	-7	-20	312	258	-147	3	214	9	5	4	3	2	1	1
1/13	1	-16	314	259	-148	3	216	8	3	4	4	3	1	2
1/14	1	-18	312	257	-144	4	222	6	3	2	2	5	1	4
1/15	-9	-43	293	240	-172	6	233	11	12	5	6	21	0	2
1/16	-18	-51	297	242	-195	6	235	5	3	4	4	2	0	1
1/17	-16	-50	298	243	-197	5	231	2	3	3	3	2	0	2
1/18	-25	-70	272	219	-193	4	226	14	19	22	21	16	0	2
1/19	33	-44	77	199	-180	4	222	19	18	189	21	12	0	1
1/20	26	-33	207	239	-177	3	218	11	8	159	9	5	0	1
1/21	30	-22	312	254	-168	3	218	9	4	5	3	8	0	1
1/22	29	-20	319	256	-158	3	216	2	1	1	0	1	0	1
1/23	23	-25	311	248	-166	3	216	4	4	5	4	4	0	1
1/24	16	-29	308	243	-171	4	215	1	1	1	0	2	1	1
1/25	15	-29	308	244	-164	3	216	1	1	0	0	1	0	1
1/26	11	-30	308	243	-164	3	214	1	1	0	0	0	0	2
1/27	12	-31	308	243	-164	3	214	1	1	1	0	0	0	2
1/28	12	-31	310	242	-166	3	214	1	1	0	1	1	0	1
1/29	11	-30	311	242	-168	3	214	1	0	1	0	0	0	1
1/30	13	-32	307	239	-173	3	208	7	4	5	4	6	0	6
1/31	15	-30	311	240	-186	3	208	2	3	4	3	3	0	1

Table 17

Record of SP, Soil Temperature, Soil Moisture, and Standard Deviation at Long-Term Monitoring Site for February 1987 (Data reduced to 24-hr average from ADC record)

Date	#1 (sp)	#2 (sp)	#3 (sp)	#4 (sp)	#5 (sp)	Soil Temp	Soil Mois	#1 (std)	#2 (std)	#3 (std)	#4 (std)	#5 (std)	ST (std)	SM (std)
2/1	8	-24	320	244	-192	3	209	2	1	2	1	1	0	1
2/2	17	-26	315	240	-191	3	208	13	7	12	10	3	0	2
2/3	36	-4	302	229	-188	2	205	32	32	8	6	17	0	3
2/4	24	6	300	227	-187	2	208	15	11	8	7	9	1	2
2/5	-1	-14	319	239	-217	3	211	19	7	5	4	15	1	2
2/6	5	-15	327	243	-211	3	212	17	6	4	4	14	1	3
2/7	-3	-2	314	232	-218	4	217	15	23	12	10	13	1	4
2/8	-19	-2	315	227	-220	4	219	14	28	11	10	13	1	3
2/9	-13	-14	342	251	-215	2	214	11	5	7	6	15	0	4
2/10	-3	-7	348	253	-165	2	210	6	5	5	6	25	0	2
2/11	1	-5	341	245	-136	2	212	8	4	5	5	8	0	3
2/12	-23	-37	305	211	-143	4	219	22	28	31	29	19	1	4
2/13	-7	-31	323	229	-150	4	224	14	4	5	5	10	1	4
2/14	1	-23	339	242	-165	4	223	9	4	5	5	11	1	2
2/15	7	-23	337	239	-180	4	222	7	3	3	3	5	1	1
2/16	6	-20	346	246	-180	3	219	2	4	5	4	7	0	4
2/17	14	-14	343	243	-174	2	213	3	1	1	1	3	0	1
2/18	21	-15	337	240	-184	2	213	1	1	2	1	3	0	1
2/19	16	-20	333	236	-190	3	214	3	2	2	2	4	0	2
2/20	14	-20	336	239	-189	3	215	7	4	4	4	6	0	1
2/21	16	-19	337	240	-188	4	214	6	3	5	4	4	1	1
2/22	-9	-34	327	229	-200	3	214	5	3	4	4	3	0	1
2/23	25	-28	329	233	-204	4	211	40	5	7	7	8	1	3
2/24	36	-23	337	236	-212	4	208	32	8	8	8	5	1	1
2/25	52	8	343	241	-201	4	210	50	41	6	6	6	1	2
2/26	31	3	344	240	-197	4	209	51	16	5	4	3	1	1
2/27	9	-6	339	234	-196	5	211	5	4	1	2	1	0	1
2/28	18	7	289	190	-194	5	211	18	19	66	57	11	0	3

Table 18

Record of SP, Soil Temperature, Soil Moisture, and Standard Deviation at Long-Term Monitoring Site for March 1987 (Data reduced to 24-hr average from ADC record)

Date	#1 (sp)	#2 (sp)	#3 (sp)	#4 (sp)	#5 (sp)	Soil Temp	Soil Mois	#1 (std)	#2 (std)	#3 (std)	#4 (std)	#5 (std)	ST (std)	SM (std)
3/1	-11	-20	43	165	-215	4	212	34	32	32	19	19	1	6
3/2	-70	-64	11	188	-205	4	224	12	21	35	23	19	1	5
3/3	-54	-60	-82	191	-200	5	229	18	7	61	4	24	1	5
3/4	-13	-23	-83	206	-212	4	229	21	10	98	4	11	1	3
3/5	15	-8	312	243	-205	4	227	23	5	5	14	10	1	5
3/6	17	-10	319	255	-208	5	231	19	6	4	5	6	2	7
3/7	12	-14	330	256	-210	6	239	19	7	5	6	9	2	7
3/8	14	-15	342	263	-210	7	244	11	4	5	4	6	1	4
3/9	9	-26	329	250	-212	9	251	18	21	24	23	15	1	3
3/10	-31	-49	322	238	-227	7	246	16	16	20	18	9	1	5
3/11	-2	-25	349	261	-213	5	234	23	8	5	5	8	1	4
3/12	12	-21	346	259	-199	5	235	17	6	4	4	4	1	5
3/13	8	-23	348	260	-198	5	237	16	8	4	5	5	1	5
3/14	15	-18	350	262	-172	5	236	19	6	6	5	9	1	5
3/15	17	-21	345	257	-162	5	238	12	4	5	4	4	1	2
3/16	28	-21	341	253	-157	5	233	18	6	5	6	5	1	5
3/17	7	-38	321	234	-186	4	229	13	15	18	15	22	1	6
3/18	-2	-42	332	243	-192	5	234	13	8	8	8	6	1	5
3/19	2	-41	336	246	-193	6	238	7	3	3	3	7	0	1
3/20	2	-38	343	254	-206	6	237	17	7	5	5	9	1	8
3/21	-4	-36	352	260	-207	6	243	13	6	5	5	6	2	6
3/22	-4	-36	348	257	-193	7	247	15	7	7	6	7	1	8
3/23	0	-38	344	255	-178	7	250	16	7	6	7	5	2	6
3/24	2	-38	343	255	-161	8	252	14	8	7	6	7	1	7
3/25	9	-39	340	253	-144	9	255	11	8	4	4	9	0	1
3/26	7	-42	339	256	-161	9	259	12	7	5	6	8	1	7
3/27	2	-44	343	258	-184	10	262	8	6	6	7	3	1	5
3/28	-35	-79	313	228	-226	11	270	17	19	24	23	28	1	6
3/29	-22	-65	353	259	-228	11	276	11	4	6	7	9	2	6
3/30	6	-66	170	214	-223	12	275	21	24	165	39	20	0	2
3/31	-28	-58	149	208	-219	11	271	28	10	28	28	17	2	3

Table 19

Record of SP, Soil Temperature, Soil Moisture, and Standard Deviation at Long-Term Monitoring Site for April and May 1987 (Data reduced to 24-hr average from ADC record)

Date	#1 (sp)	#2 (sp)	#3 (sp)	#4 (sp)	#5 (sp)	Soil Temp	Soil Mois	#1 (std)	#2 (std)	#3 (std)	#4 (std)	#5 (std)	ST (std)	SM (std)
4/1	-1	-48	136	182	-230	*	256	15	7	120	18	4	*	4
4/2	-3	-44	338	264	-228	*	255	9	7	10	8	3	*	3
4/3	17	-44	337	259	-224	11	248	10	3	5	2	5	3	3
4/4	6	-50	323	250	-248	9	239	9	2	2	2	7	0	2
4/5	-2	-37	328	255	-245	7	231	21	7	8	8	21	1	3
4/6	-31	-6	224	235	-212	8	227	36	47	104	19	20	1	1
4/7	-29	-40	130	238	-256	8	240	21	8	69	4	5	2	11
4/8	-29	-43	188	212	-244	8	256	10	6	53	26	3	1	9
4/9	-22	-41	181	182	-231	9	261	14	8	111	15	4	1	8
4/10	-14	-48	323	255	-213	10	267	17	9	12	15	6	2	8
4/11	5	-50	341	267	-192	10	267	18	7	5	6	9	1	4
4/12	20	-44	340	270	-182	10	268	9	4	3	4	4	1	4
4/13	21	-46	341	271	-184	11	272	19	8	5	5	7	2	9
4/14	31	-55	340	268	-165	11	278	12	3	4	5	8	1	4
4/15	33	-45	234	197	-185	11	278	17	24	81	68	29	0	1
4/16	-53	-76	153	32	-204	12	272	10	23	16	71	18	2	2
4/17	-53	-55	175	137	-206	11	271	15	9	27	64	16	1	3
4/18	25	-39	169	131	-207	11	276	37	5	17	17	11	1	6
4/19	35	-64	86	95	-233	12	286	21	10	35	11	12	2	7
4/20	14	-68	9	84	-236	14	294	23	11	25	10	3	2	9
4/21	-18	-79	-45	77	-225	14	301	19	11	19	10	6	2	9
4/22	-35	-81	-76	126	-199	16	308	10	7	26	31	10	2	9
4/23	-27	-74	-114	106	-175	15	307	13	10	20	9	14	0	2
4/24	-71	-96	4	19	-212	*	302	33	38	58	45	25	*	2
4/25	-104	-85	88	127	-189	*	296	30	52	35	34	13	*	4
4/26	31	-38	97	92	-214	*	287	25	20	31	27	19	*	7
4/27	-4	-64	38	61	-232	*	287	14	8	20	9	4	*	5
4/28	-28	-59	-59	78	-192	*	306	4	38	12	15	4	*	8
4/29	-10	-57	-68	48	-192	*	296	1	5	5	8	4	*	4
5/1	48	-33	-131	43	-197	*	304	17	14	43	12	6	*	10
5/2	69	-10	-78	78	-196	*	307	12	14	111	36	13	*	8
5/3	84	-30	120	157	-198	*	311	7	8	22	12	7	*	6
5/4	13	-77	-18	102	-225	*	306	24	13	20	14	14	*	5
5/5	-16	-64	89	174	-227	*	299	19	7	103	41	12	*	8
5/6	-43	-74	249	241	-255	*	302	16	8	18	5	10	*	10
5/7	-31	-73	304	242	-253	*	308	16	9	13	8	5	*	9
5/8	38	-46	308	233	-230	*	306	32	16	8	8	10	*	5
5/9	60	-56	277	205	-229	*	306	8	11	16	15	14	*	9
5/10	75	-69	261	194	-226	*	311	11	11	16	16	15	*	9
5/11	92	-69	262	199	-211	*	310	10	10	9	9	14	*	4

Table 20

SP Values (millivolts) at the Moore Sinkhole A, July to October 1986

DATE	7/21	7/23	7/25	7/28	7/30	8/5	8/18	9/9	9/19	10/2	10/8	10/14	10/24	10/27
TIME	1500	1900	0800	1600	5800	0900	1400	1600	1200	1200	1200	1200		
SOIL TEMP (C)			27			23	25	21	17	19	16	17	17	17
ELECTRODE #														
1	-236	-215	-224	-269	-256	-278	-298	-173	-247	-273	-287	-195	-279	-120
2	-67	-52	-52	-62	-64	-59	-56	-8	-11	-14	-47	-48	-76	-54
3	-126	-136	-132	-118	-129	-94	-18	24	27	26	-157	-128	-275	-141
4	13	9	18	13	16	39	37	26	28	37	49	-4	34	-13
5	-45	-28	-20	-15	-16	-15	-17	8	-1	-12	-15	-23	-27	-30
6	-8	-11	-4	-6	-6	10	4	13	16	30	46	-1	16	-21
7	-51	-43	-37	-38	-39	-35	-40	0	-10	-18	-12	-16	-10	-28
8	29	4	13	10	10	33	35	21	25	27	29	-2	8	-16
9	-12	-5	3	5	9	21	22	30	24	21	27	12	14	6
10	12	-12	-15	-18	-12	-18	-23	35	31	22	23	-23	13	-1
11	-49	-40	-39	-37	-43	-44	-50	4	-11	-22	-24	-19	-16	-16
12	-278	-252	-287	-360	-337	-382	-375	-158	-310	-342	-355	-227	-320	-121
13	-104	-60	-68	-68	-68	-80	-72	-14	-34	-48	-50	-38	-51	-35
14	8	-2	12	13	4	26	23	24	29	36	43	-9	22	-21
15	-60	-47	-55	-52	-46	-33	-32	-6	-11	-13	-26	-32	-80	-132
16	-8	-5	2	2	-2	22	23	19	31	48	53	-11	21	-31
17	11	-2	14	13	4	43	37	26	32	53	66	-3	26	-21
18	38	17	35	21	28	84	79	29	45	82	109	-1	50	-9
19	10	2	15	17	9	33	13	-23	7	14	15	-14	-26	-16
20	-168	-165	-175	-140	-109	-78	-7	16	7	7	8	-10	-4	-18
21	-44	-53	-70	-99	-127	-207	-203	-64	-158	-195	-182	-106	-190	-74
22	-41	-48	-45	-38	-83	-135	-141	-70	-172	-189	-158	-38	-138	-29
23	-99	-86	-98	-93	-78	-89	-32	42	39	31	13	-1	6	0
24	-19	-33	-28	-31	-33	-51	-79	-43	-68	-95	-117	-100	-116	-90
25	-83	-83	-79	-80	-84	-86	-108	-52	-67	-86	-118	-114	-134	-110
26	-10	-16	-17	-25	-21	-50	-79	-23	-31	-78	-96	-52	-66	-38
27	16	14	23	30	27	33	6	30	32	10	5	-31	-1	-8
28	16	9	20	27	32	57	35	42	41	36	37	2	10	-1
29	-302	-202	-271	-368	-312	-386	-369	-82	-235	-253	-245	-115	-134	-35
30	-37	-16	-6	-2	-5	16	4	16	20	19	18	-17	3	-17
31	-80	-35	-32	-22	-9	13	-2	18	19	19	18	-20	2	-28
32	14	3	16	18	3	33	18	18	12	28	31	0	6	-22

Table 21

SP Values (millivolts) at the Three Moore Sinkholes from January to April 1987

	Moore A				Moore B				Moore C			
DATE	1/13	1/23	3/3	4/29	1/13	1/30	3/4	4/28	1/13	1/20	3/4	4/29
SOIL TEMP (C)	0	3	3	9	0	3	2	10	0	3	2	11
ELECTRODE #												
1	173	98	85	33	20	-9	3	-11	-64	-154	-156	-246
2	148	69	37	-27	105	76	58	22	-121	-190	-205	-245
3	141	61	45	-10	110	47	78	22	-66	-130	-108	-213
4	289	195	165	70	74	43	54	-5	-72	-155	-154	-196
5	194	98	68	-31	113	69	36	29	-60	-120	-162	-290
6	169	63	-3	-109	227	181	183	64	-152	-195	-167	-173
7	135	48	5	-224	205	126	85	2	-96	-183	-179	-286
8	278	192	160	67	200	122	109	-26	-35	-103	-69	10
9	212	121	97	10	219	146	125	28	138	77	91	30
10	300	202	177	60	220	141	118	14	-7	-63	-23	-76
11	275	174	134	40	61	36	22	-14	133	57	16	-88
12	112	41	9	-103	58	48	24	-33	-125	-165	-135	-133
13	135	89	55	-44	90	30	44	33	25	-23	-27	-133
14	223	141	137	42	150	99	65	32	22	71	-82	-60
15	170	97	113	24	308	228	205	101	-73	-121	-126	-190
16	155	68	51	-29	56	47	36	17	-39	-117	-160	-229
17	76	-22	-65	-154	27	-25	-27	-106	109	23	85	38
18	221	149	118	38	-78	-129	-106	-145	22	-56	-67	-121
19	156	85	55	-9	-59	-169	-189	-294	-53	-146	-153	-214
20	214	135	95	-26	-16	-133	-202	-341	45	-14	-13	-72
21	221	192	193	78	117	32	-2	-175	-45	-120	-150	-273
22	311	213	195	95	10	-10	-23	-65	-66	-128	-128	-328
23	308	224	192	55	172	97	88	22	68	-32	114	-215
24	170	62	15	-60	68	13	15	-51	-92	-157	-179	-366
25	158	68	38	-11	190	128	100	16	-44	-48	-73	-166
26	248	190	165	78	6	-32	-55	-204	80	9	-16	-87
27	226	144	125	67	127	50	23	-62	104	33	3	-88
28	200	127	84	26	178	108	90	3	-122	-200	-219	-289
29	228	145	138	53	122	69	64	-11	-34	-101	-92	-120
30	91	33	65	27	100	48	68	18	180	28	-41	-82
31	-89	-149	-130	-168	214	177	147	74	88	20	19	-18
32	85	6	18	-9	-132	-175	-172	-158	-65	-123	-99	-179
Center	-63	-149	-155	-159	225	158	187	28	-56	-115	-165	-176

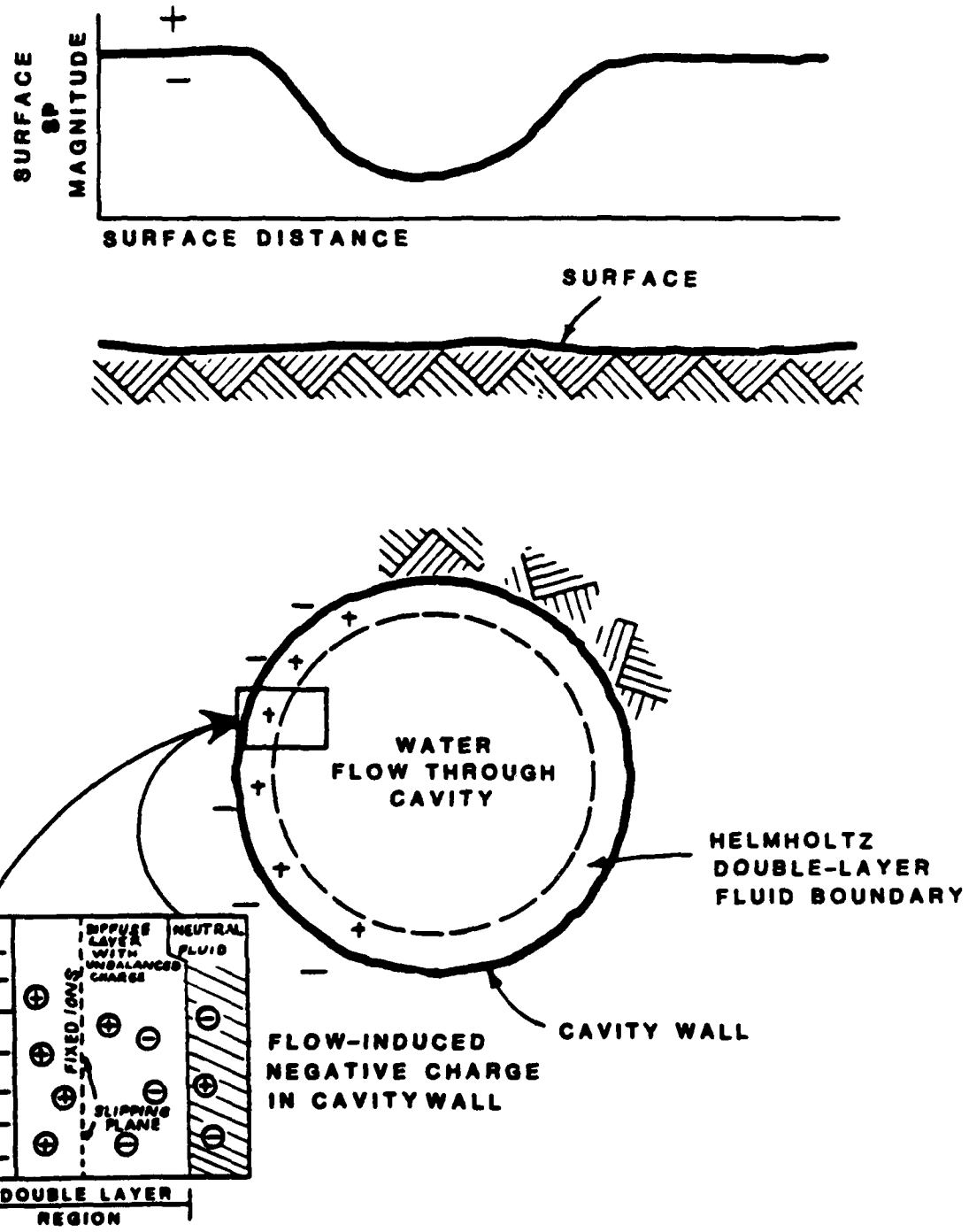

Figure 1. Schematic of flow-induced negative streaming potentials (from Cooper 1983)

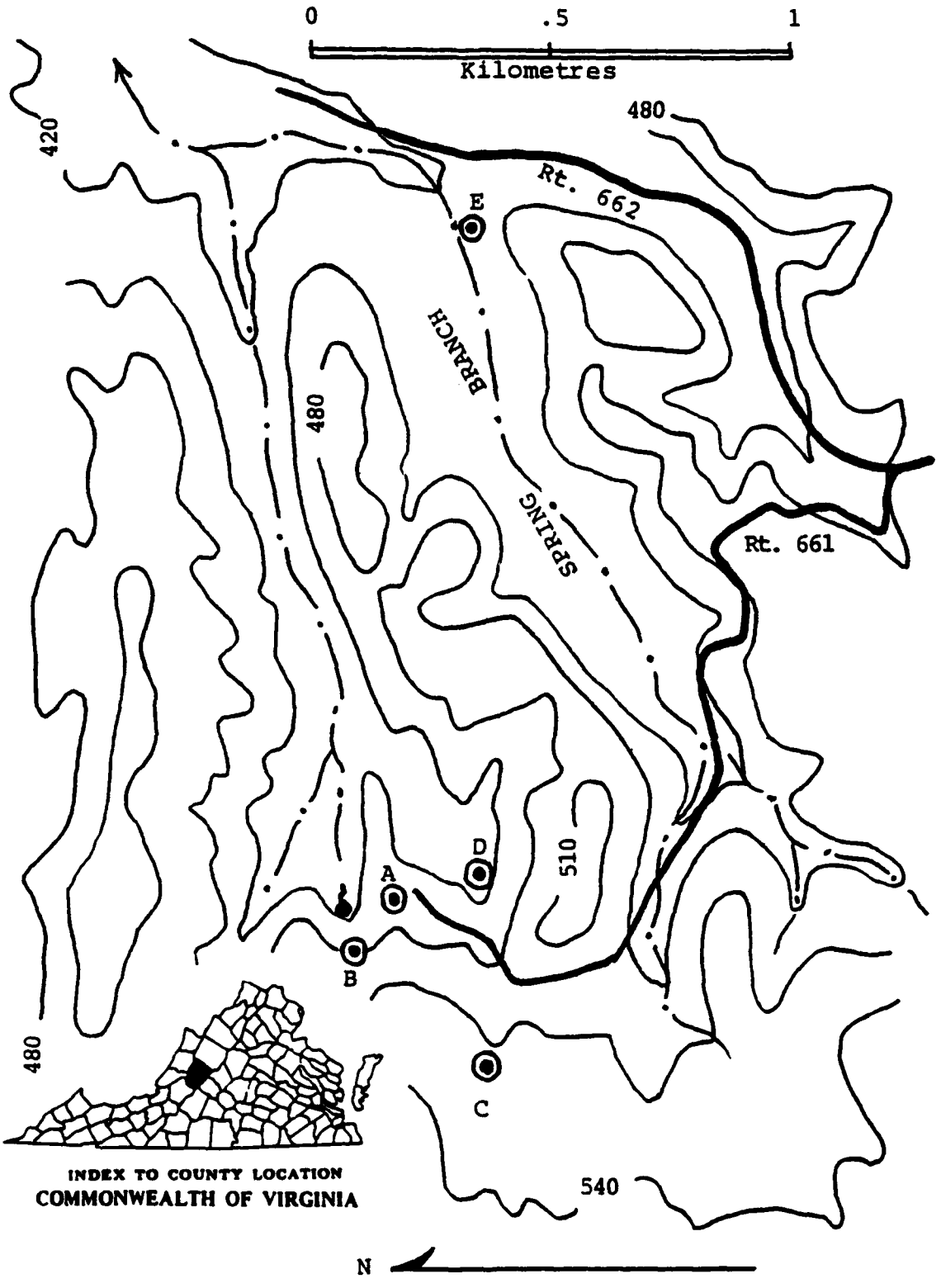

Figure 2. Topographic map of study area (contours in metres). A = McHenry sinkhole A; B = McHenry sinkhole B; C = Whose Hole Cave; D = Electrode monitoring site; E = Spring Branch

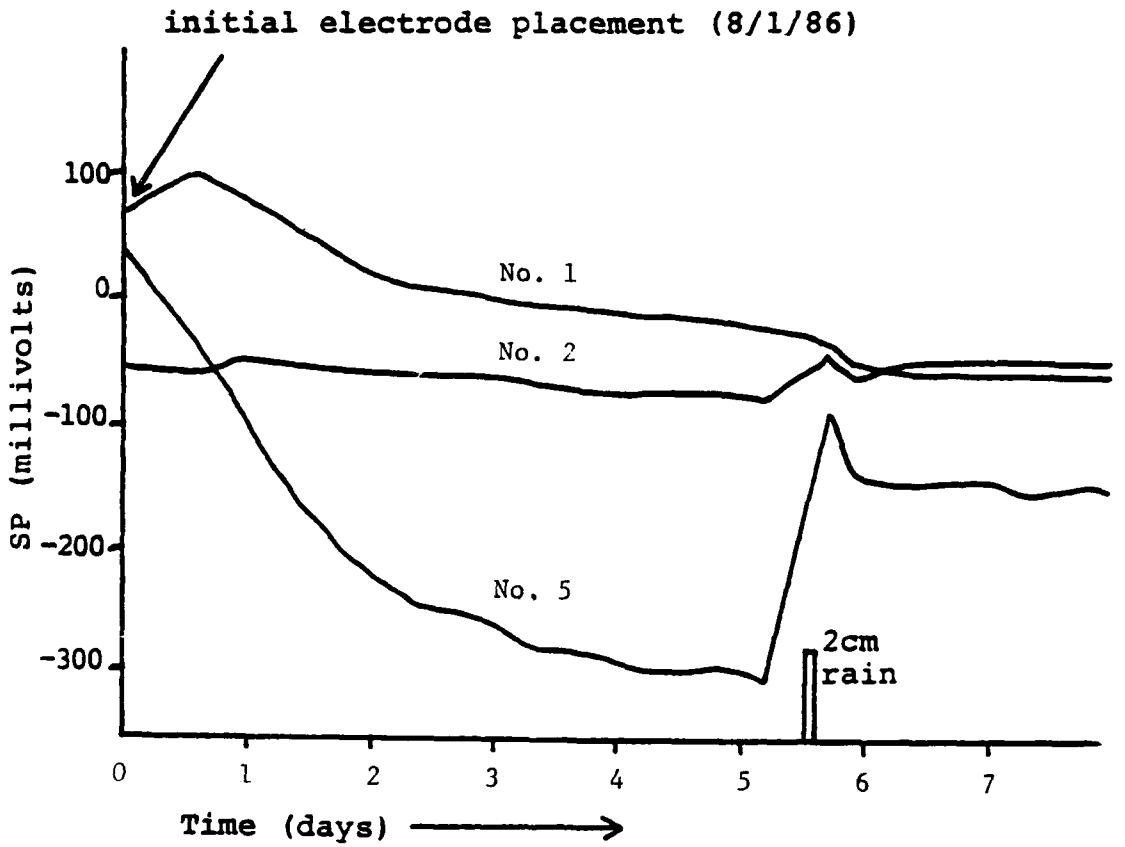

Figure 3. Polarization equilibrium of electrodes following initial placement at the electrode monitoring test site

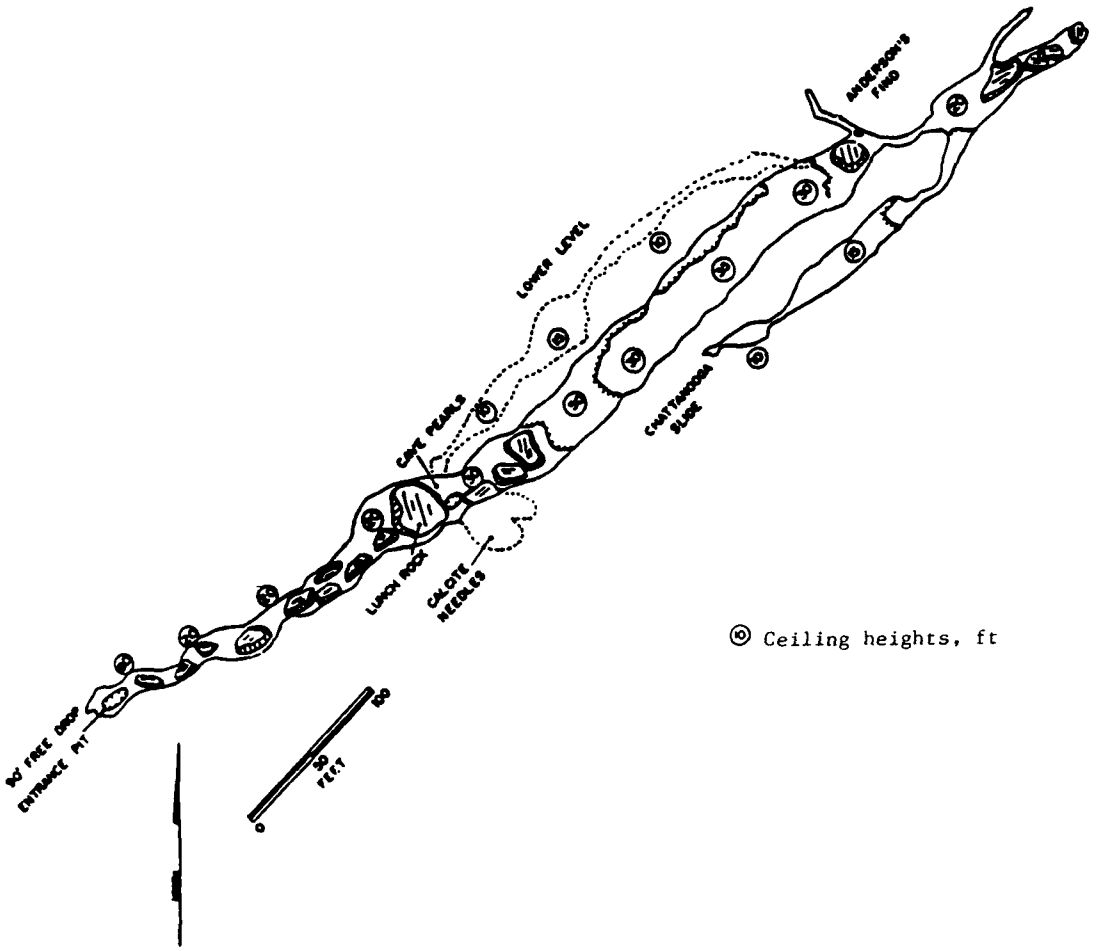

Figure 4. Map of Swinks Cave, near the Harris-Hunter sinkhole site, showing passage development along strike direction (from Holsinger 1978)

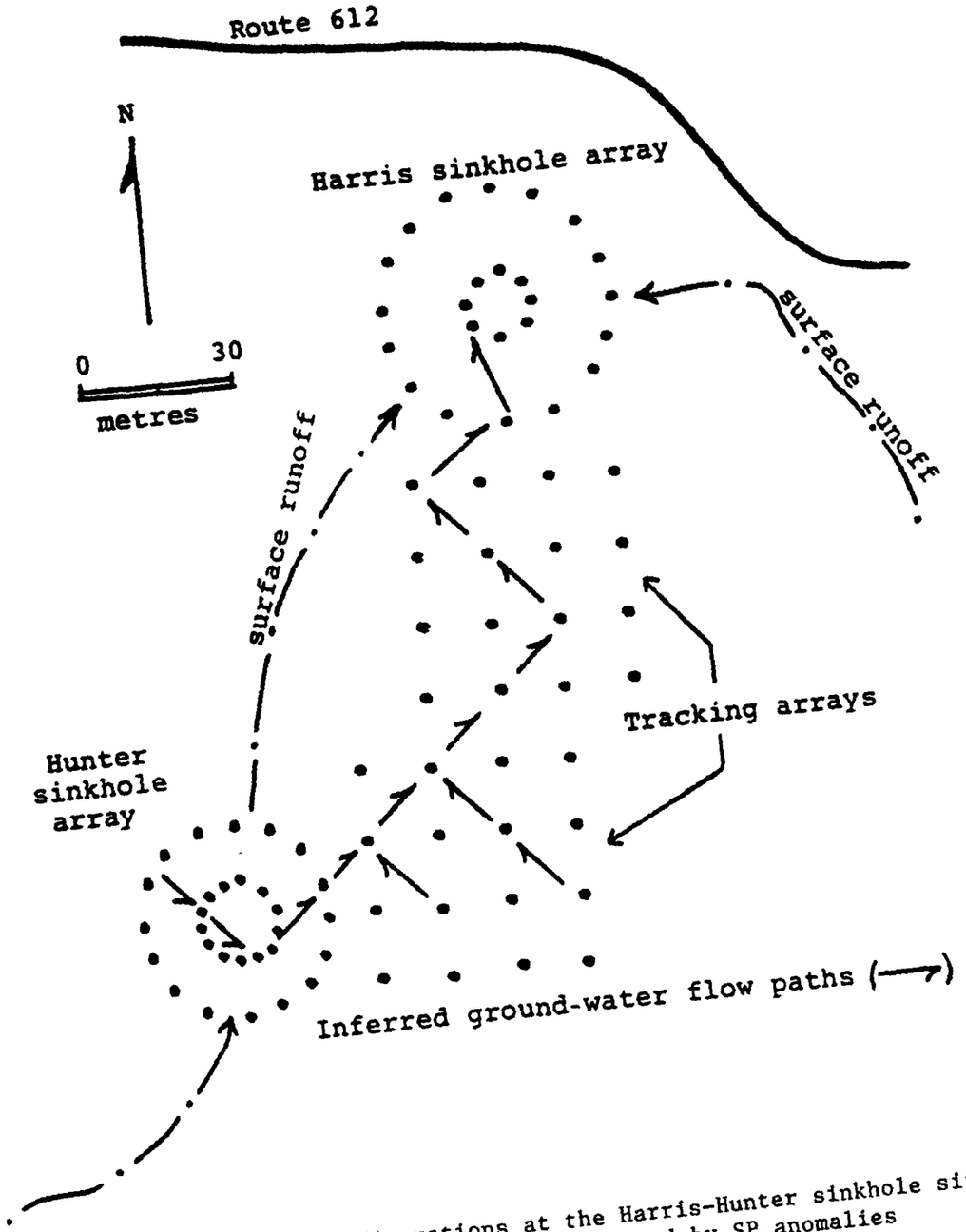

Figure 5. Electrode configurations at the Harris-Hunter sinkhole site, showing ground-water flowpaths inferred by SP anomalies

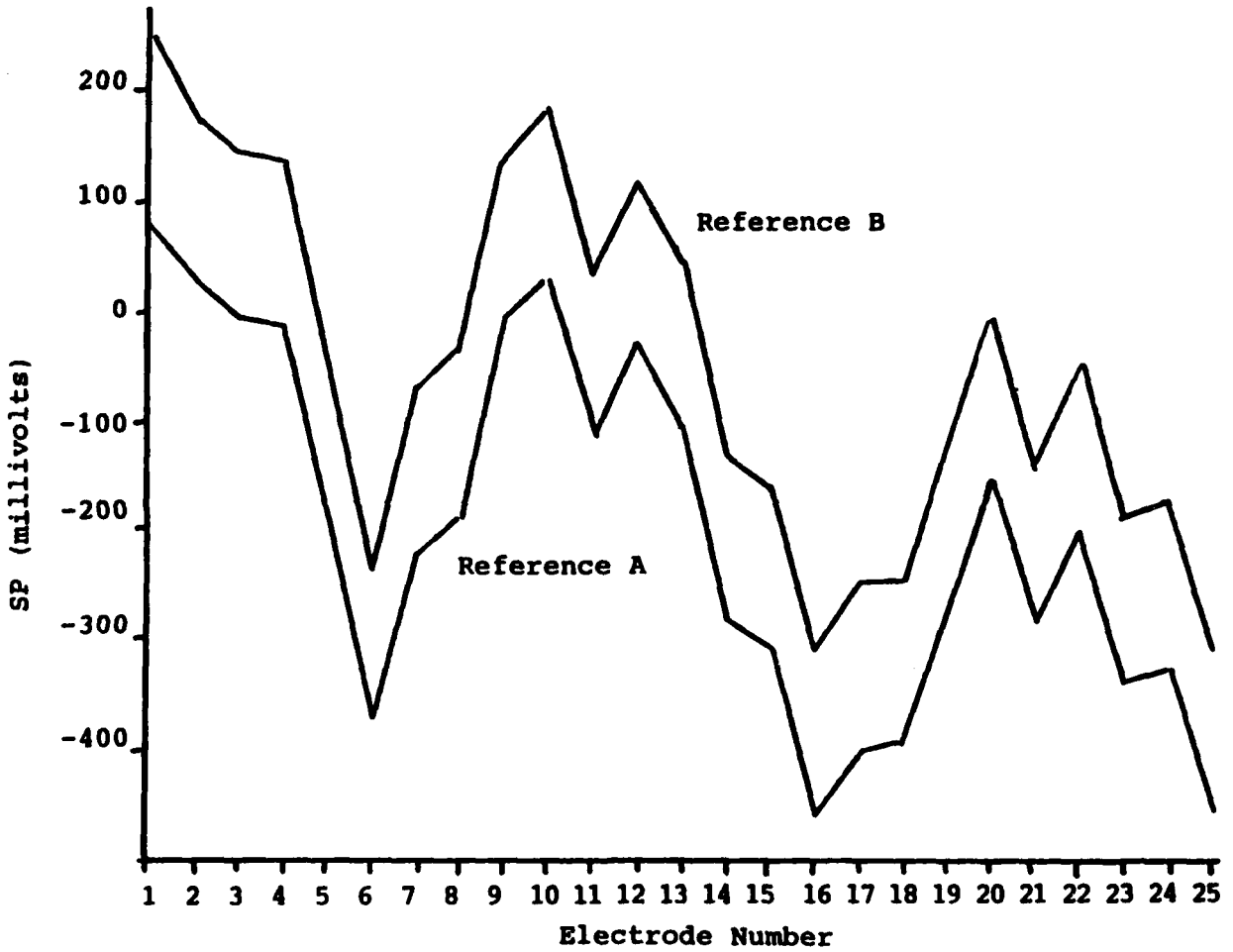

Figure 6. SP for electrode array for two different reference electrodes, 3 August 1986, Spring Branch site

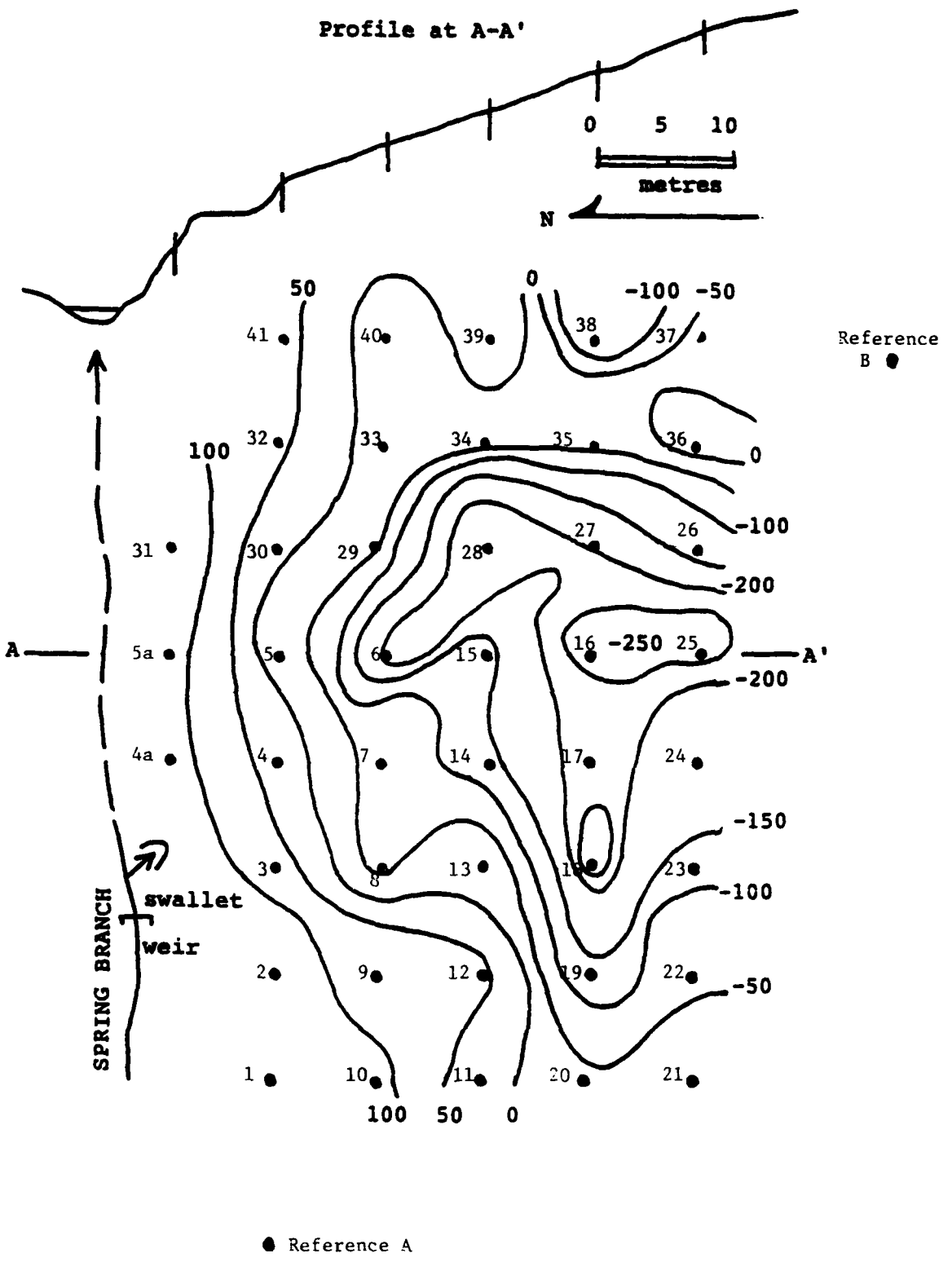

Figure 7. SP contour map (in millivolts) showing swallet, weir, and profile of slope on which array is located, Spring Branch site

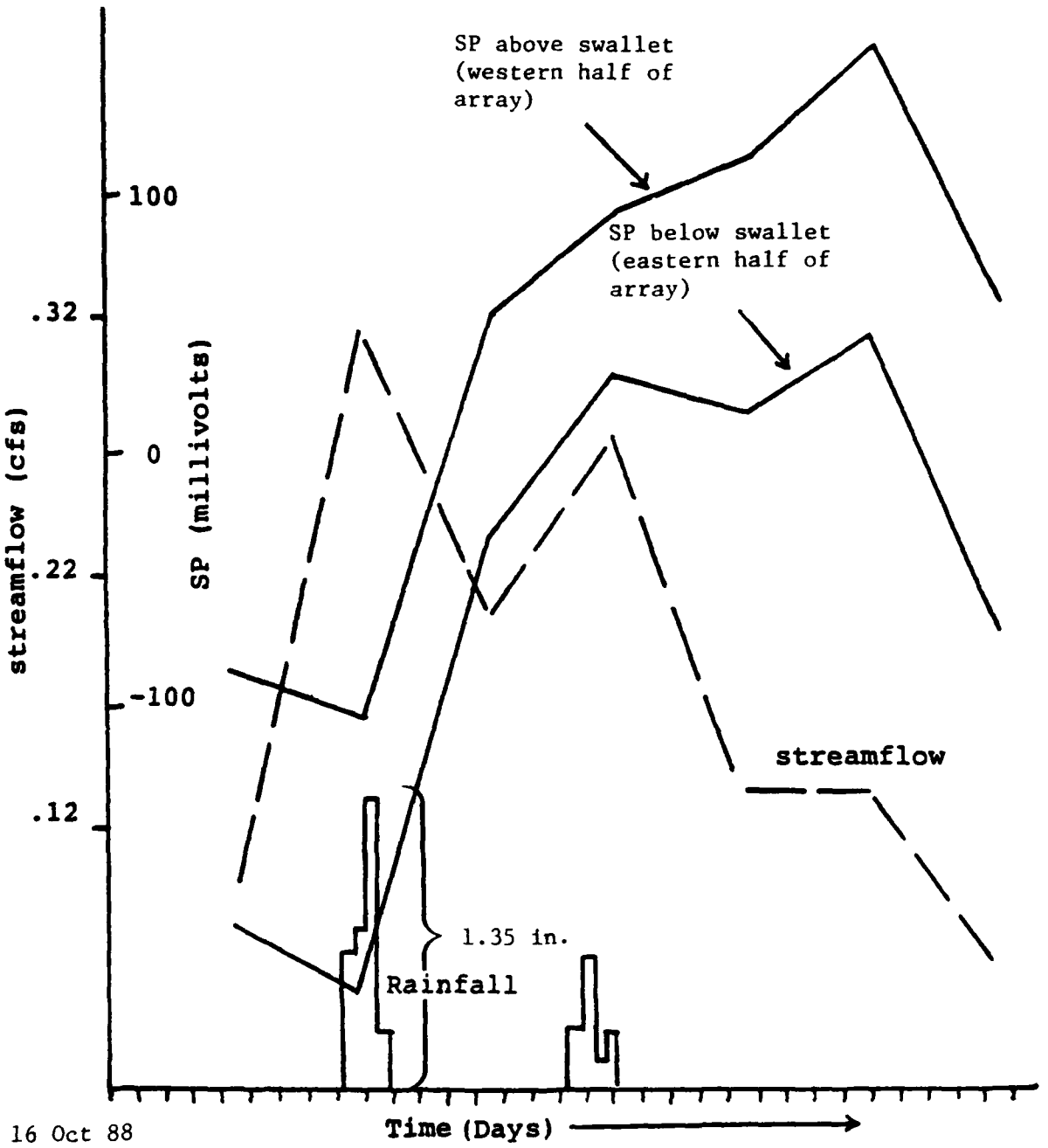

Figure 8. SP, streamflow, and rainfall, Spring Branch site. SP data show different magnitudes for the two halves of the array, relative to their position in relation to the stream sink (swallet)

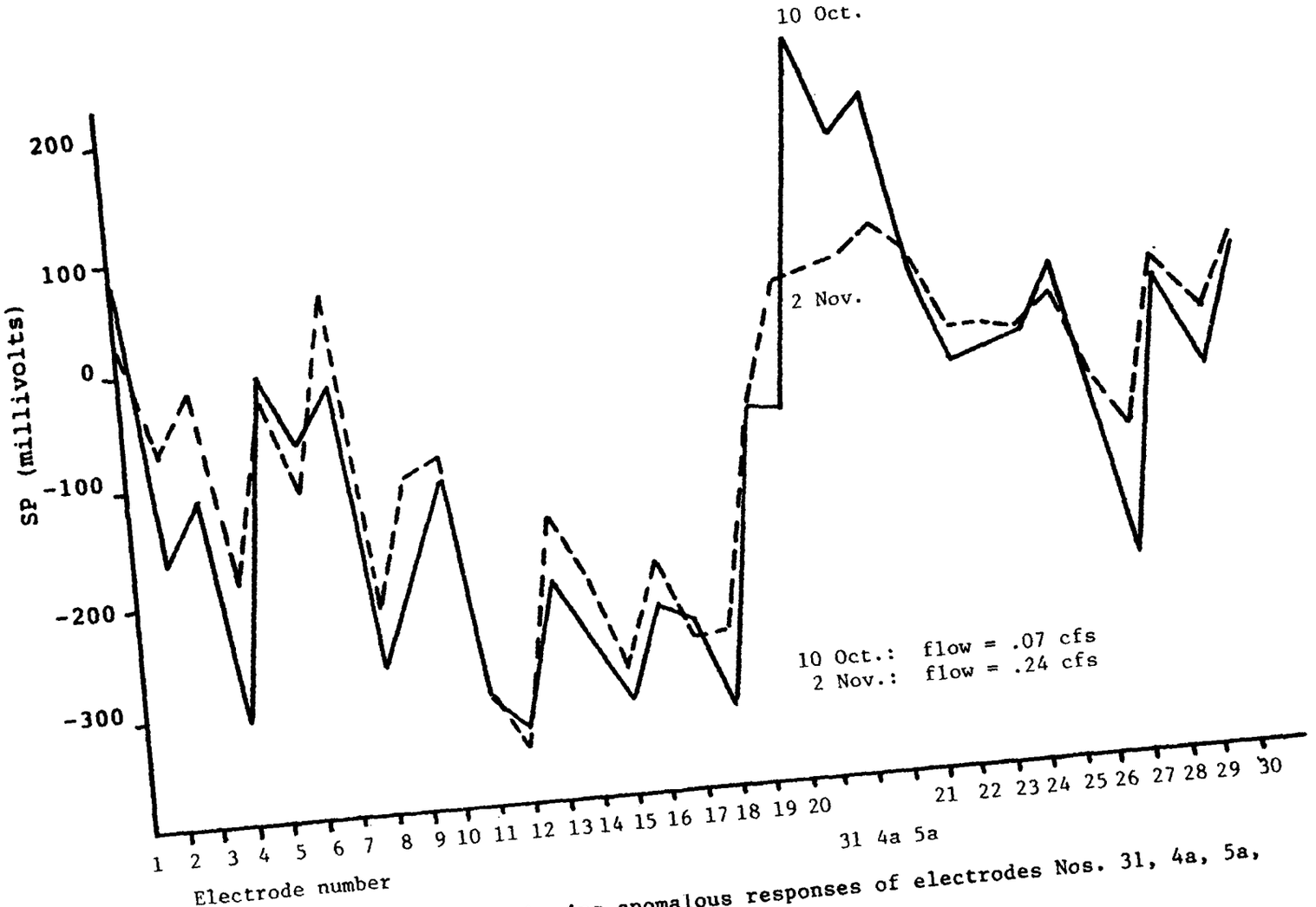

Figure 9. SP for two dates showing anomalous responses of electrodes Nos. 31, 4a, 5a, Spring Branch site

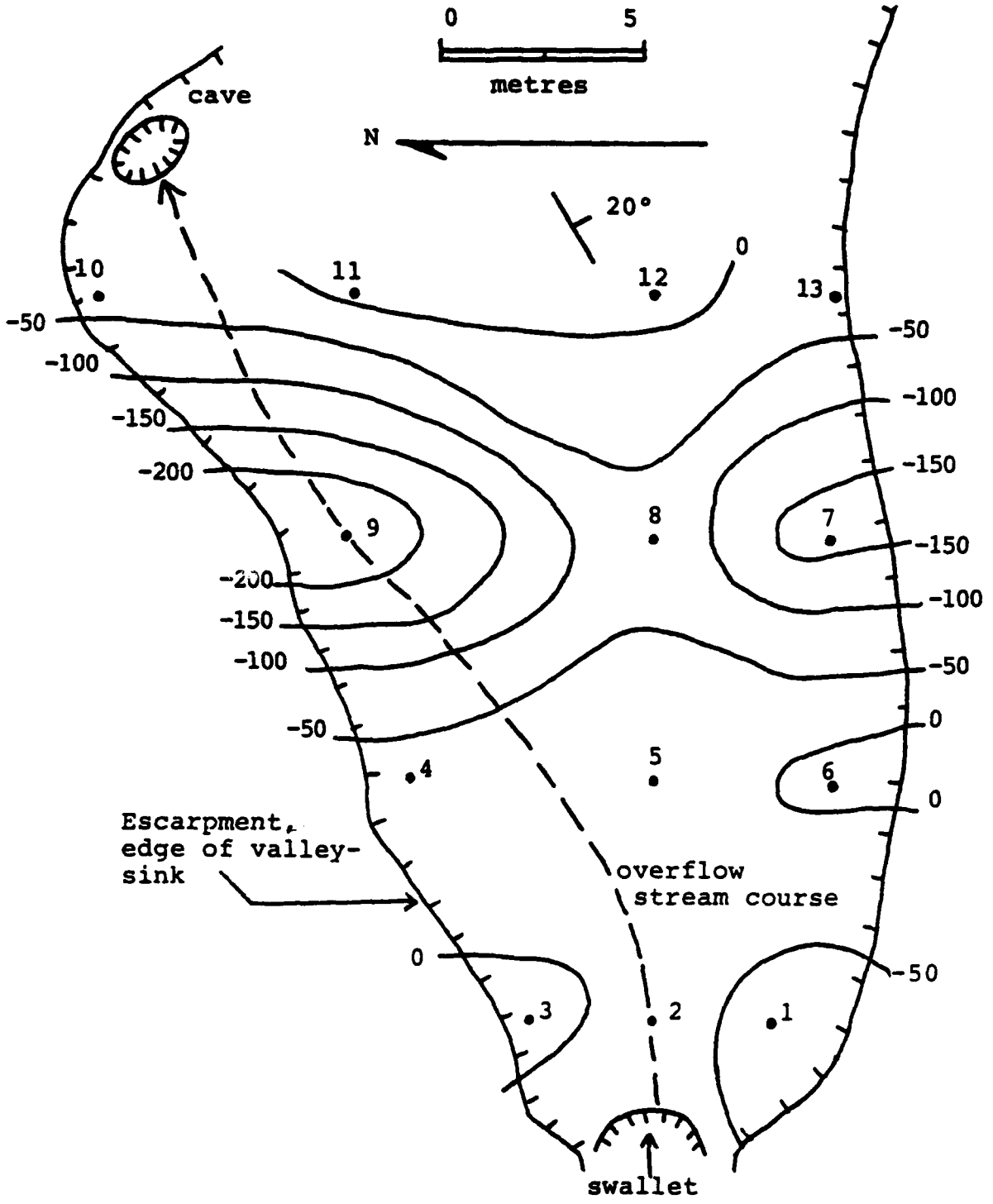

Figure 10. Map with SP contours (in millivolts) and electrode array, Ford site

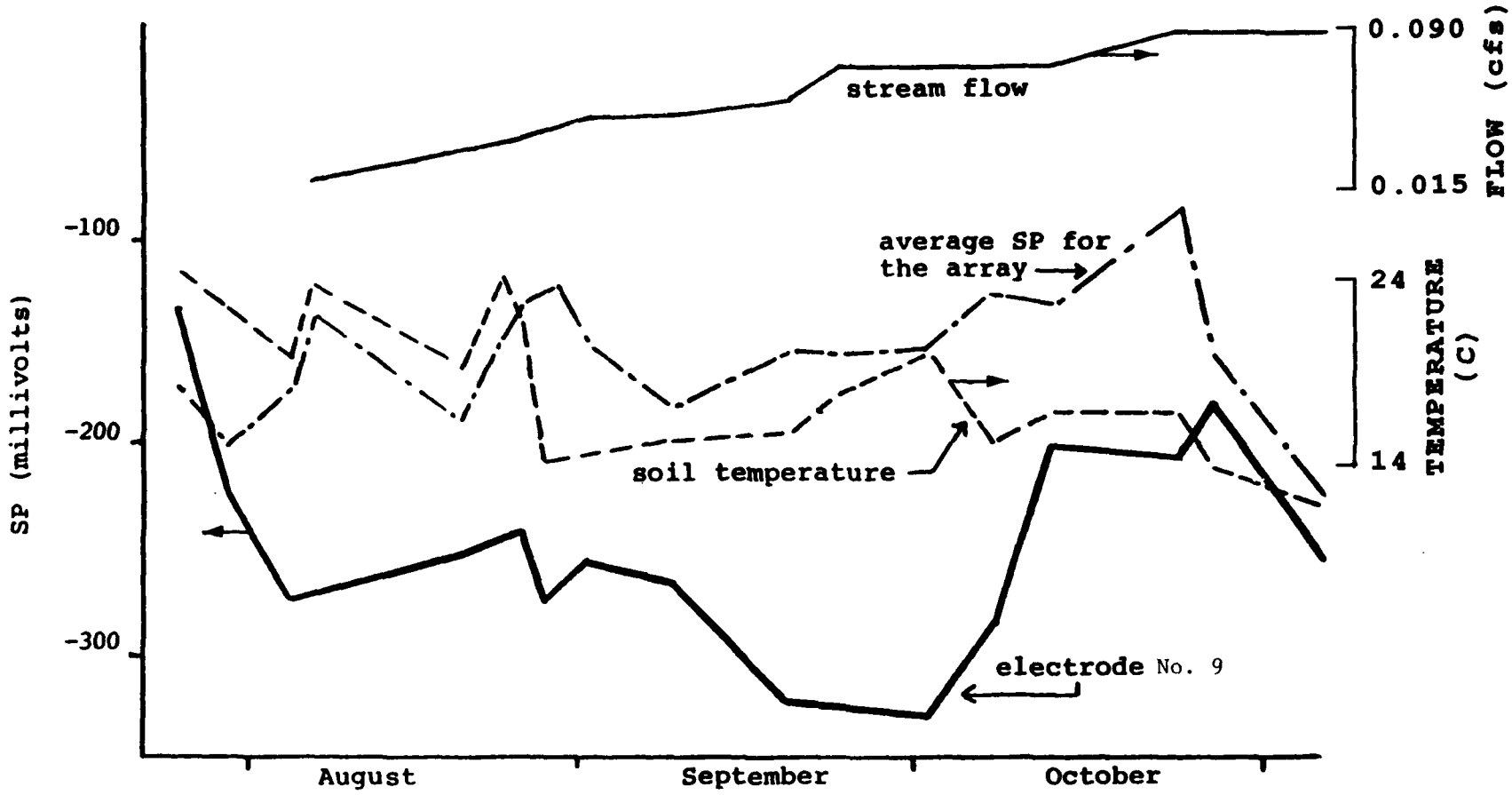

Figure 11. SP data for a 3-month period showing relationship of average SP for the array, SP for an anomalous electrode (No. 9), streamflow, and temperature, Ford site

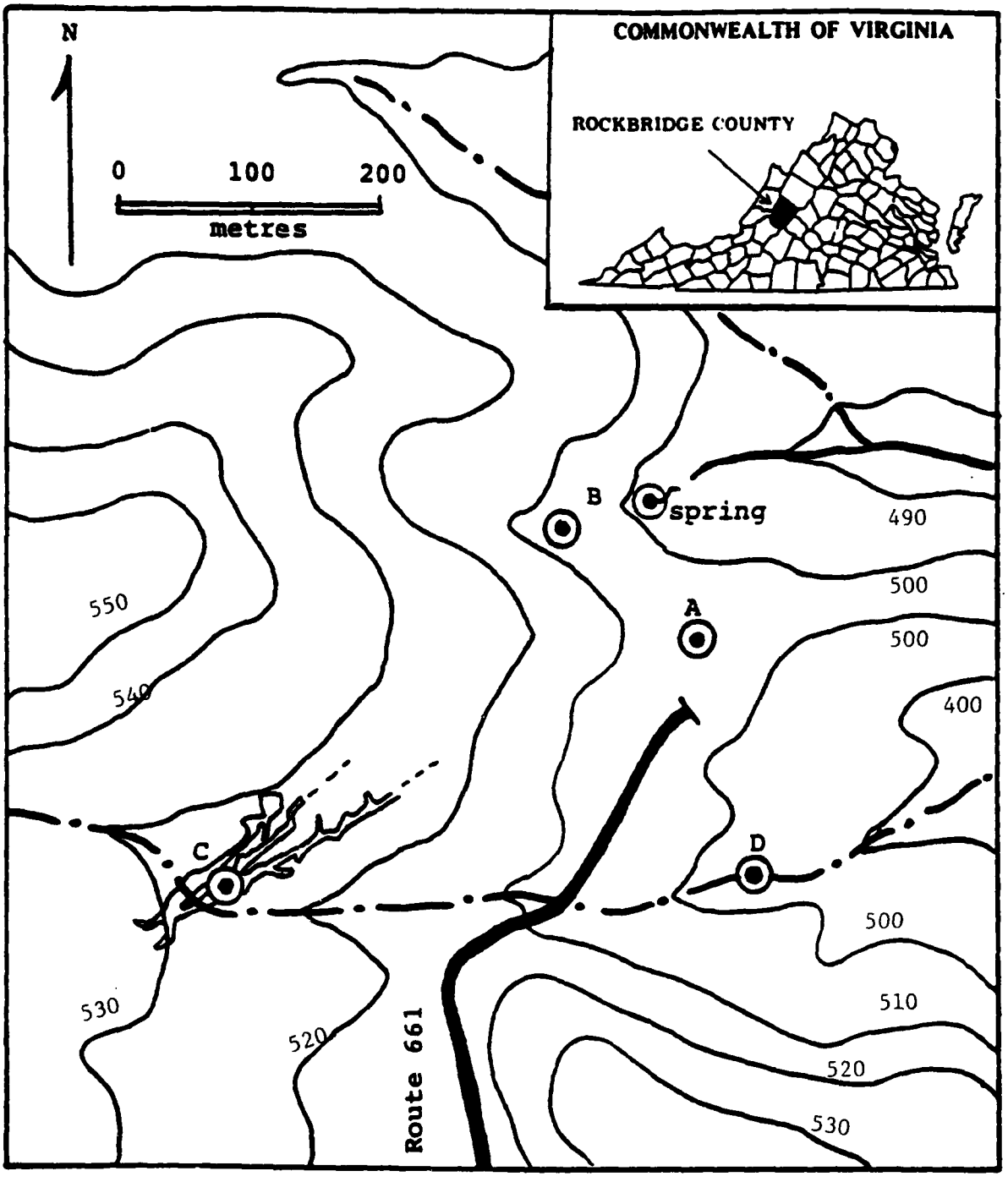

Figure 12. Topographic map of study area (contours in metres) showing relationship between: A (McHenry sinkhole A), B (McHenry sinkhole B), C (Whose Hole Cave), and D (electrode monitoring site)

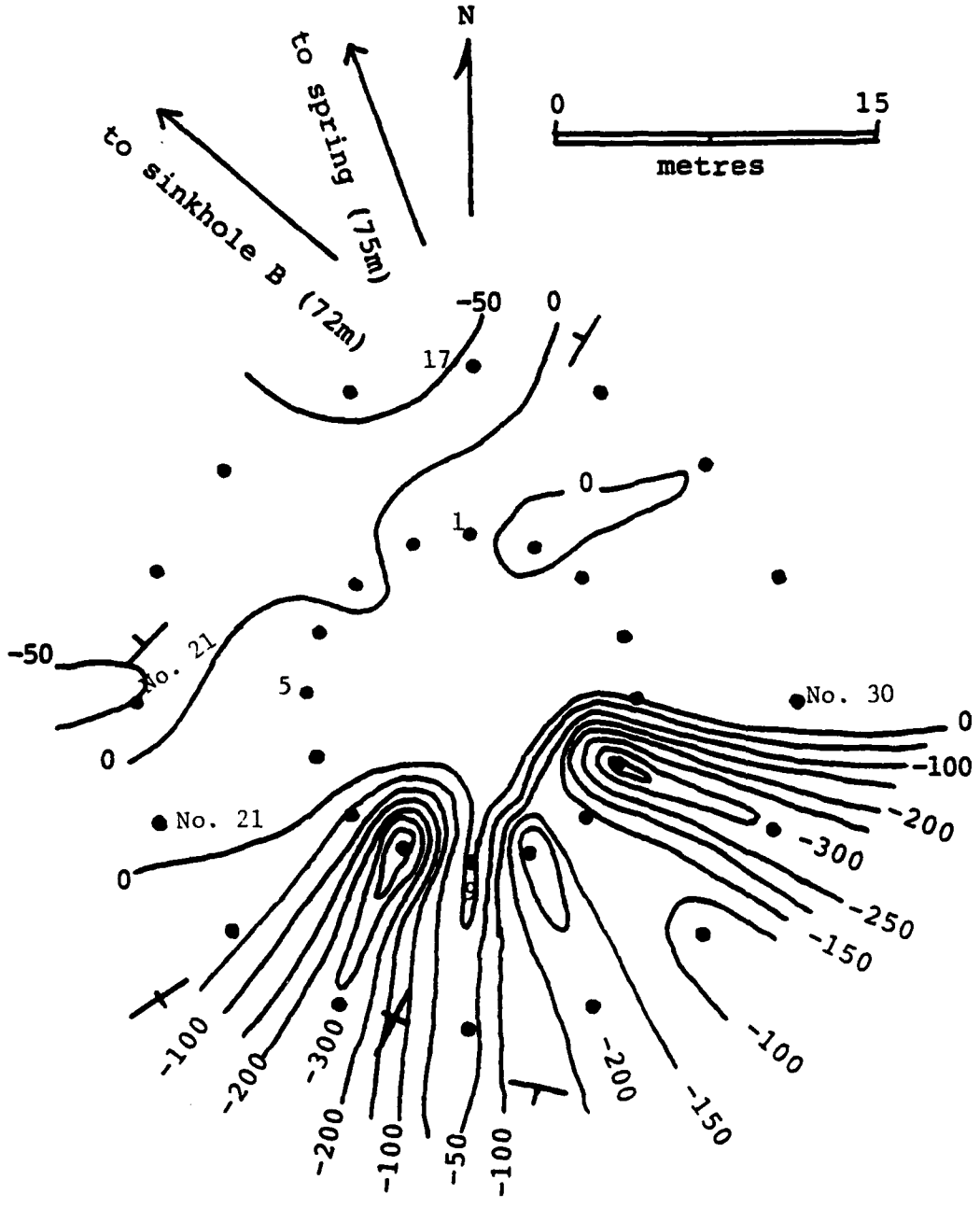

Figure 13. Electrode array and SP contours in millivolts. Strike and dip symbols indicate fault zone corresponding to anomalous SP area in southeast quadrant, McHenry sinkhole A

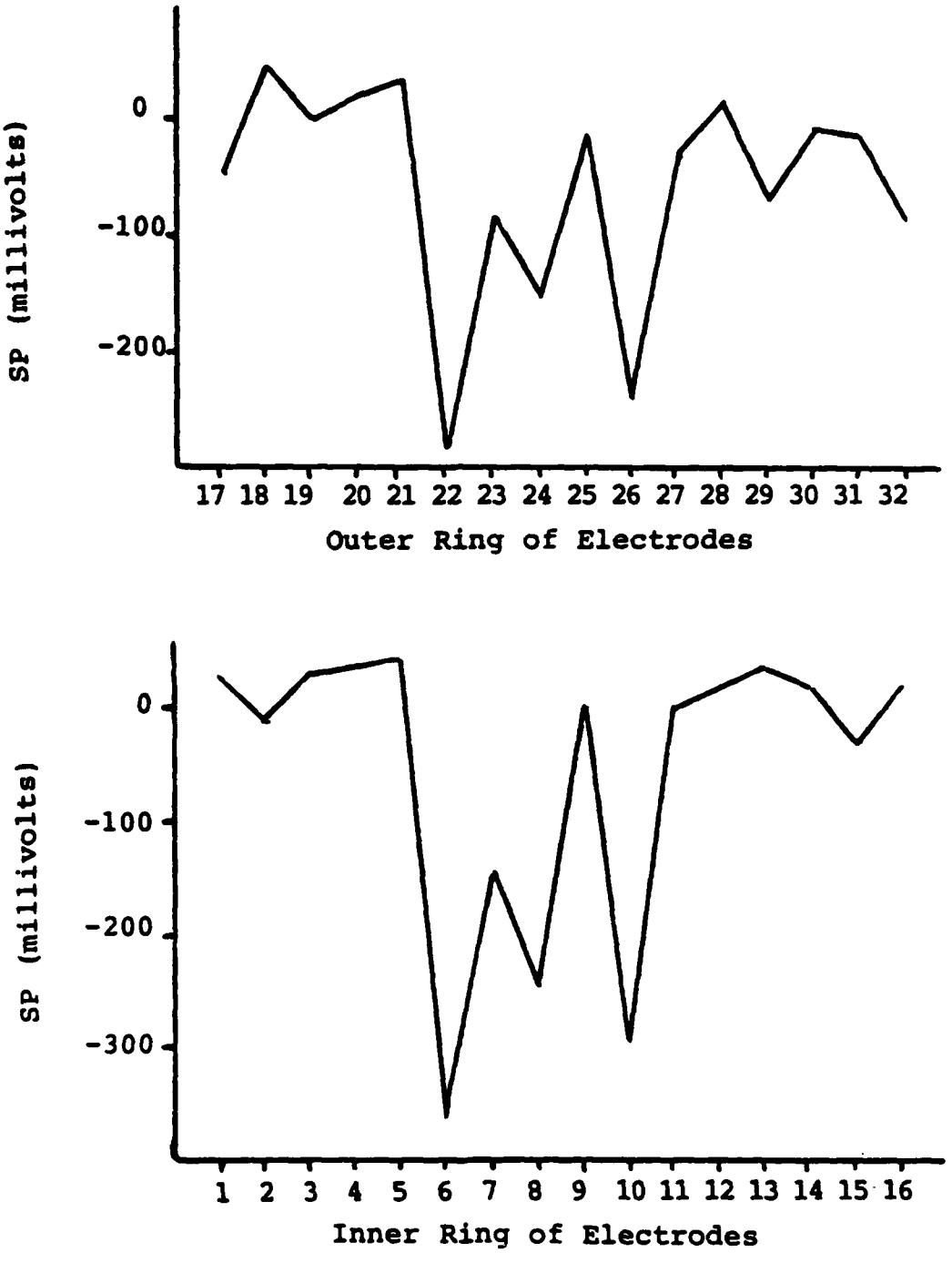

Figure 14. Correspondence of SP anomalies between the two rings of electrodes, McHenry sinkhole A. Anomalies are associated with fault zone

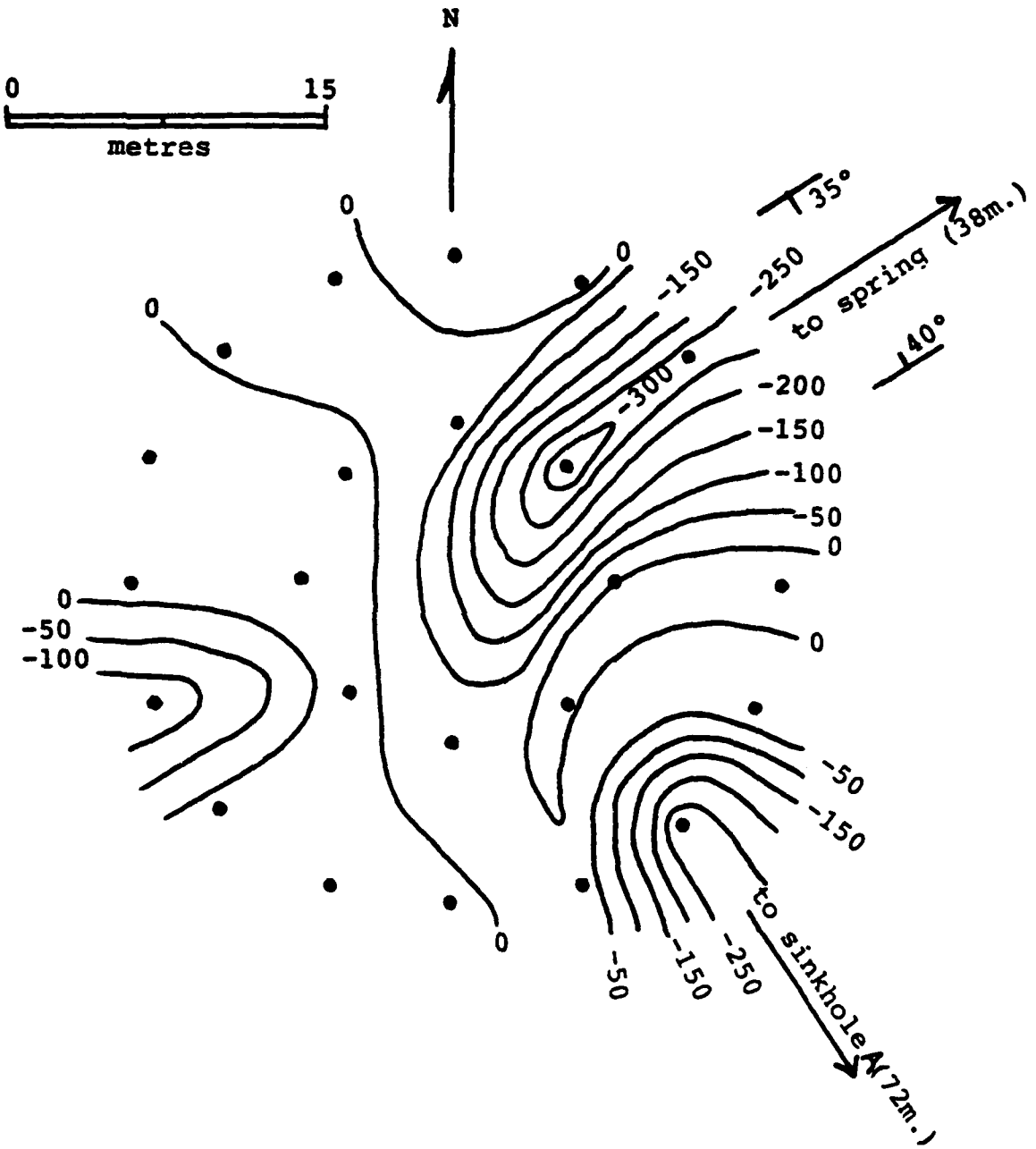

Figure 15. Electrode array and SP contours in millivolts (McHenry sinkhole B)

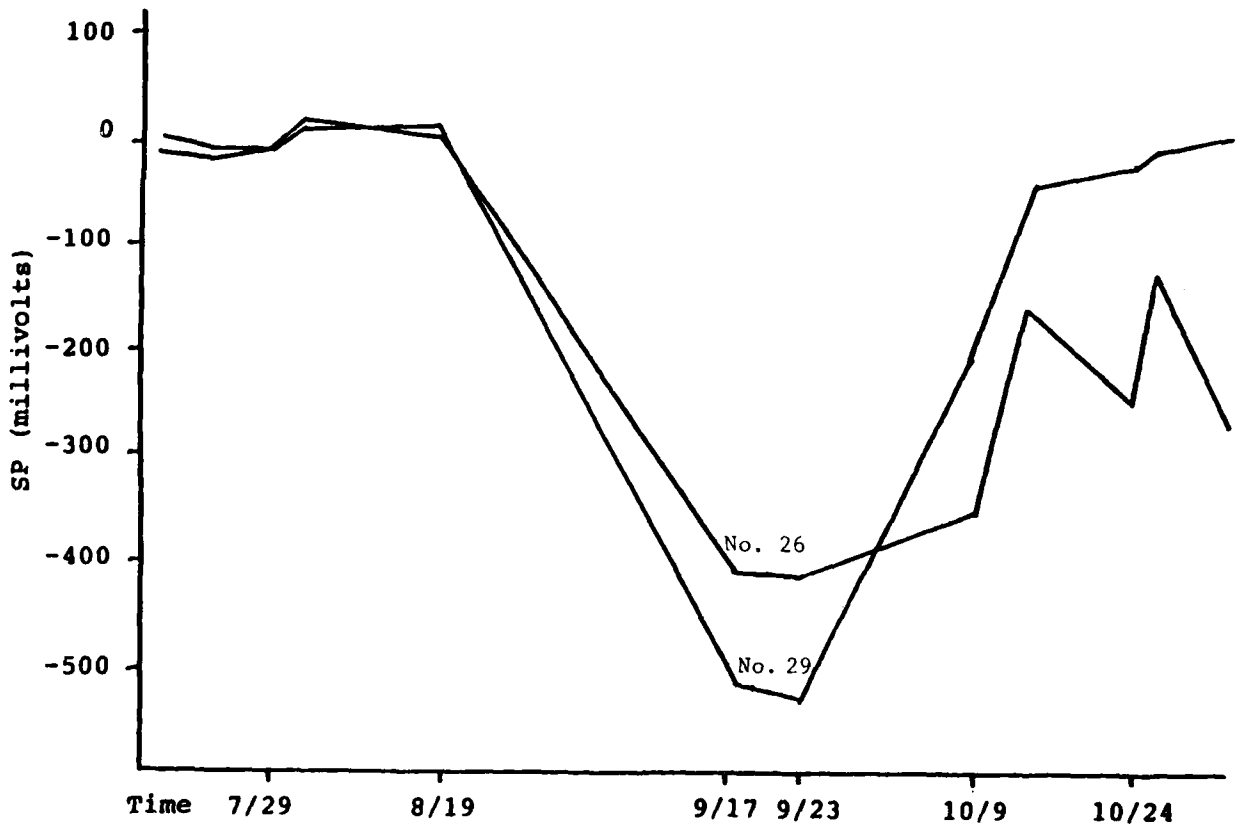

Figure 16. Short-term ephemeral anomalies for two electrodes, McHenry sinkhole A

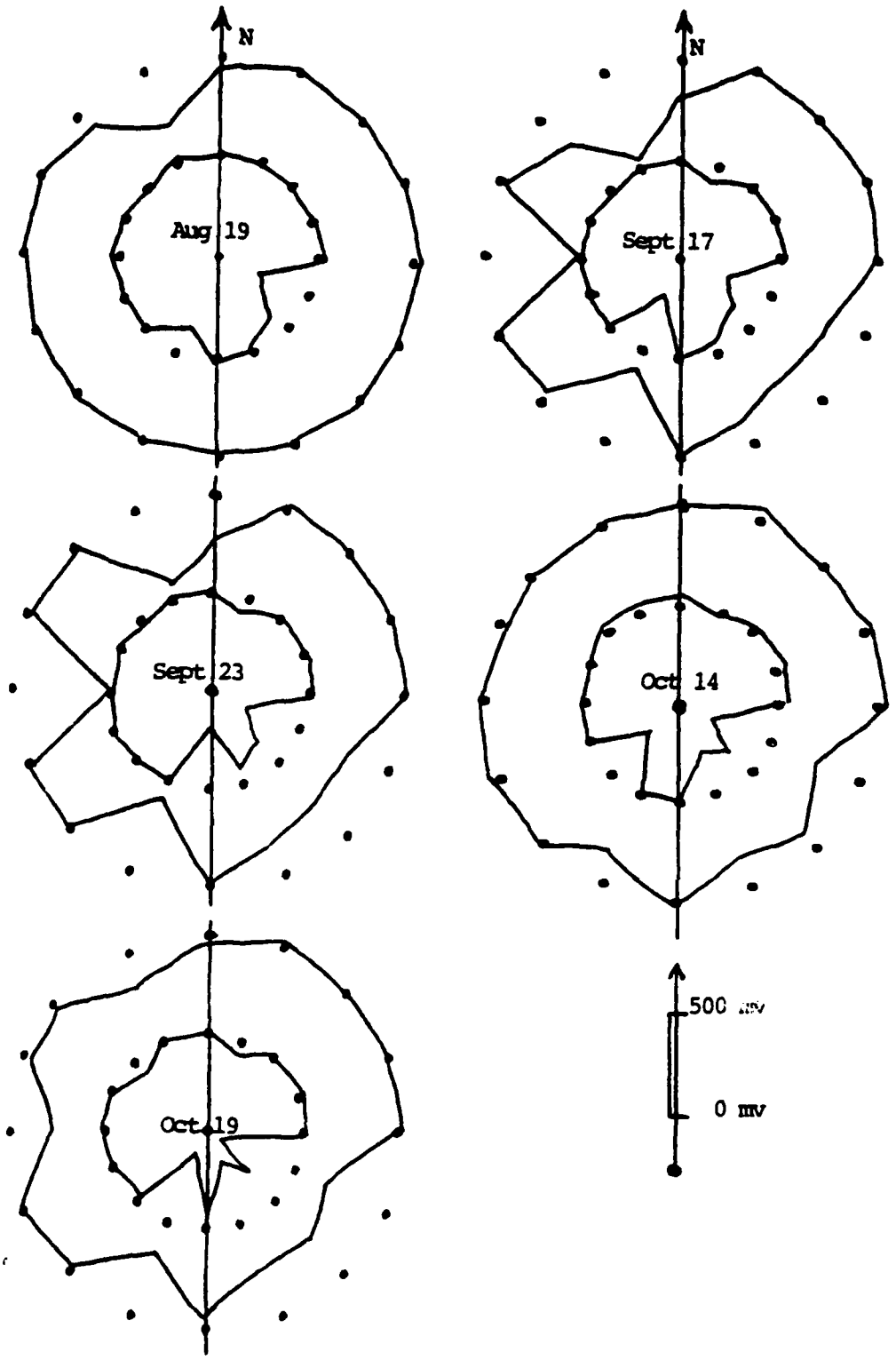

Figure 17. Polar plot of SP for various dates showing ephemeral anomalies in September, McHenry sinkhole A

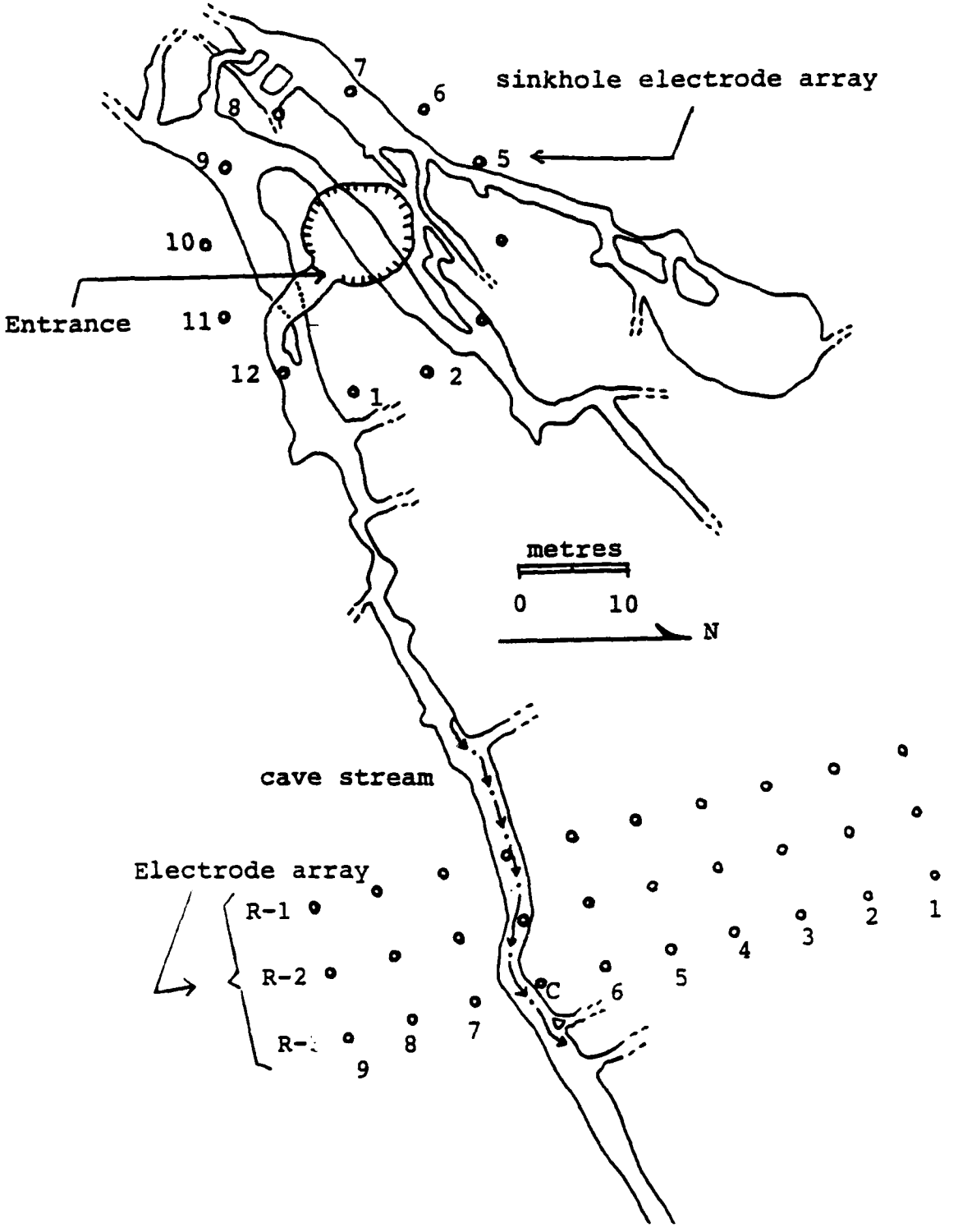

Figure 18. Plan of Whose Hole Cave, showing electrode arrays emplaced on the surface above cave

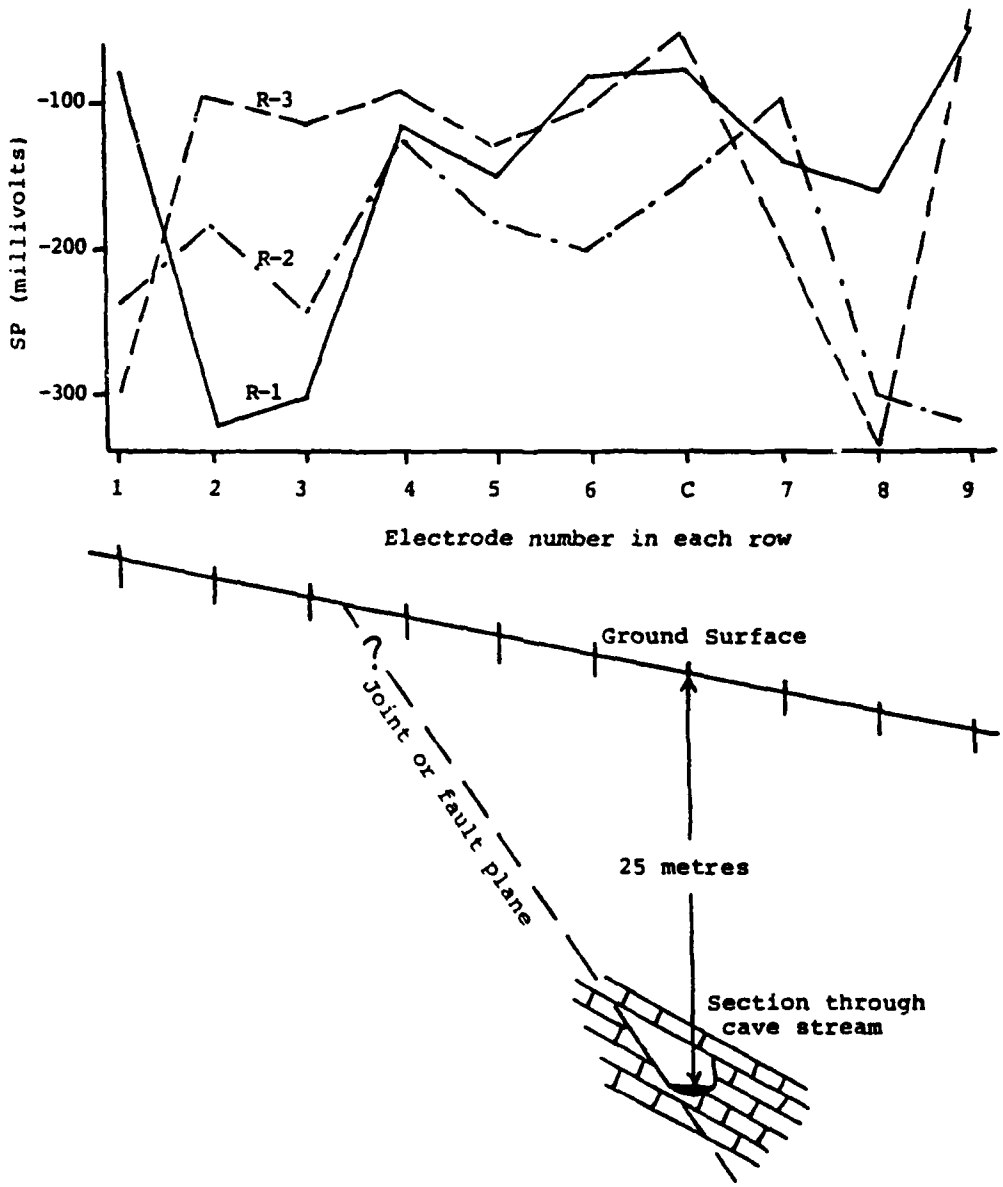

Figure 19. SP for the array of three rows (R-1, R-2, R-3) of electrodes above cave stream passage, showing dip of bedrock and influence of joint or fault plane

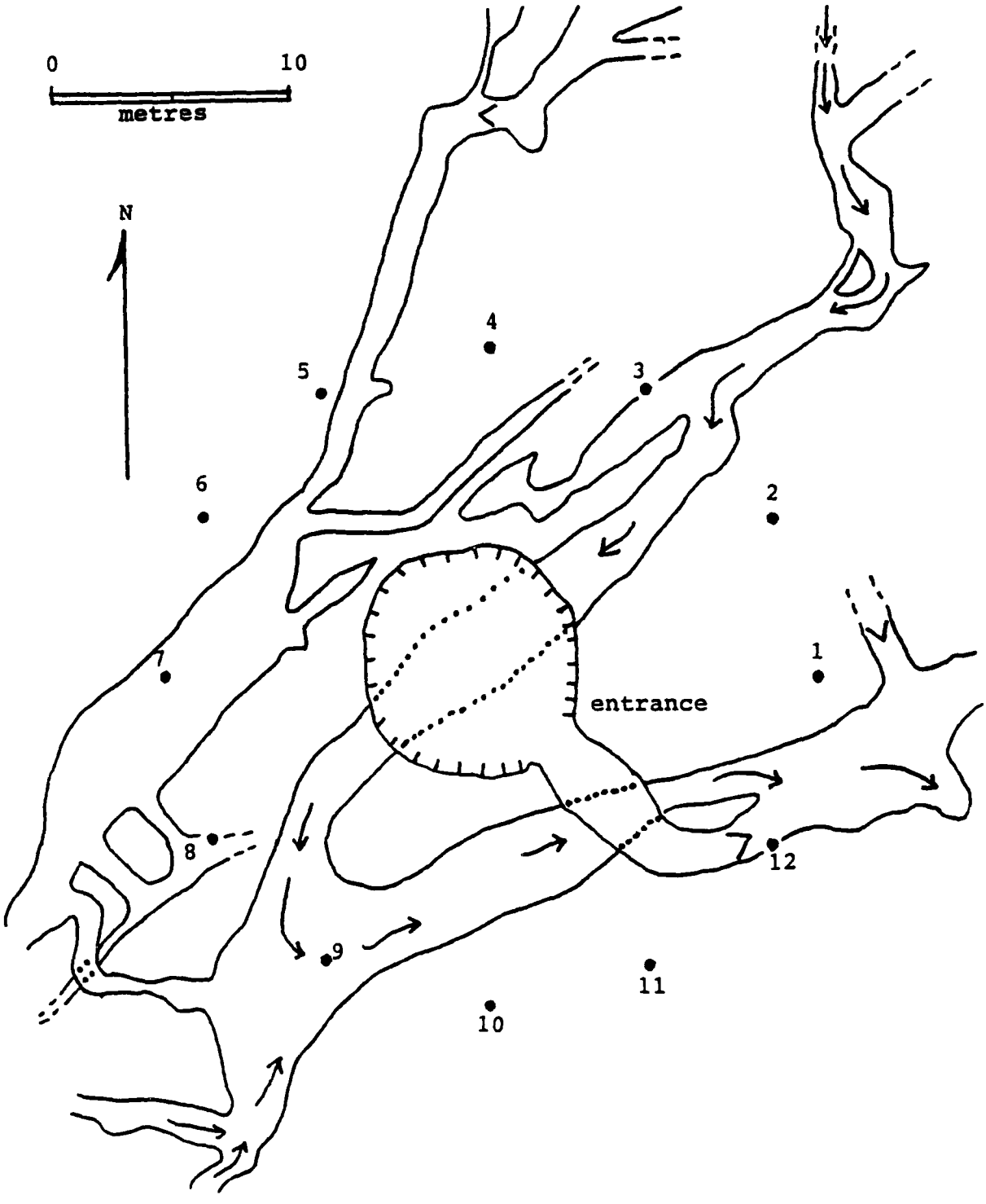

Figure 20. Array of 12 electrodes at entrance sinkhole over Whose Hole Cave (Arrows indicate direction of intermittent seepage flow into and through the cave)

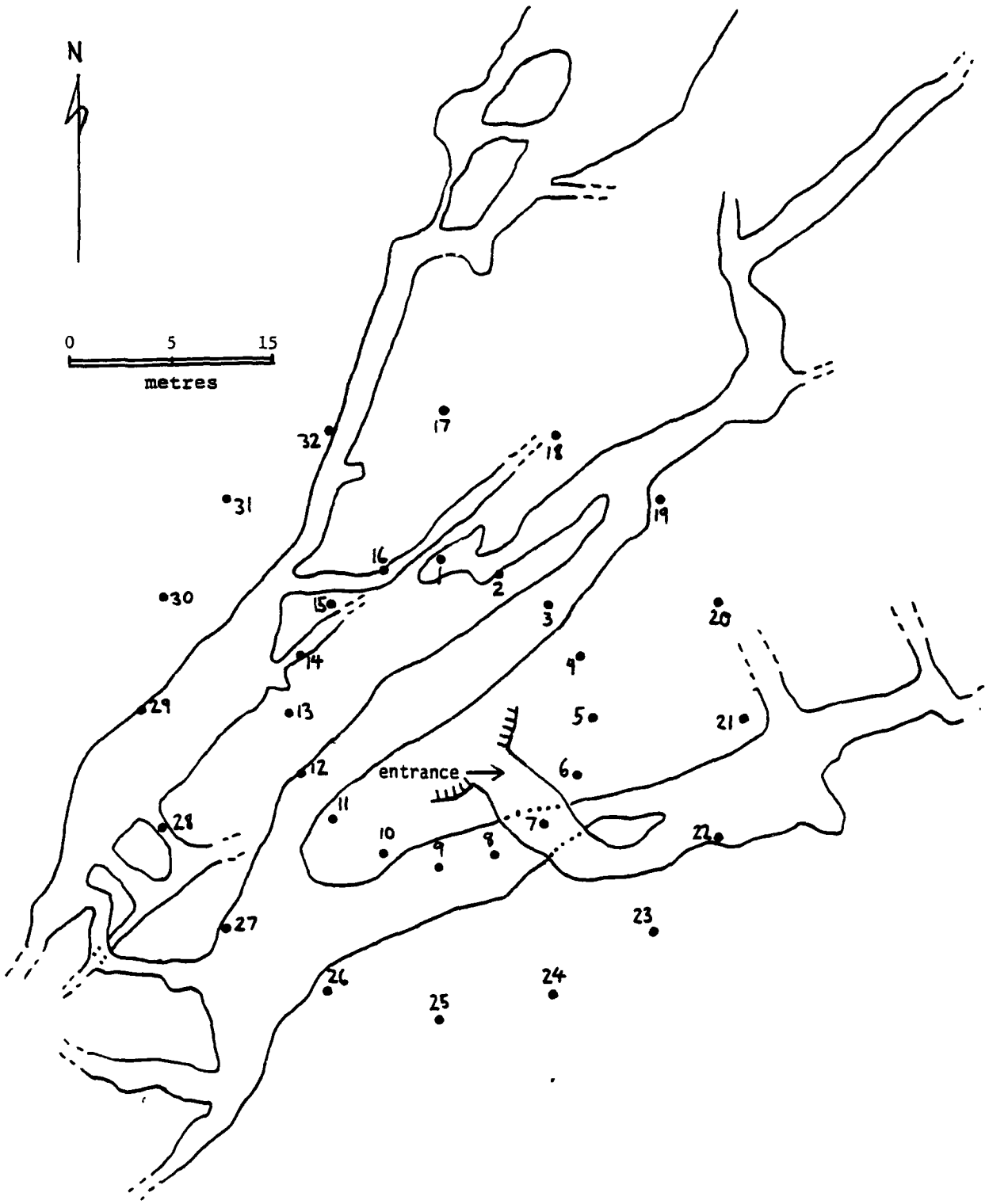

Figure 21. Map of Whose Hole Cave showing location of 32 SP electrodes in the entrance sinkhole

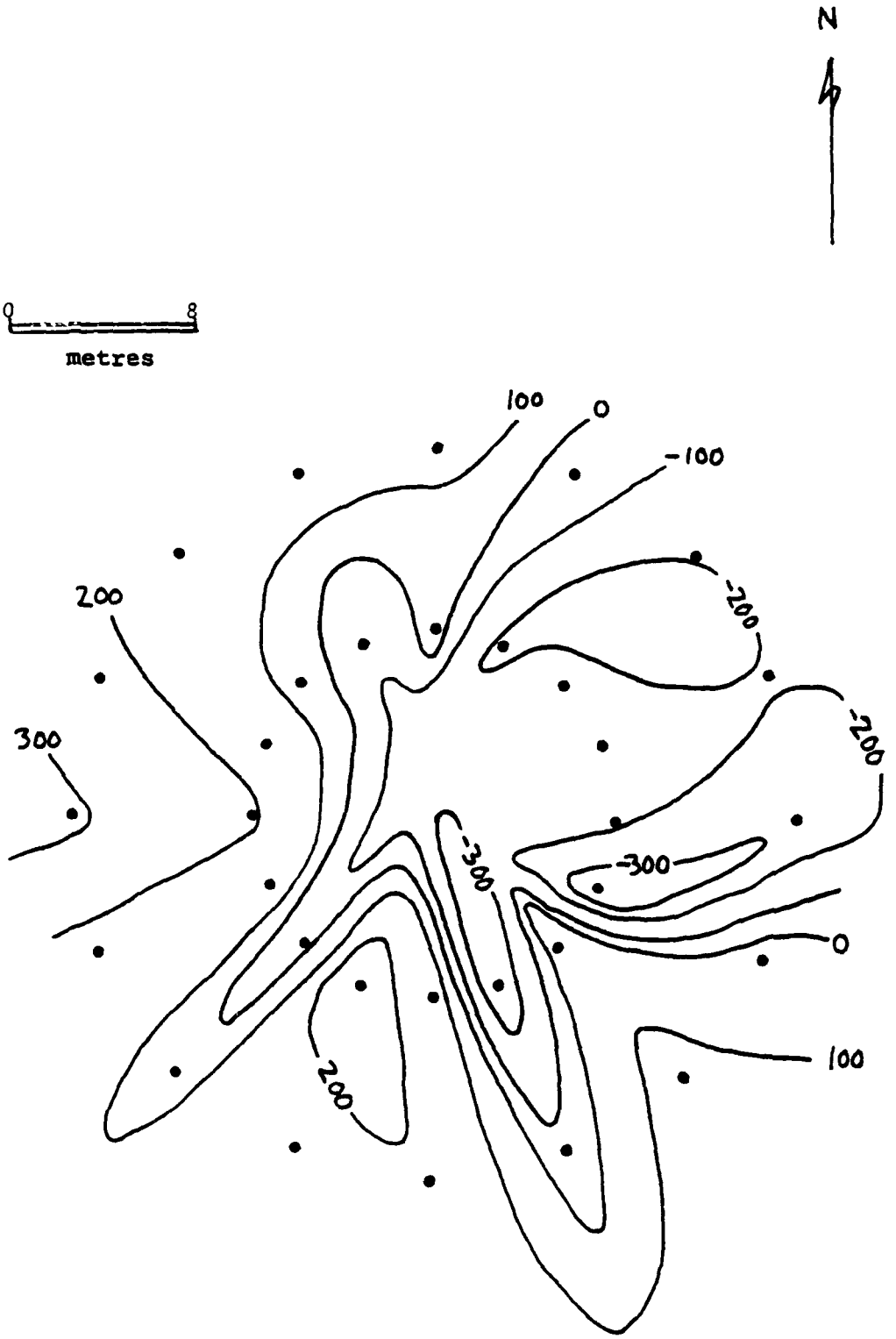

Figure 22. SP contours (in millivolts) at entrance sink, Whose Hole Cave, average of values for December 1986 and January 1987. (Dots are electrode locations for 32 electrode array)

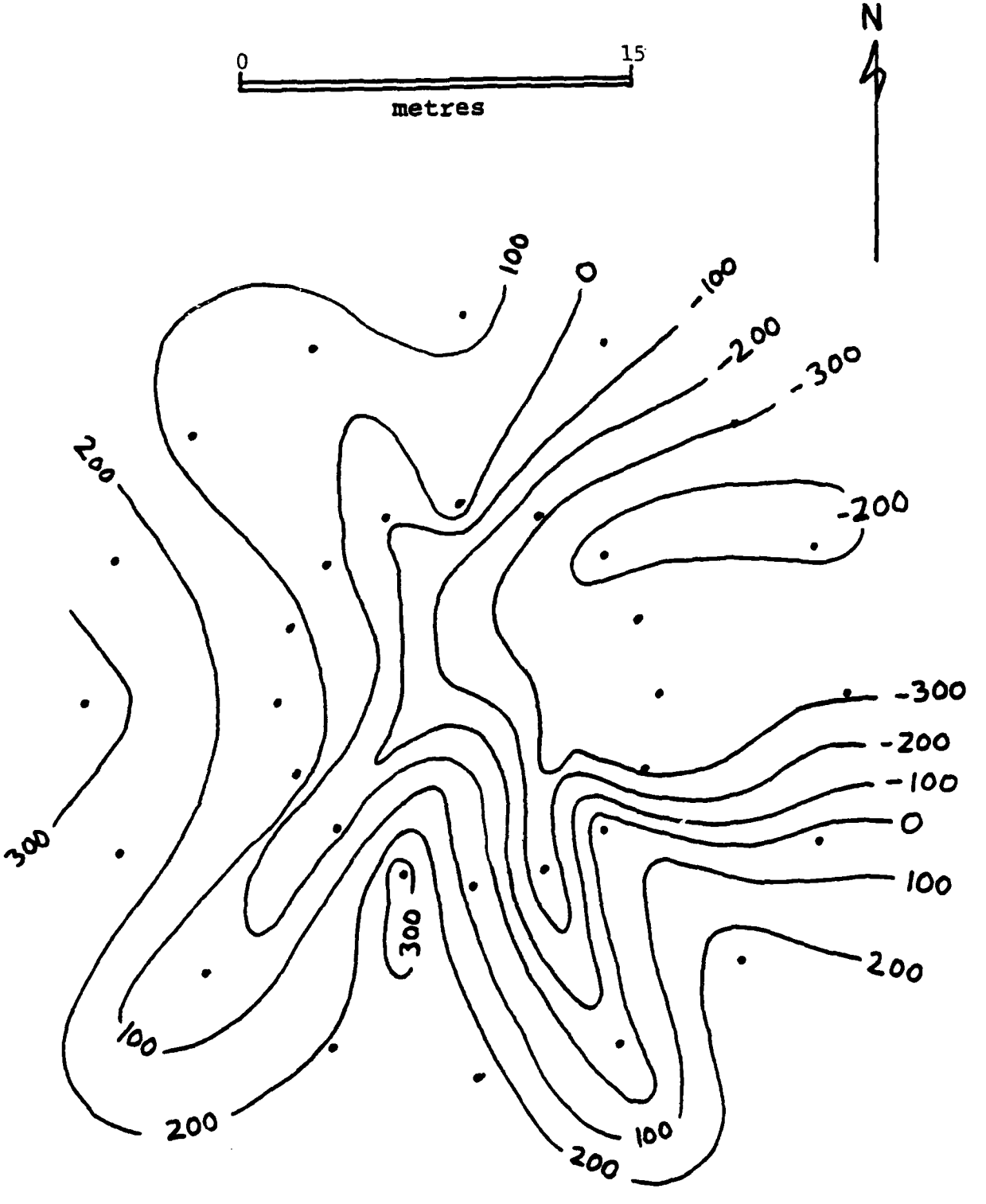

Figure 23. SP values contour map (in millivolts), Whose Hole Cave sinkhole electrode array, 5 February 1987

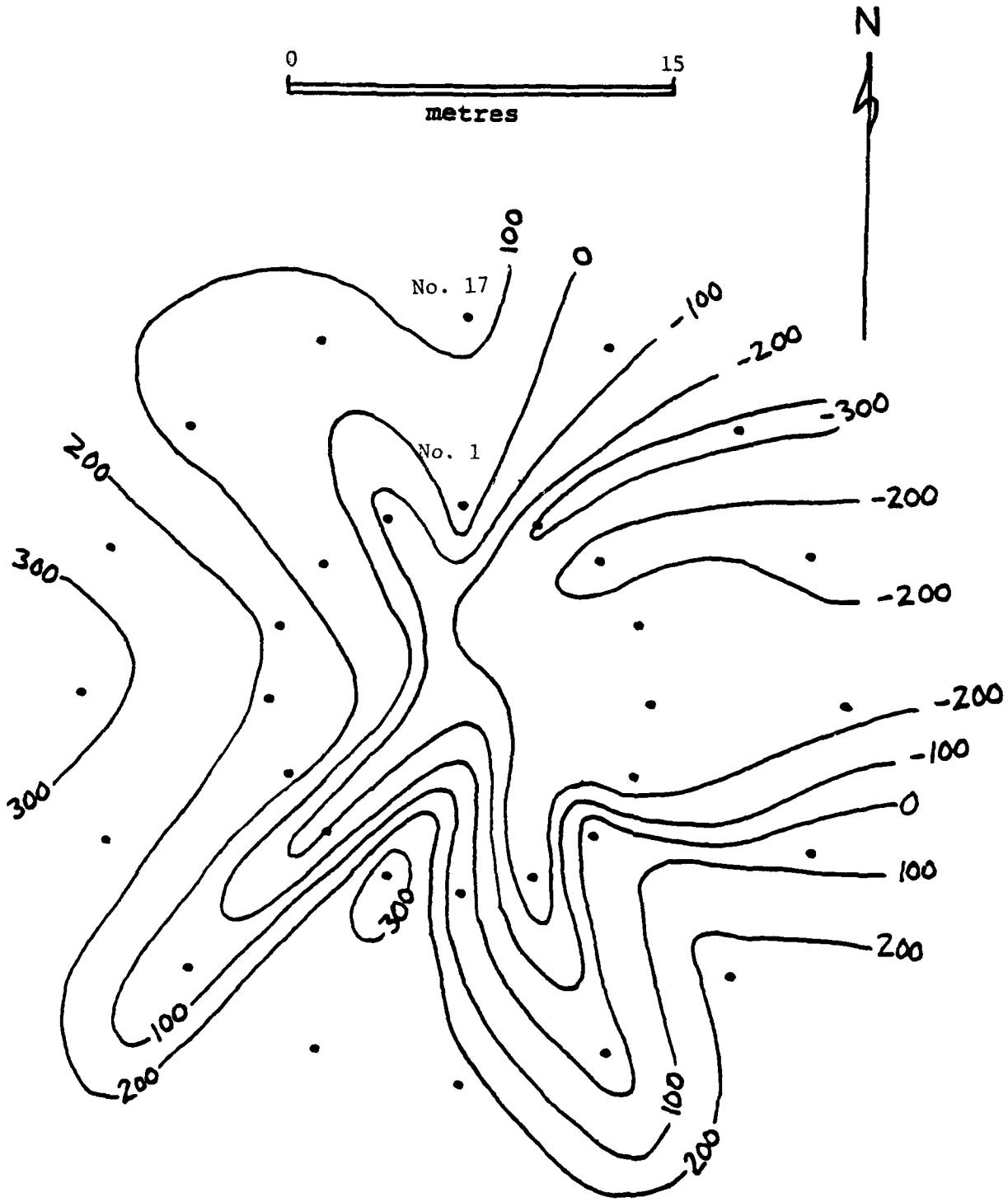

Figure 24. SP values contour map (in millivolts) Whose Hole Cave sinkhole electrode array (32 electrodes), 3 March 1987

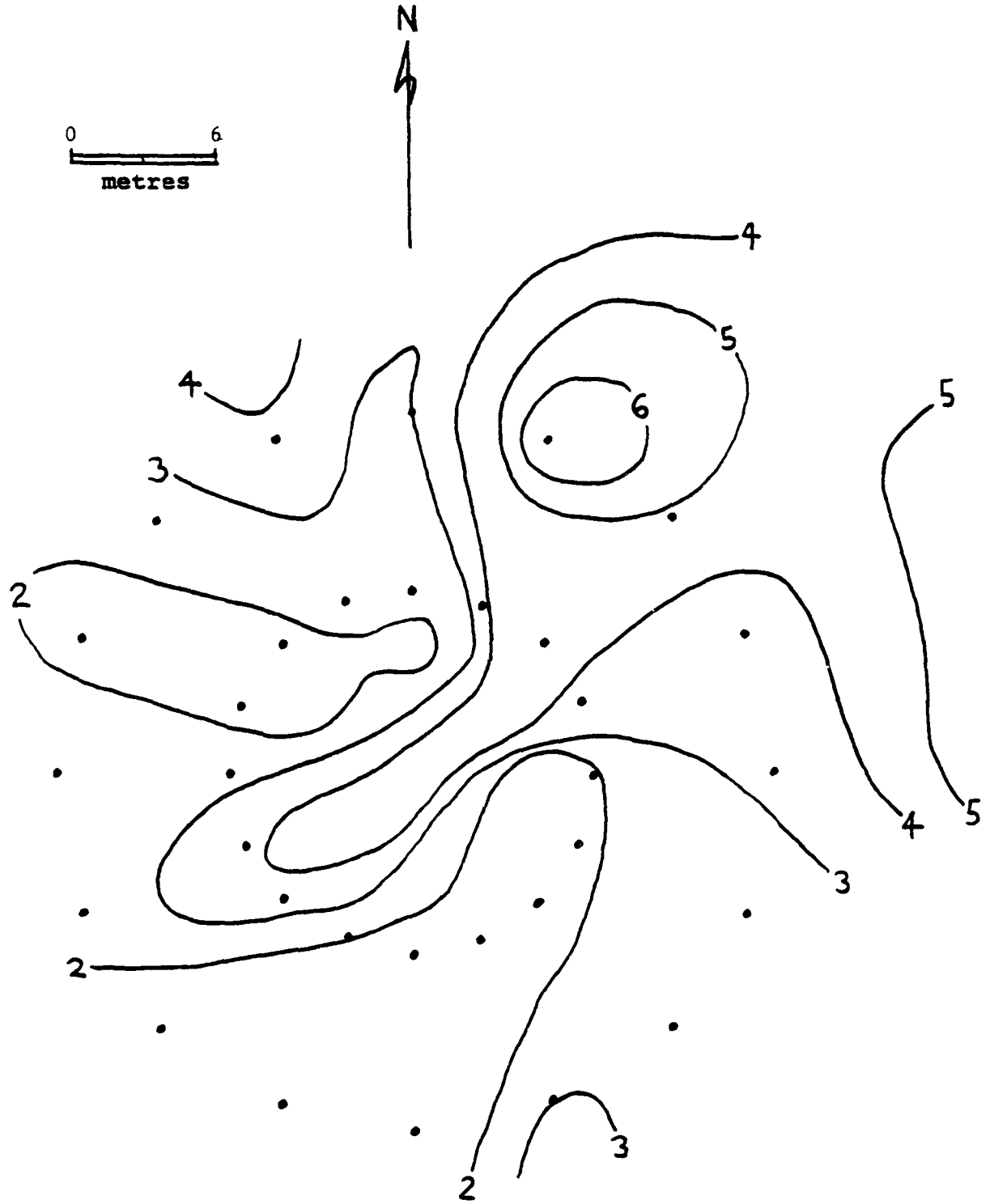

Figure 25. EM terrain conductivity survey at 10-m depth in entrance sinkhole at Whose Hole Cave. Contours are in mmhos/m and the concentric dots are the 32 SP electrodes in the array, February 1987

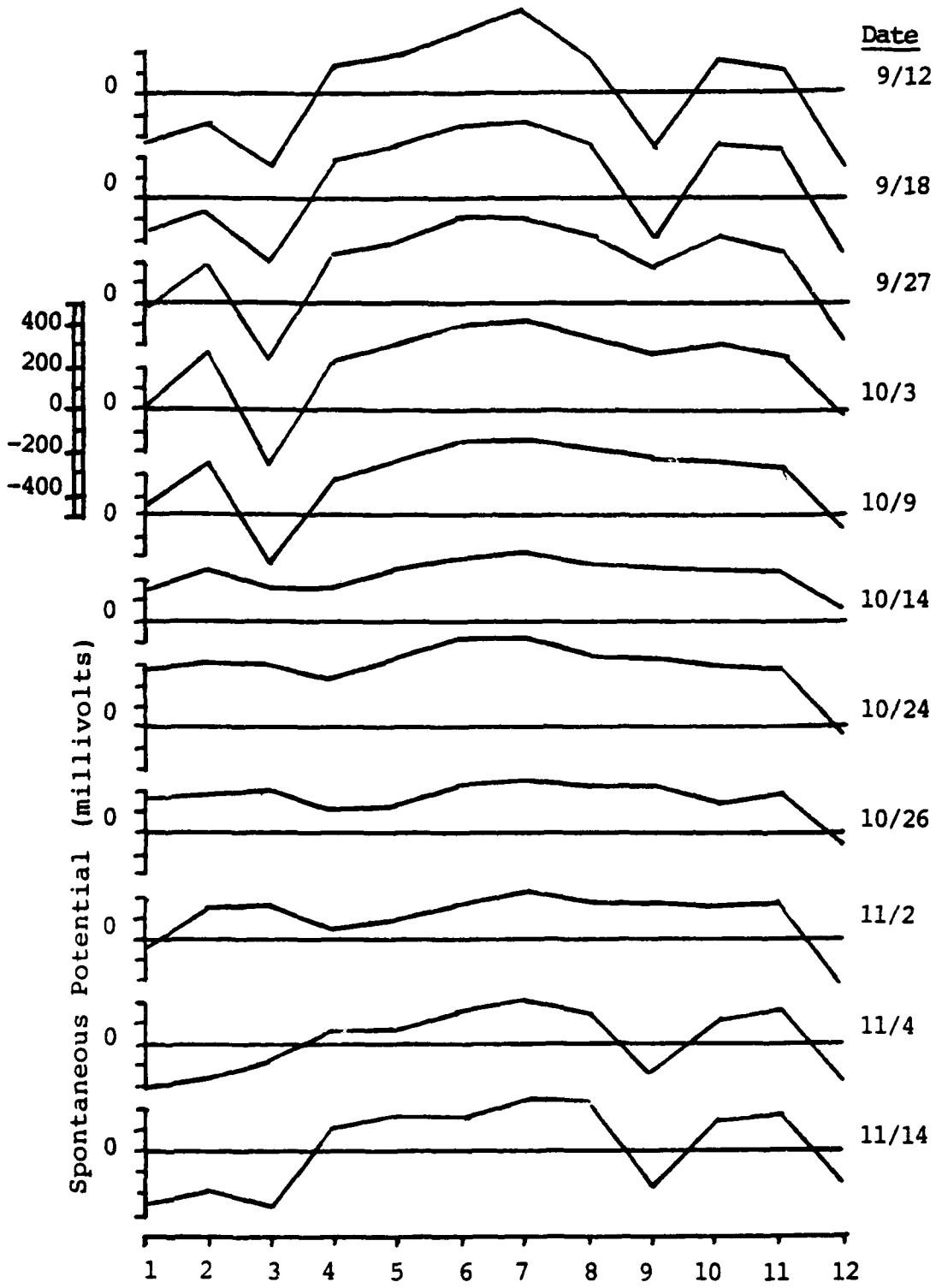

Figure 26. SP changes at sinkhole entrance, Whose Hole Cave, September to November 1986 (Loss and return of anomalies correspond to drought effects)

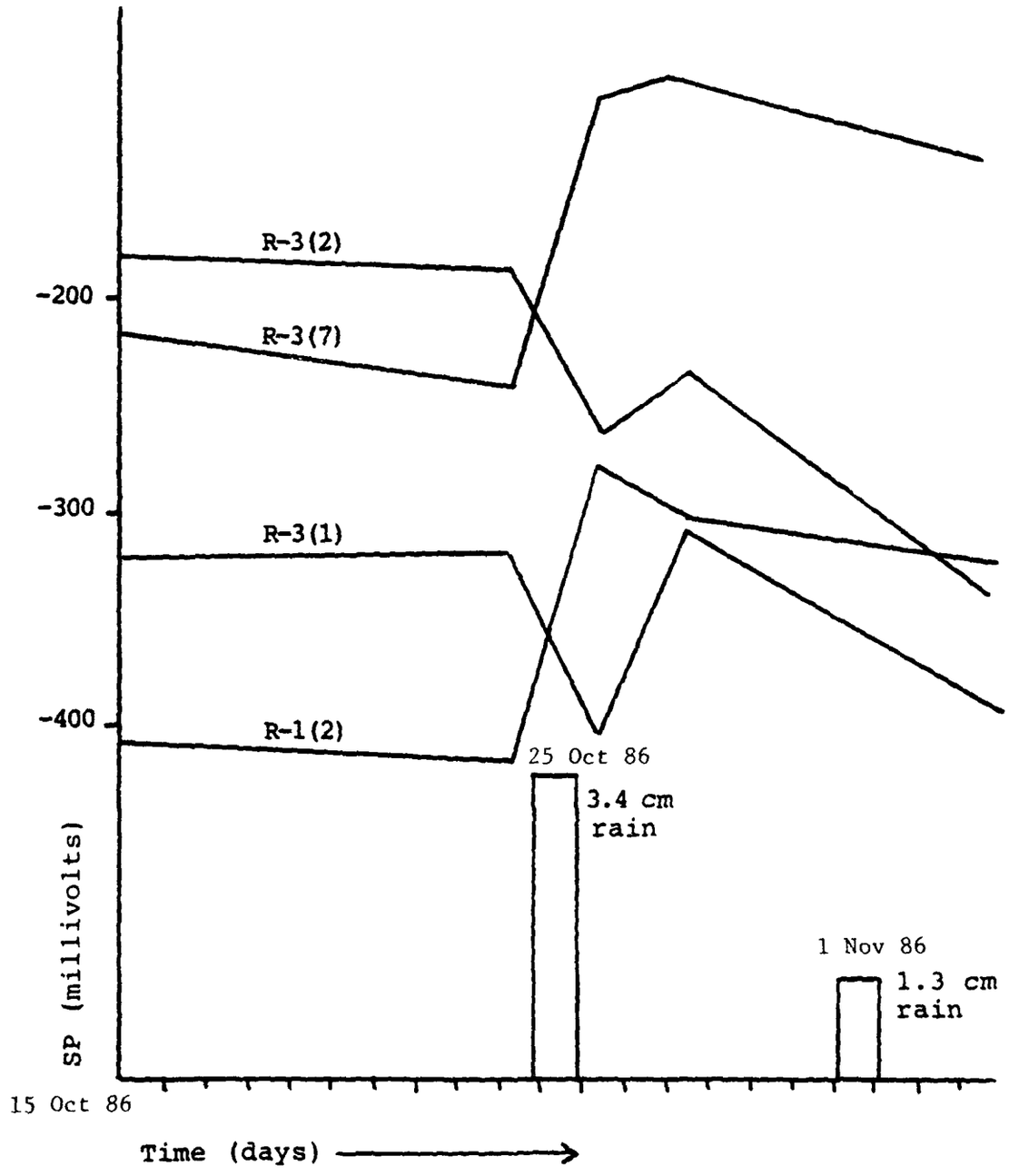

Figure 27. Varying response of four electrodes to precipitation at cave array, October 1986

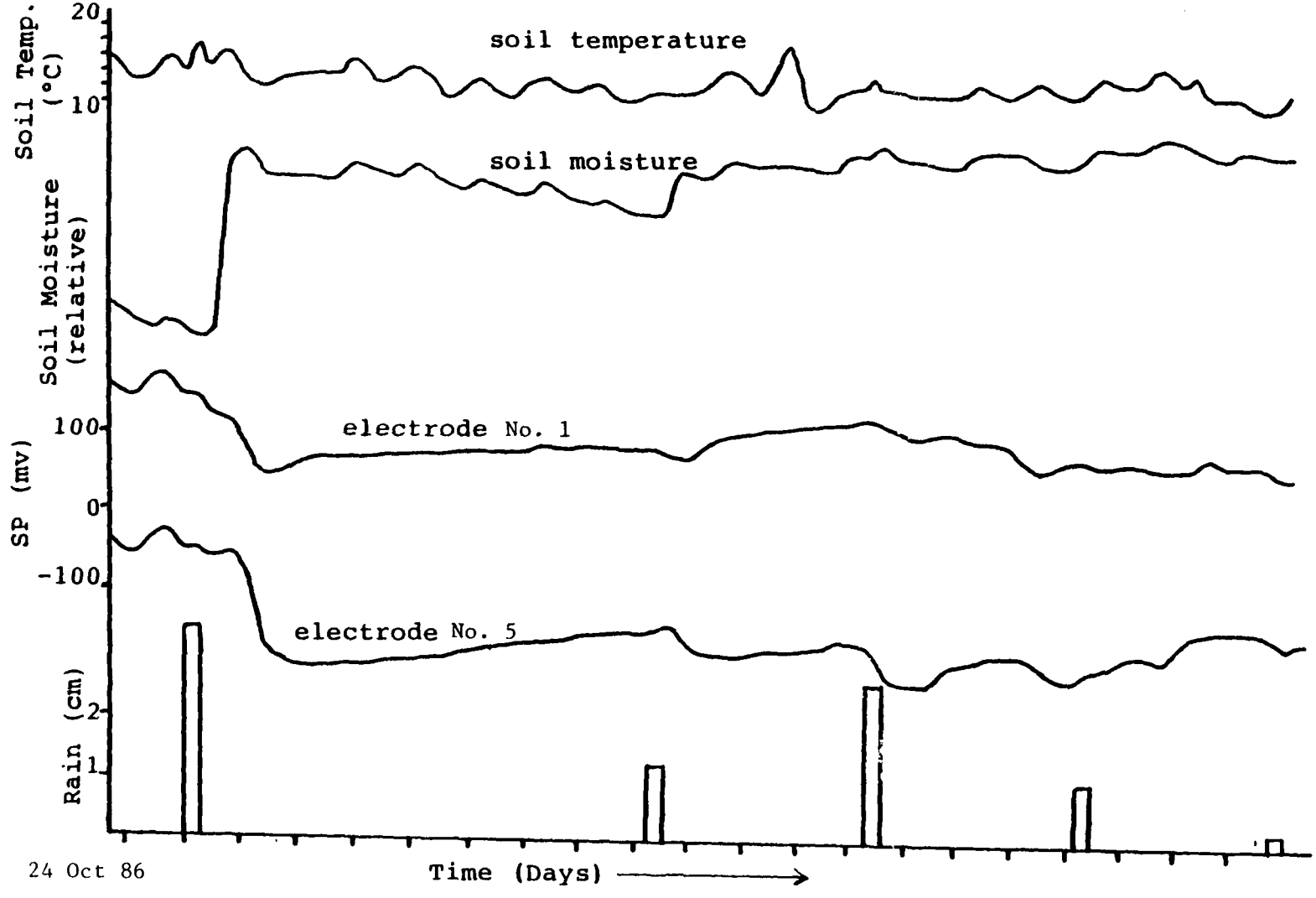

Figure 28. Record of SP for two electrodes at monitoring site showing relationship to changes in soil temperature, soil moisture, and precipitation

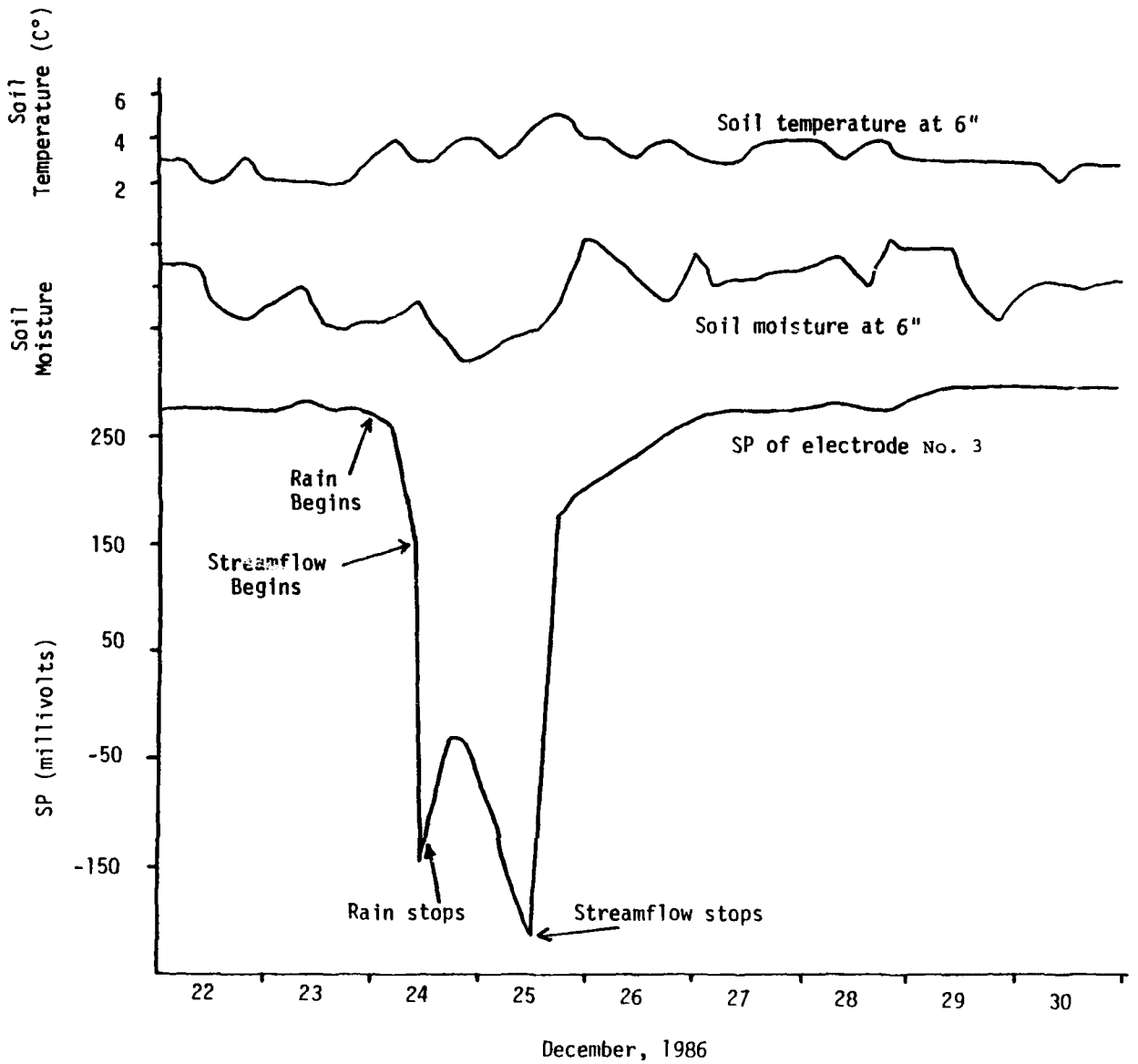

Figure 29. ACD data from electrode monitoring site showing soil temperature, soil moisture, and SP response of electrode No. 3 (in streambed) to rainfall of 2.5 in. in 24 hr

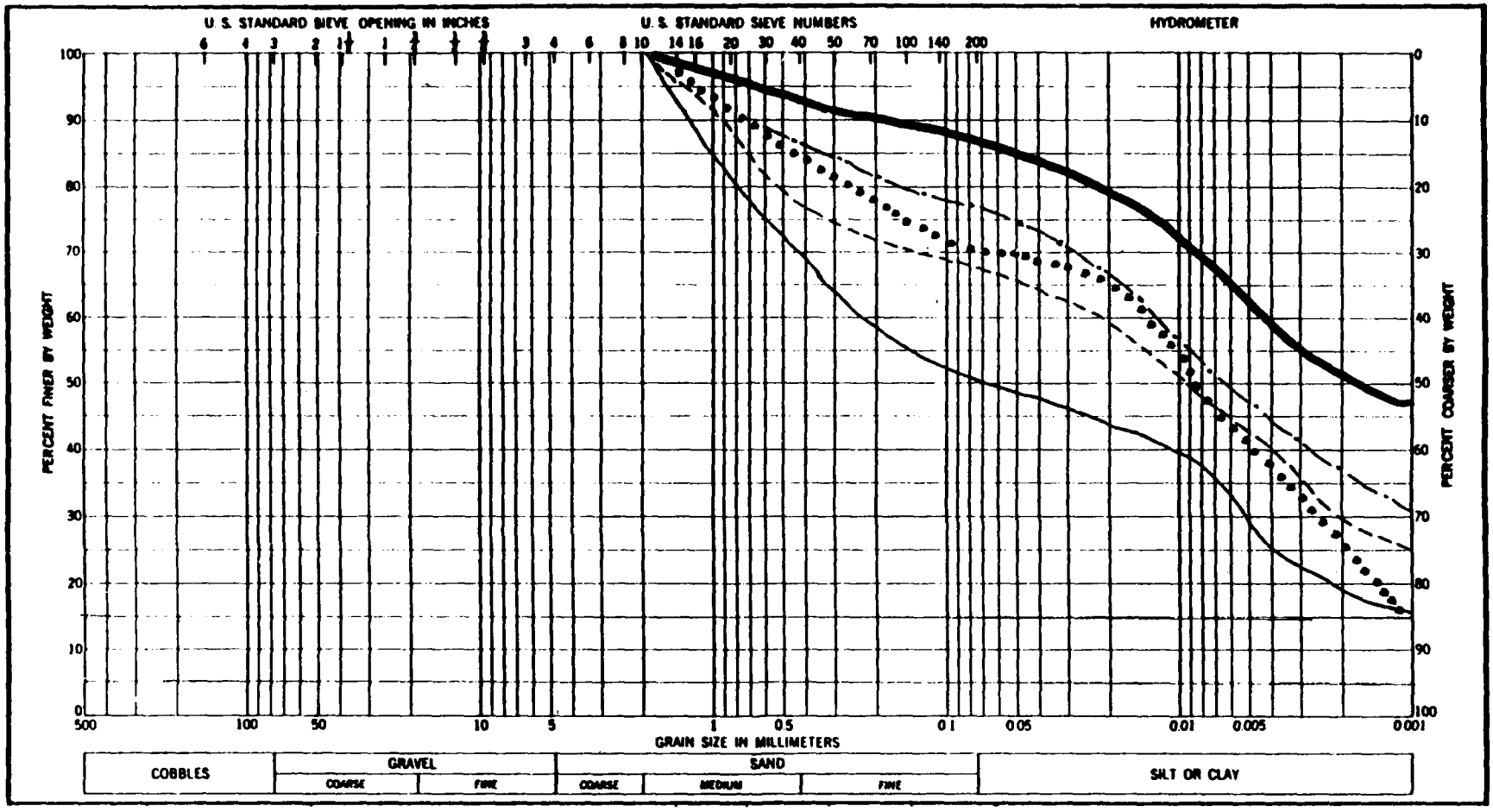

Electrode No. 1
Electrode No. 2
Electrode No. 3
Electrode No. 4
Electrode No. 5

Figure 30. Soil particle size gradation curves from hydrometer analysis of the five SP electrode sites used in the long-term monitoring experiment. Electrode No. 5 was always negative and its location shows greatest clay fraction

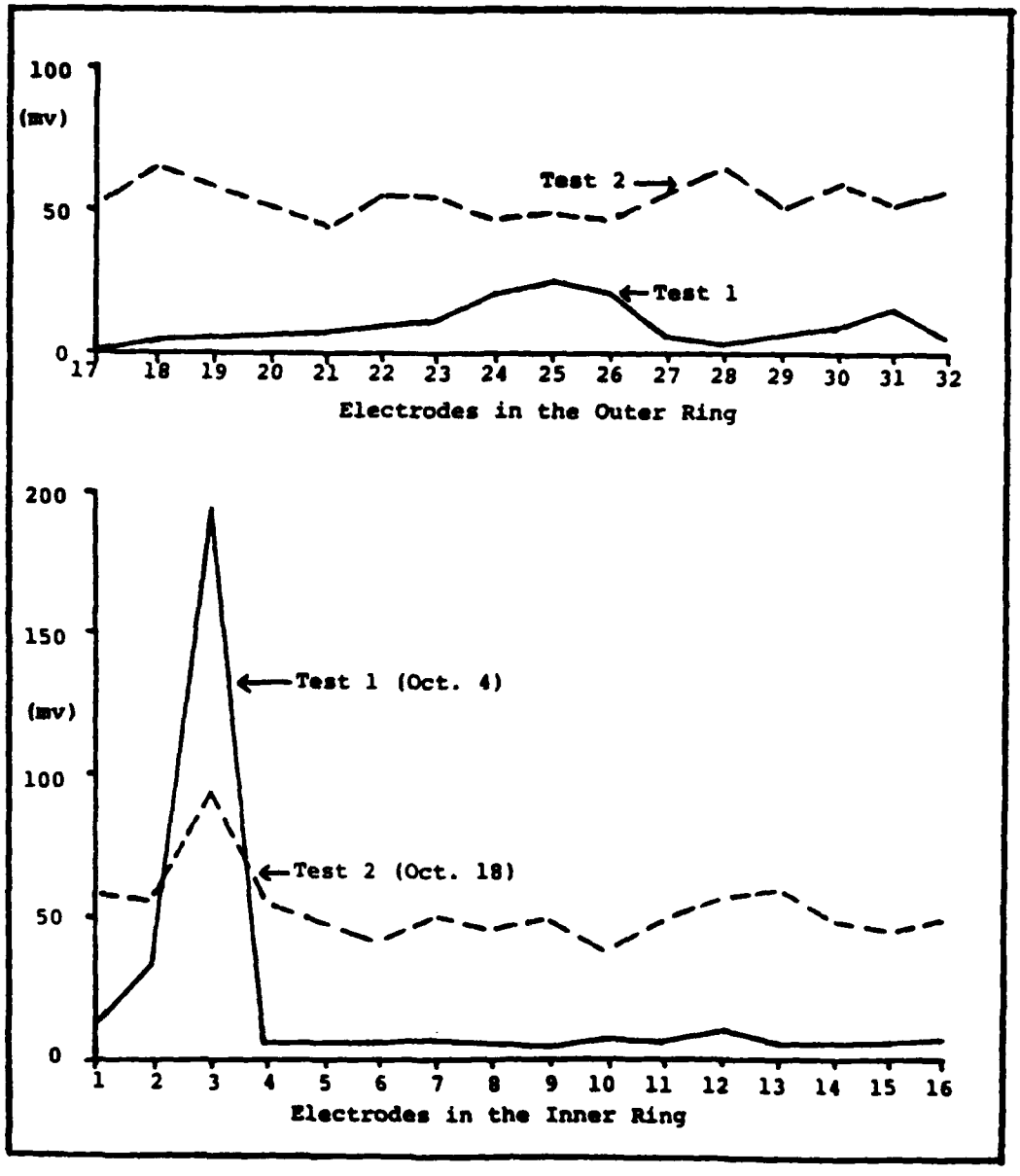

Figure 31. Change in SP induced by water discharge tests at Moore sinkhole

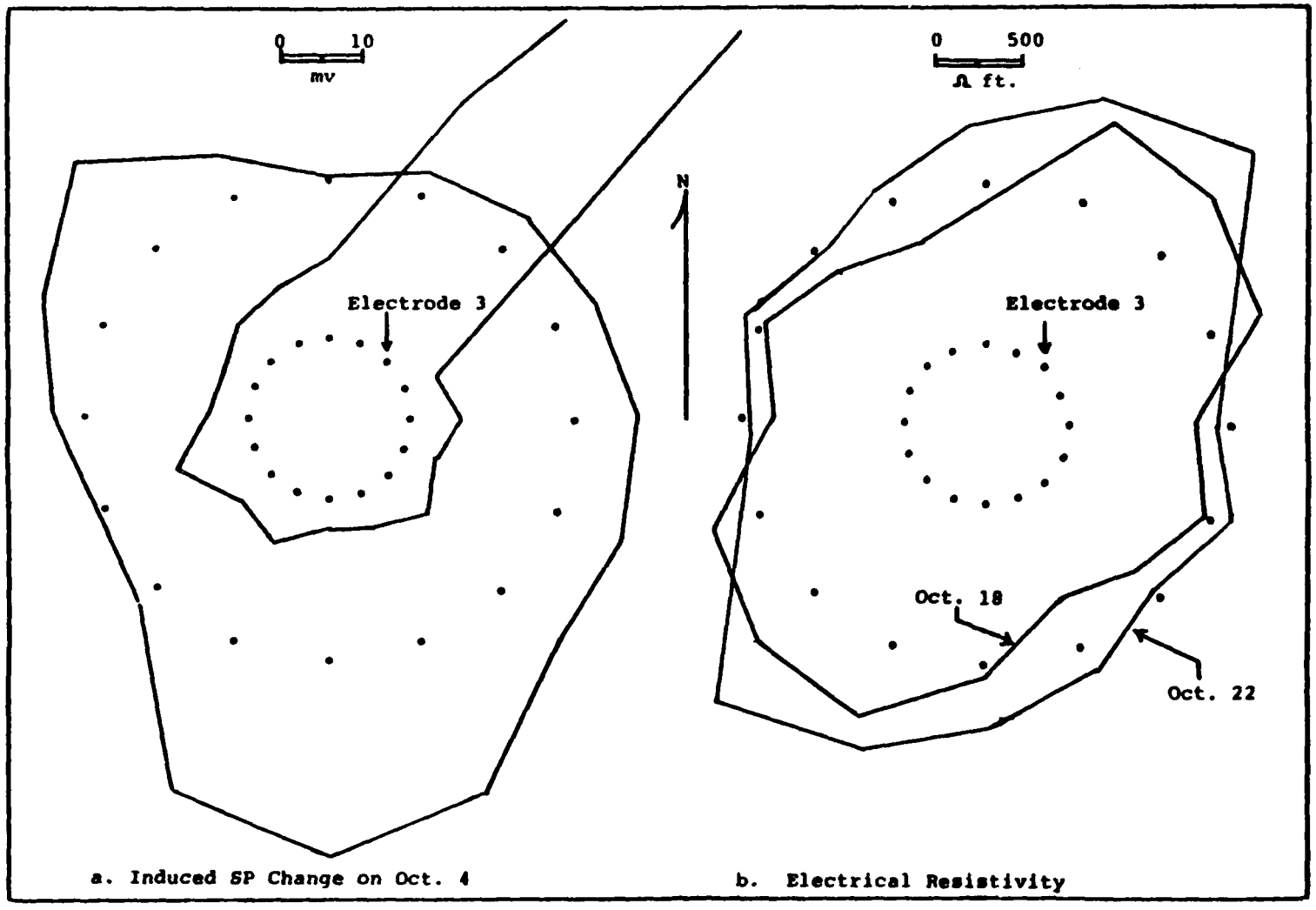

Figure 32. Polar (radial) plots of data from Moore sinkhole

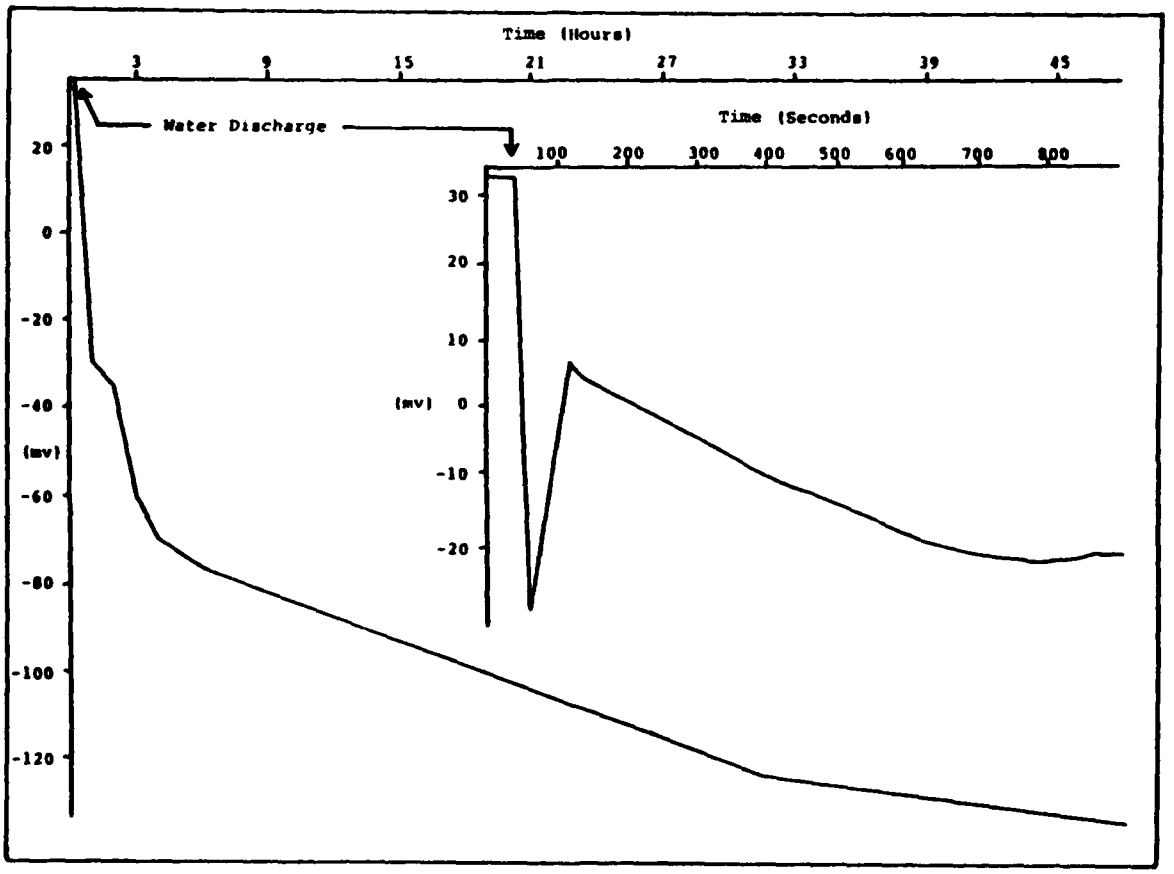

Figure 33. SP response of electrode No. 3 to water discharge test at Moore sinkhole, 4 October

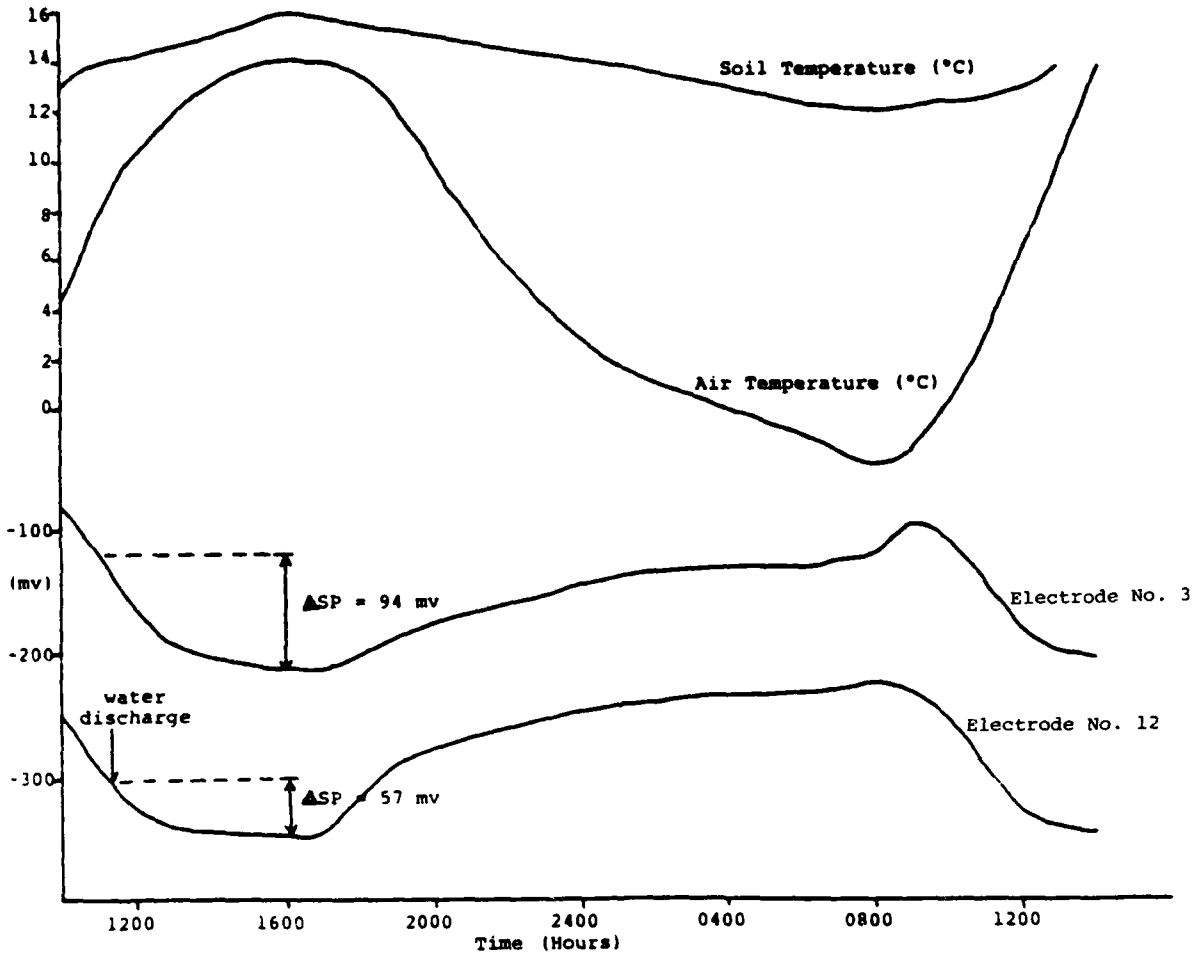

Figure 34. SP at Moore sinkhole showing change in SP induced by water discharge test and the influence of temperature, 18 and 19 October 1986

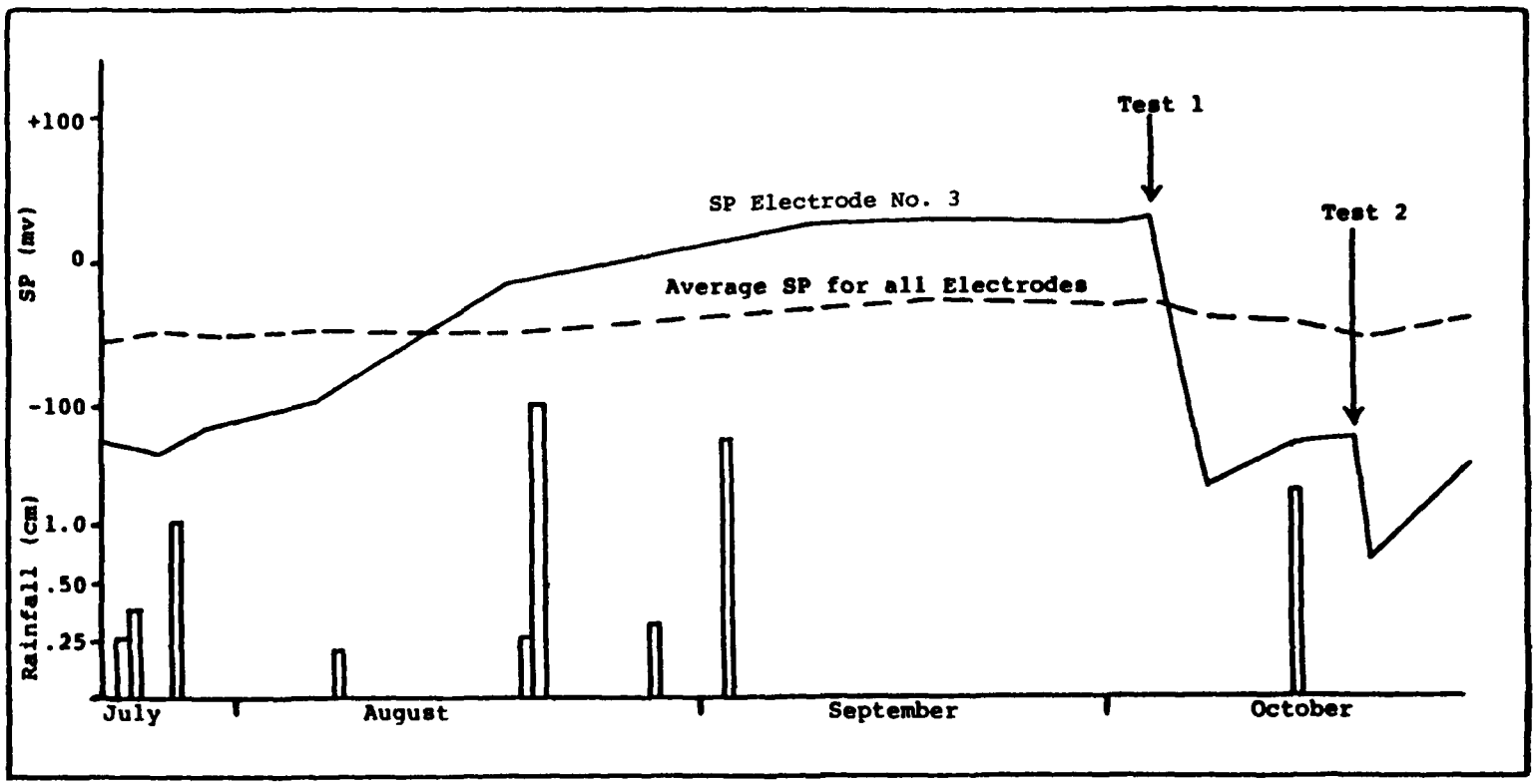

Figure 35. Precipitation and SP record for Moore sinkhole, showing effects of two water discharge tests on SP

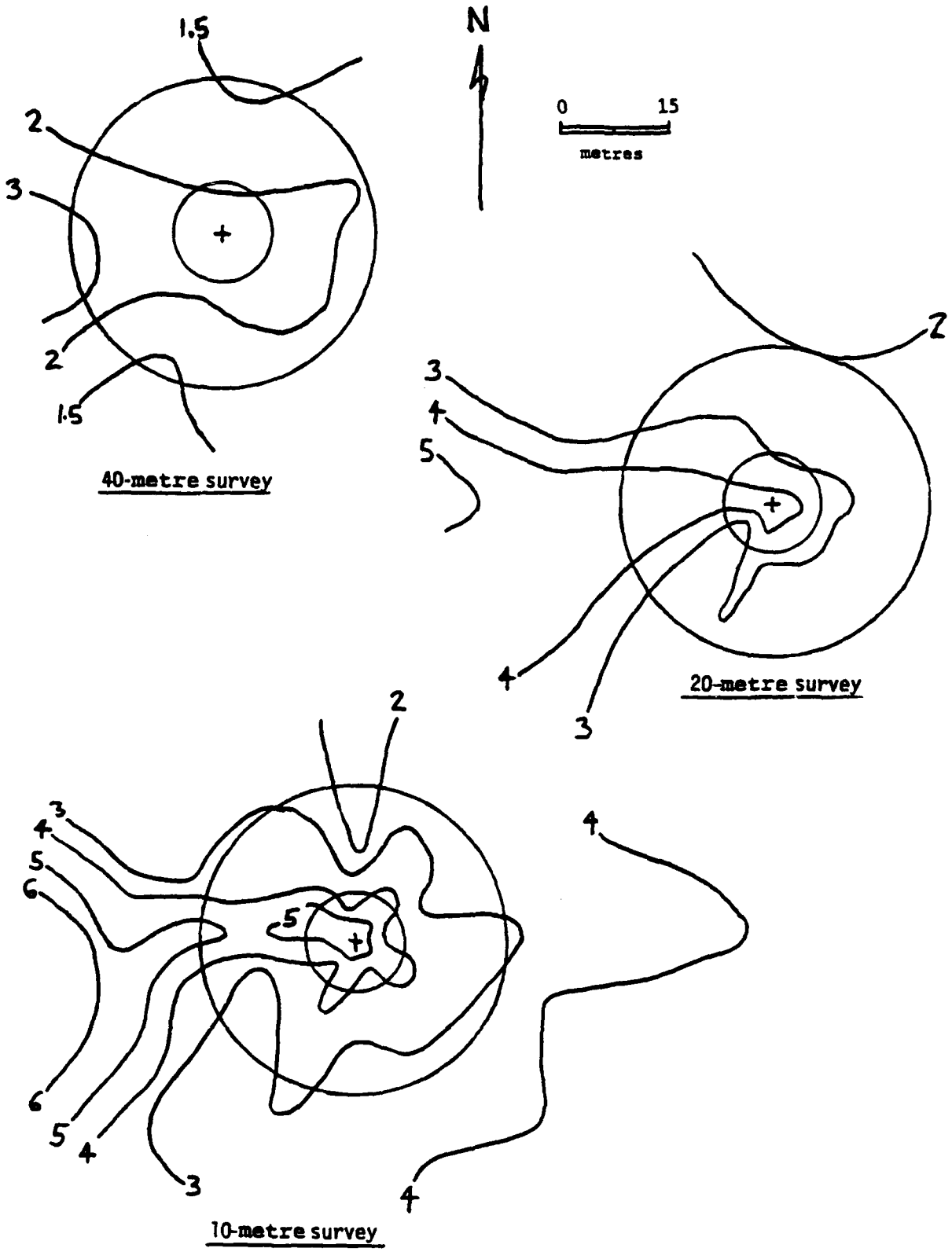

Figure 36. EM conductivity surveys at Moore sinkhole A, December 1986, contours in mmhos/m (Circles are SP electrode arrays)

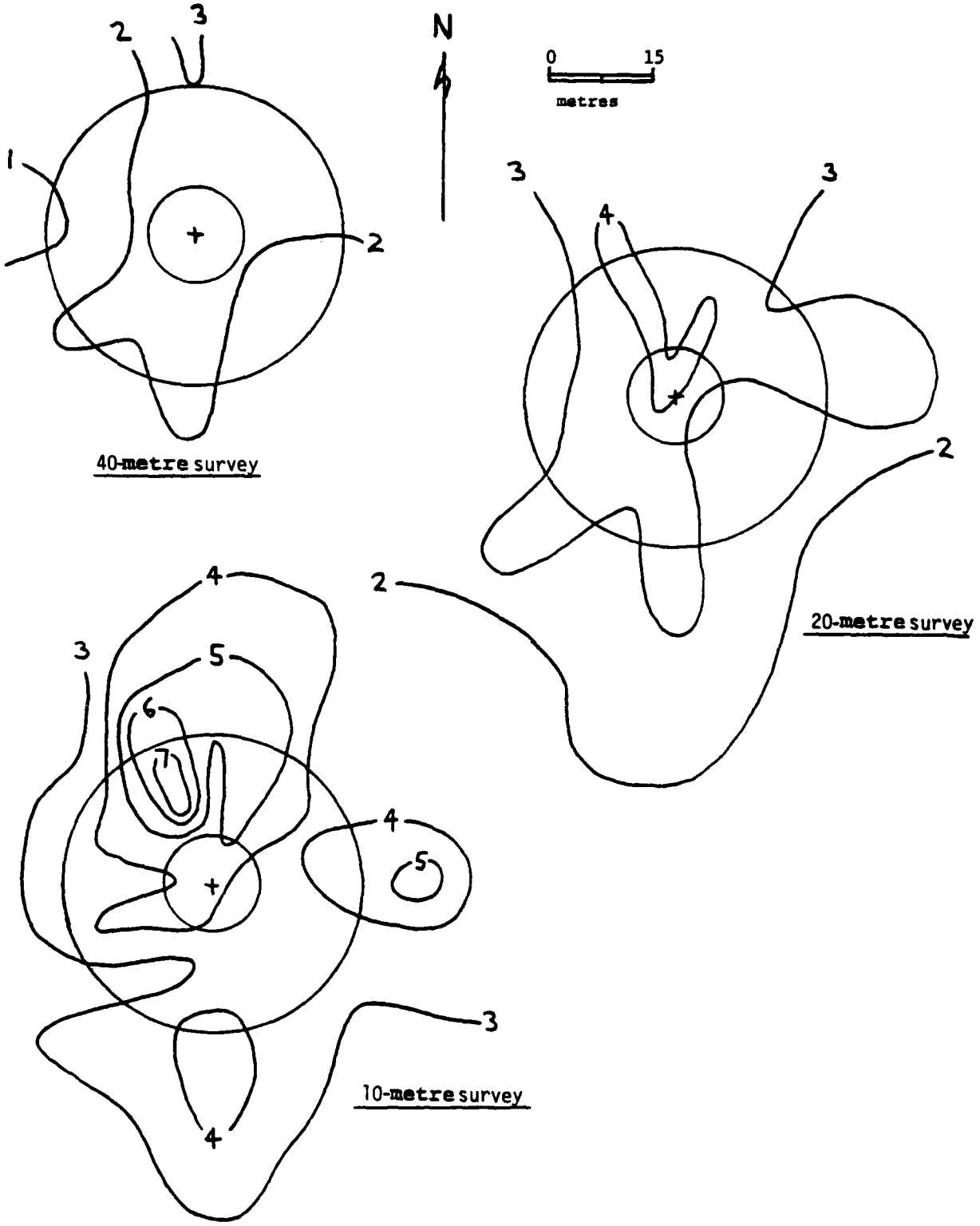

Figure 37. EM conductivity surveys at Moore sinkhole B, December 1986, contours in mmhos/m (Circles represent SP electrode arrays)

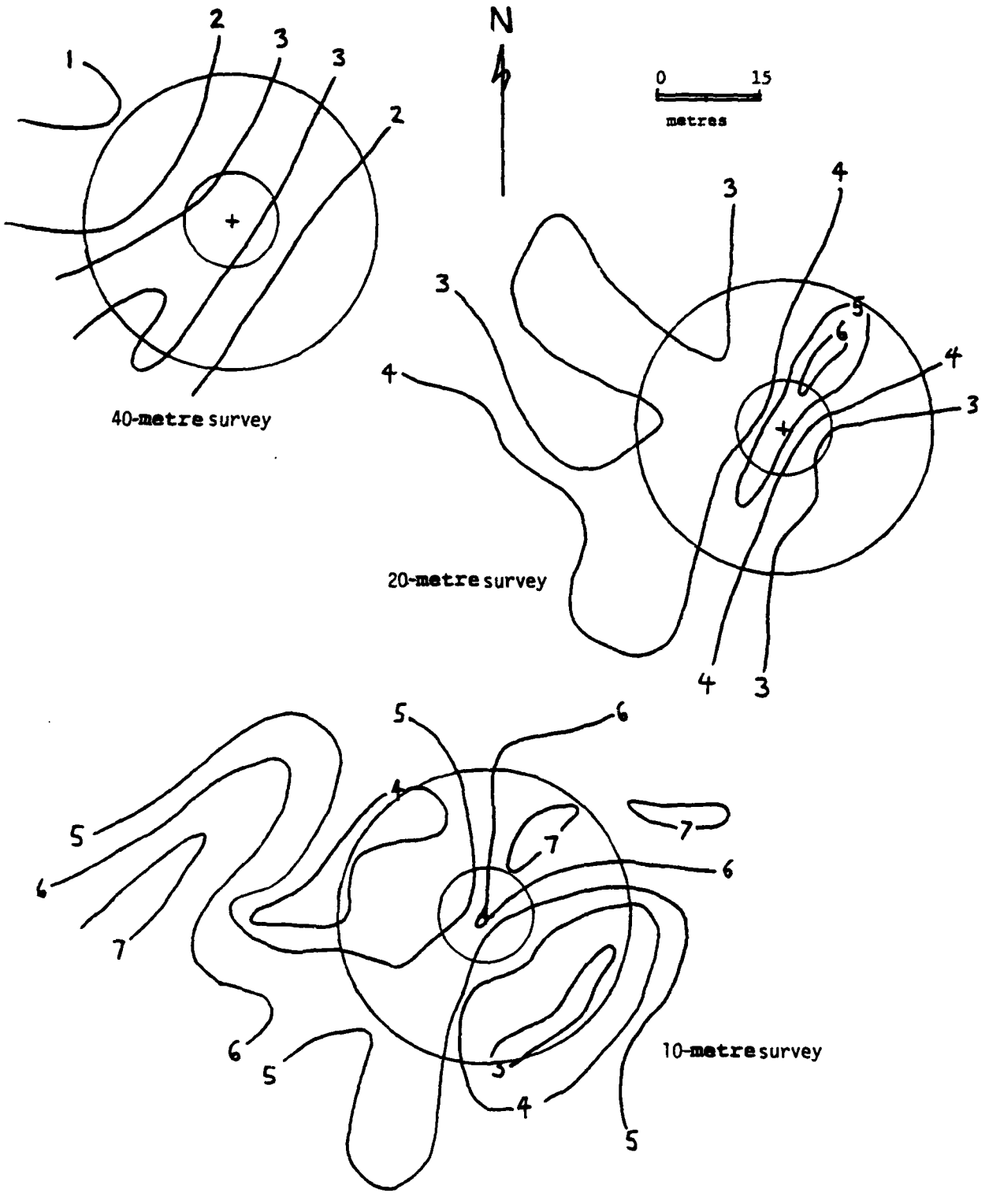

Figure 38. EM conductivity surveys of Moore sinkhole C, December 1986, contours in mmhos/m (Circles represent SP electrode arrays)

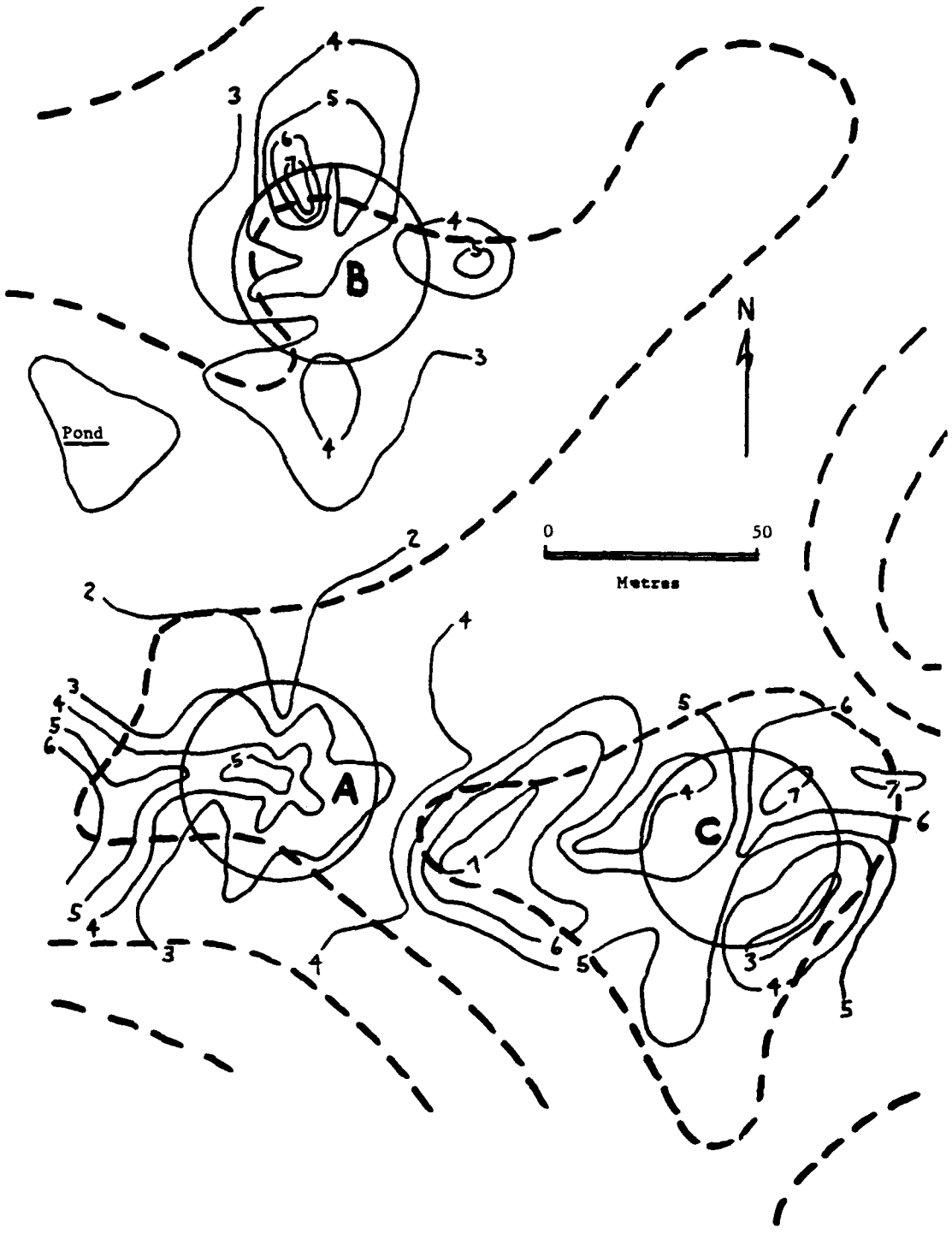

Figure 39. Moore site sinkholes A, B, and C. Dashed lines are topographic contours; solid lines are conductivity contours in mmhos/m from 10 m survey in December 1986 (Circles represent the diameter of outer ring of SP electrodes installed in each sinkhole)

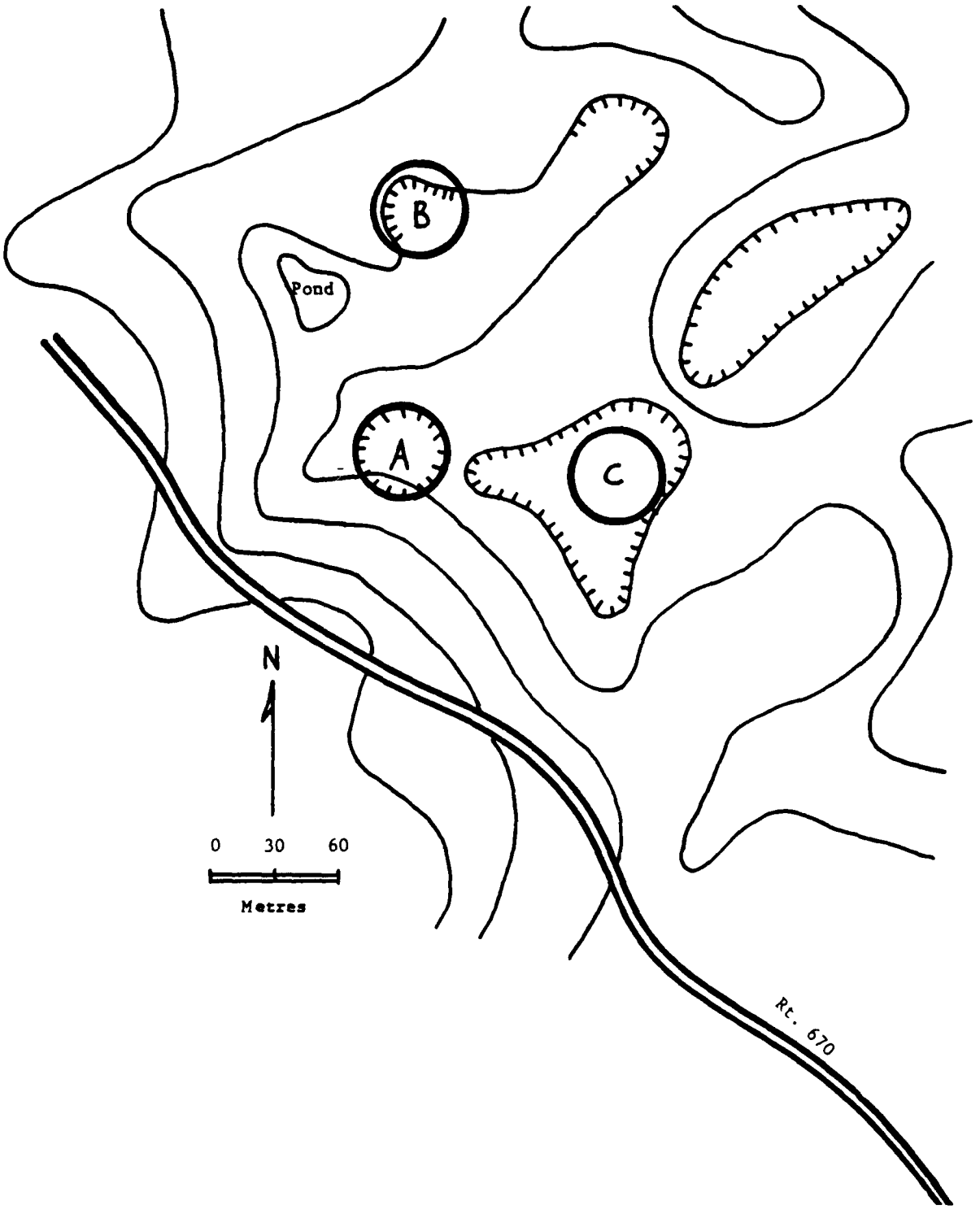

Figure 40. Topographic map of the Moores sinkholes site showing sinkholes A, B, and C, contour intervals 20 ft (Modified from the Lexington, VA, Quadrangle)

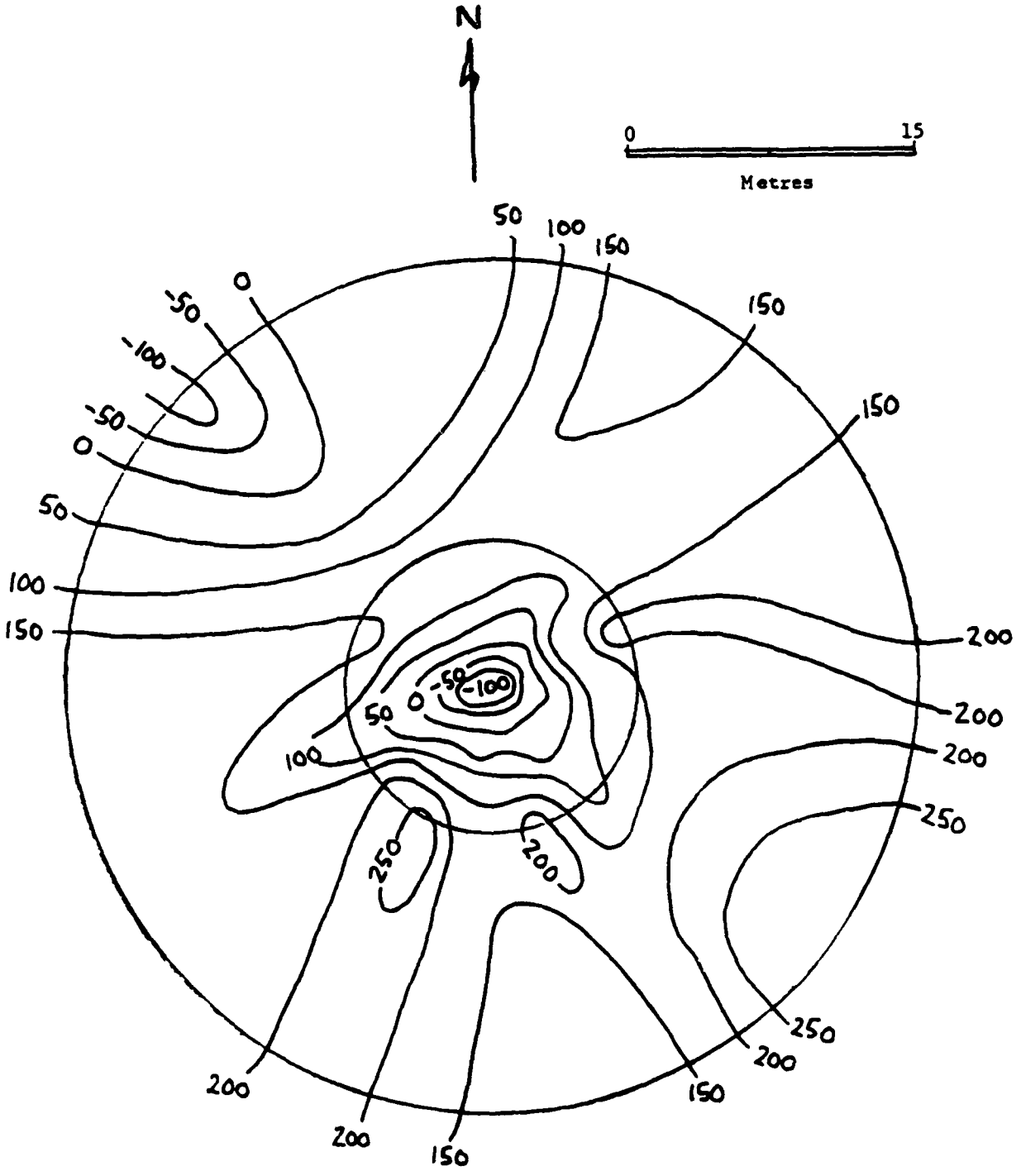

Figure 41. SP contours in millivolts at Moore sinkhole A, averaged for January 1987 (Circles represent electrode arrays)

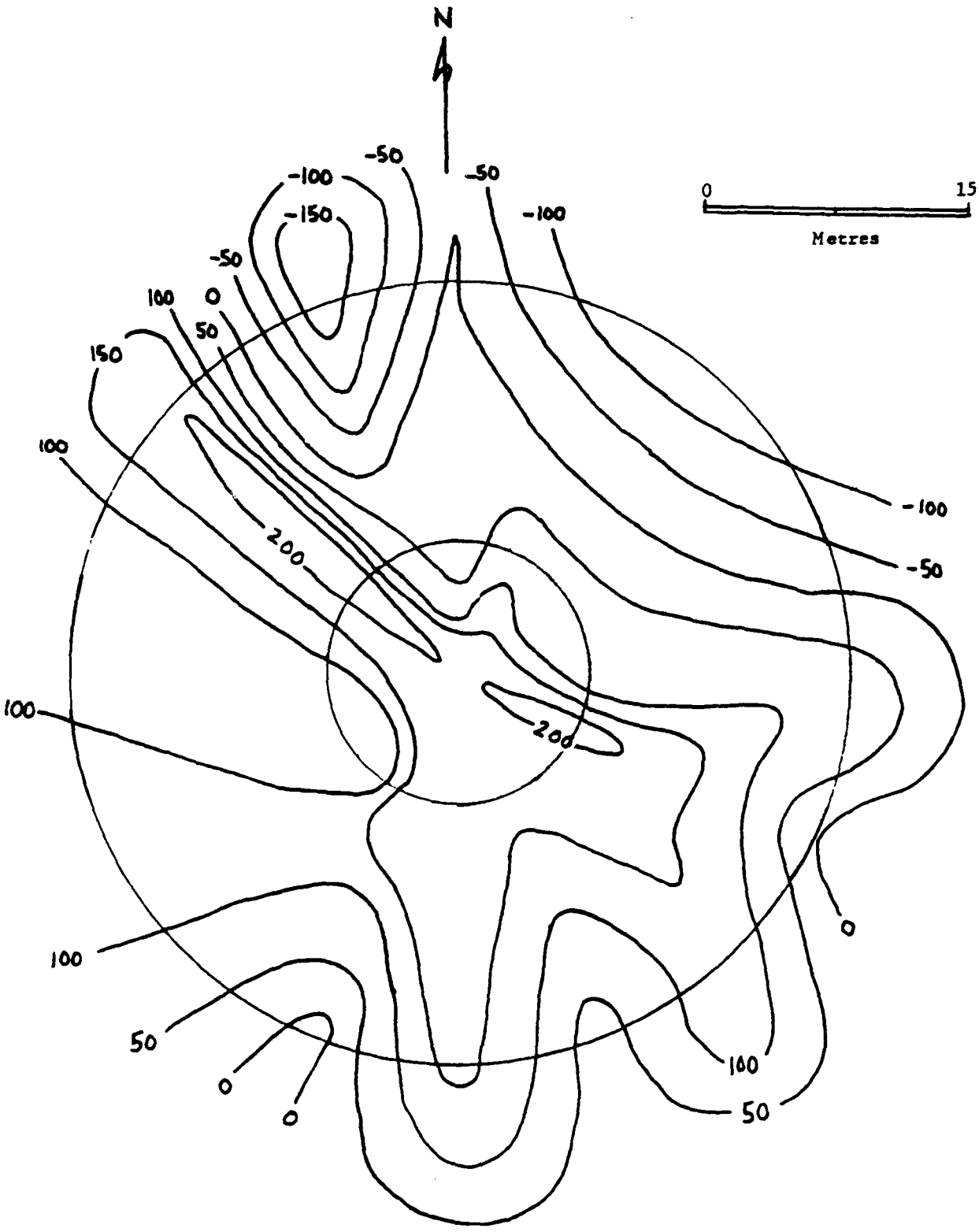

Figure 42. SP contours in millivolts at Moore sinkhole B, January 1987 (Circles represent electrode arrays)

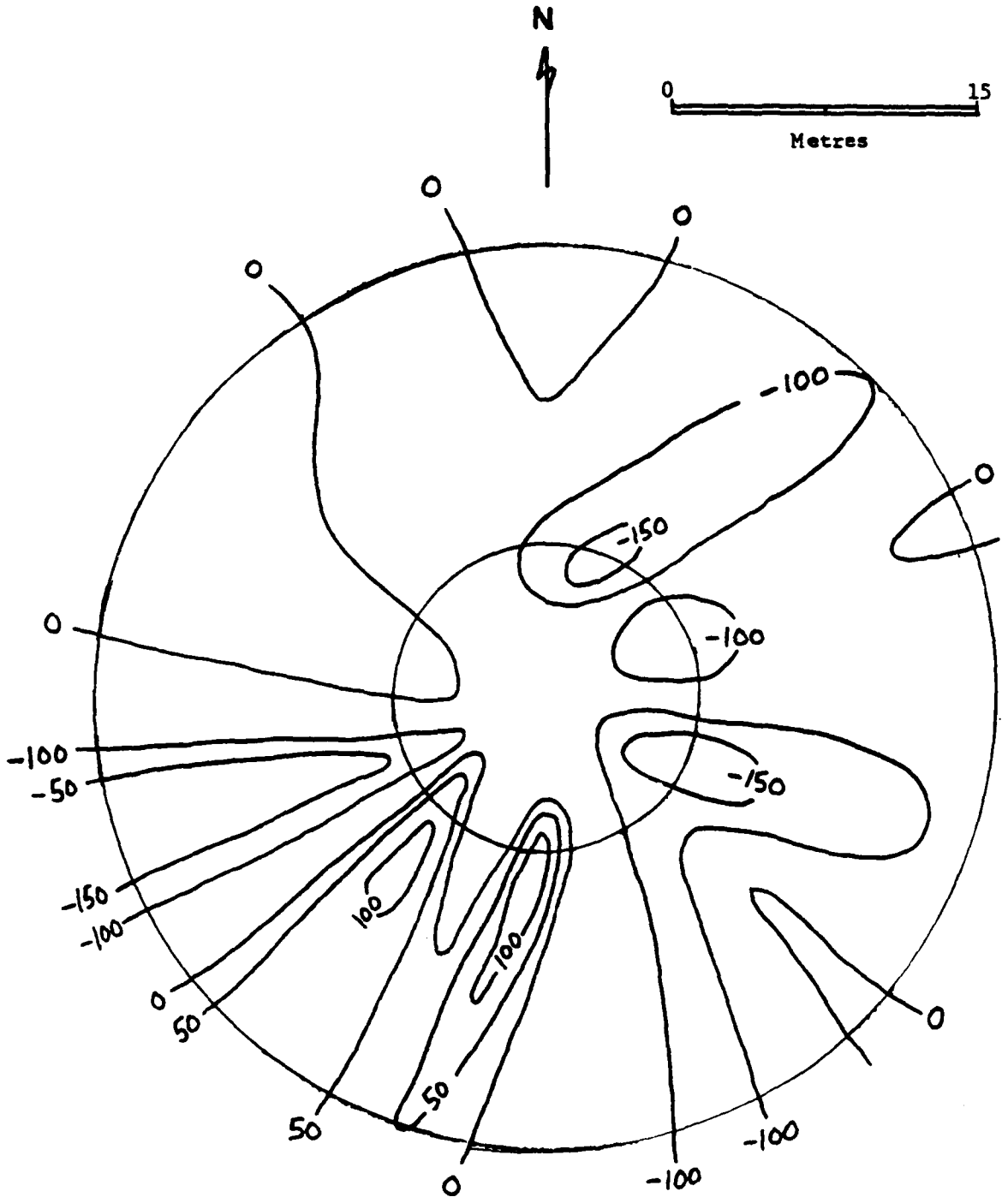

Figure 43. SP contours in millivolts at Moore sinkhole C, values for January 1987 (Circles represent electrode arrays)

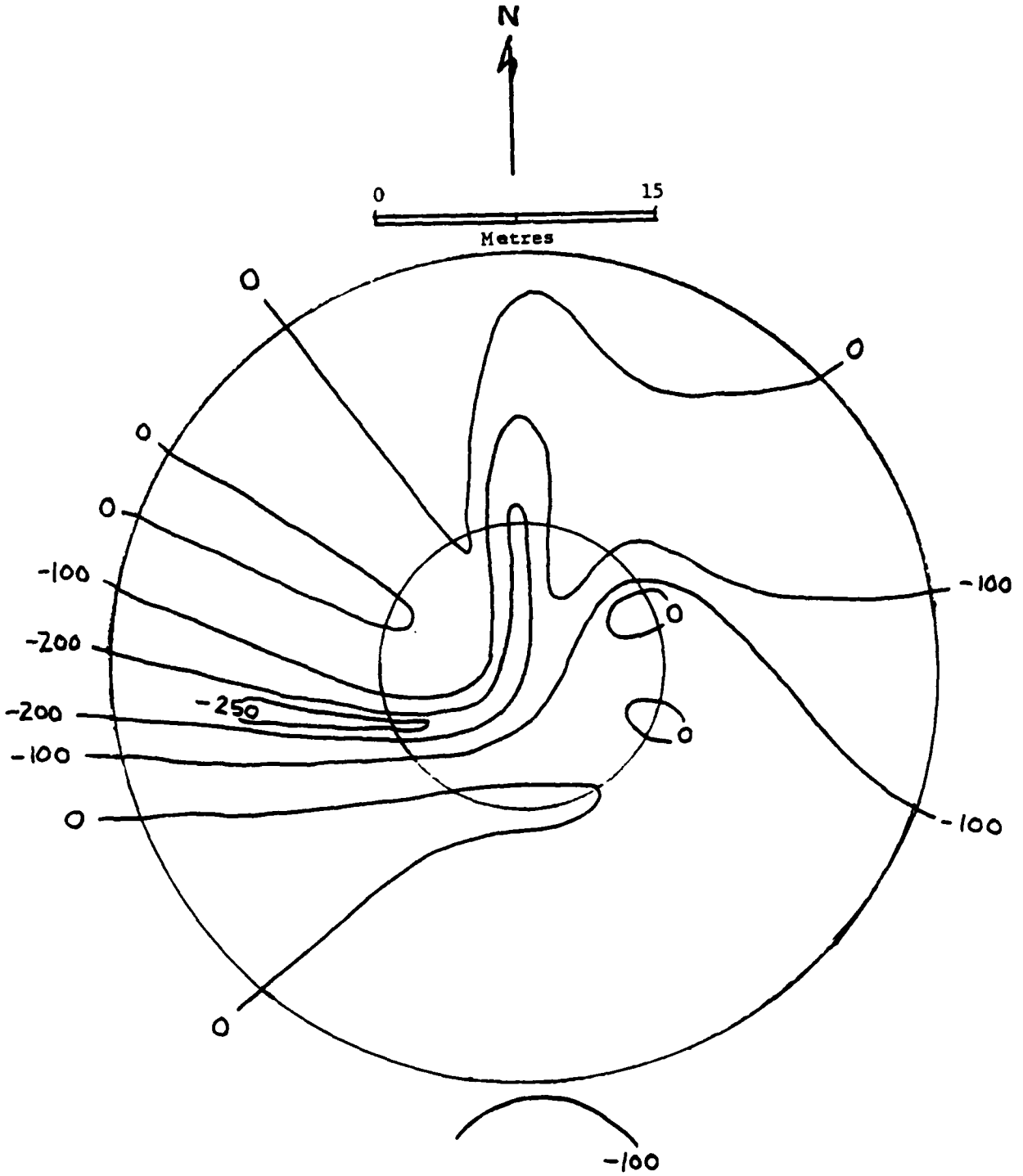

Figure 44. SP contours in millivolts at Moore sinkhole A, SP values averaged for period July - October 1986 (Circles represent electrode arrays)

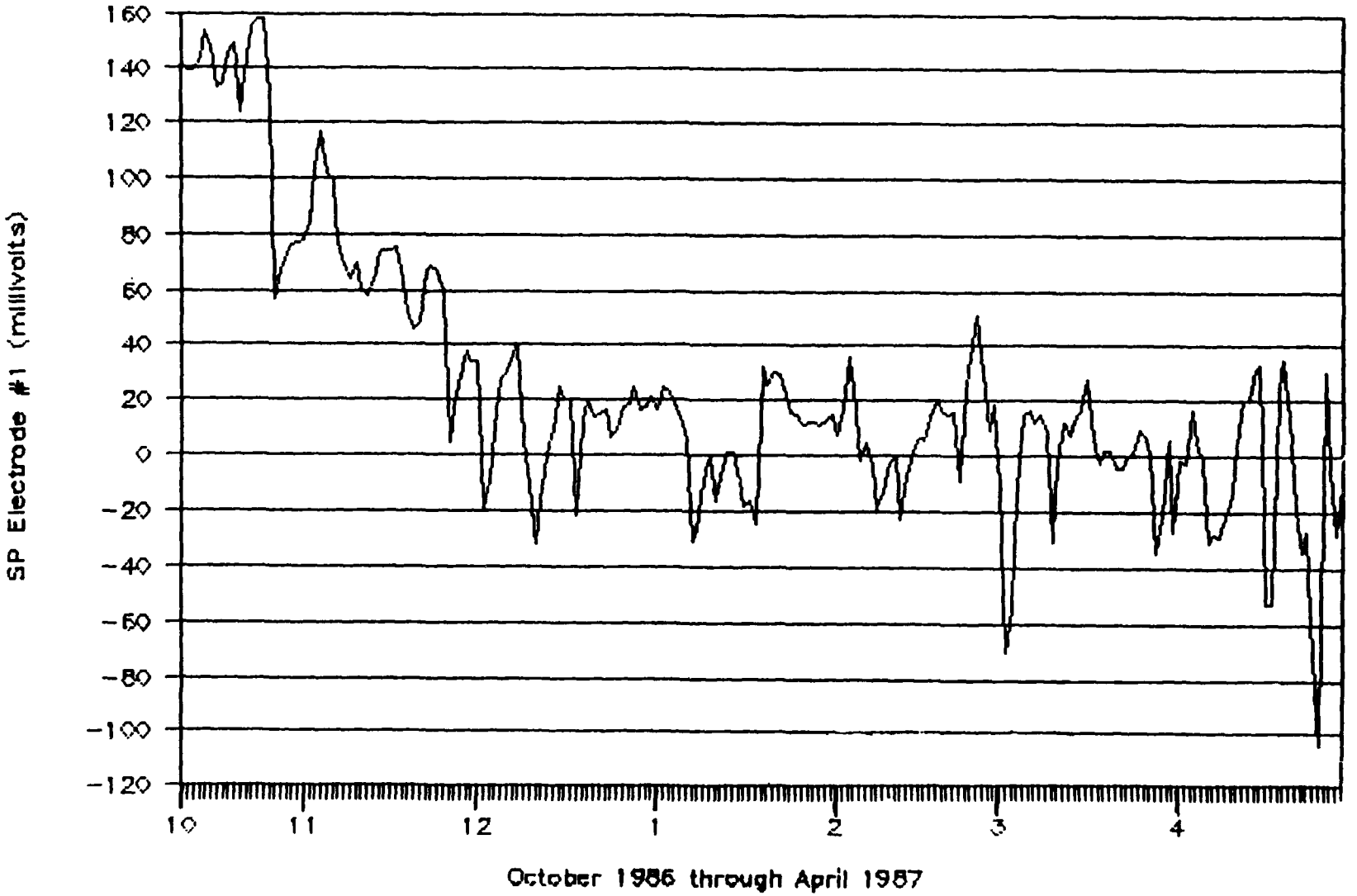

Figure 45. Daily average SP for electrode No. 1 at long-term monitoring site over 7-month period

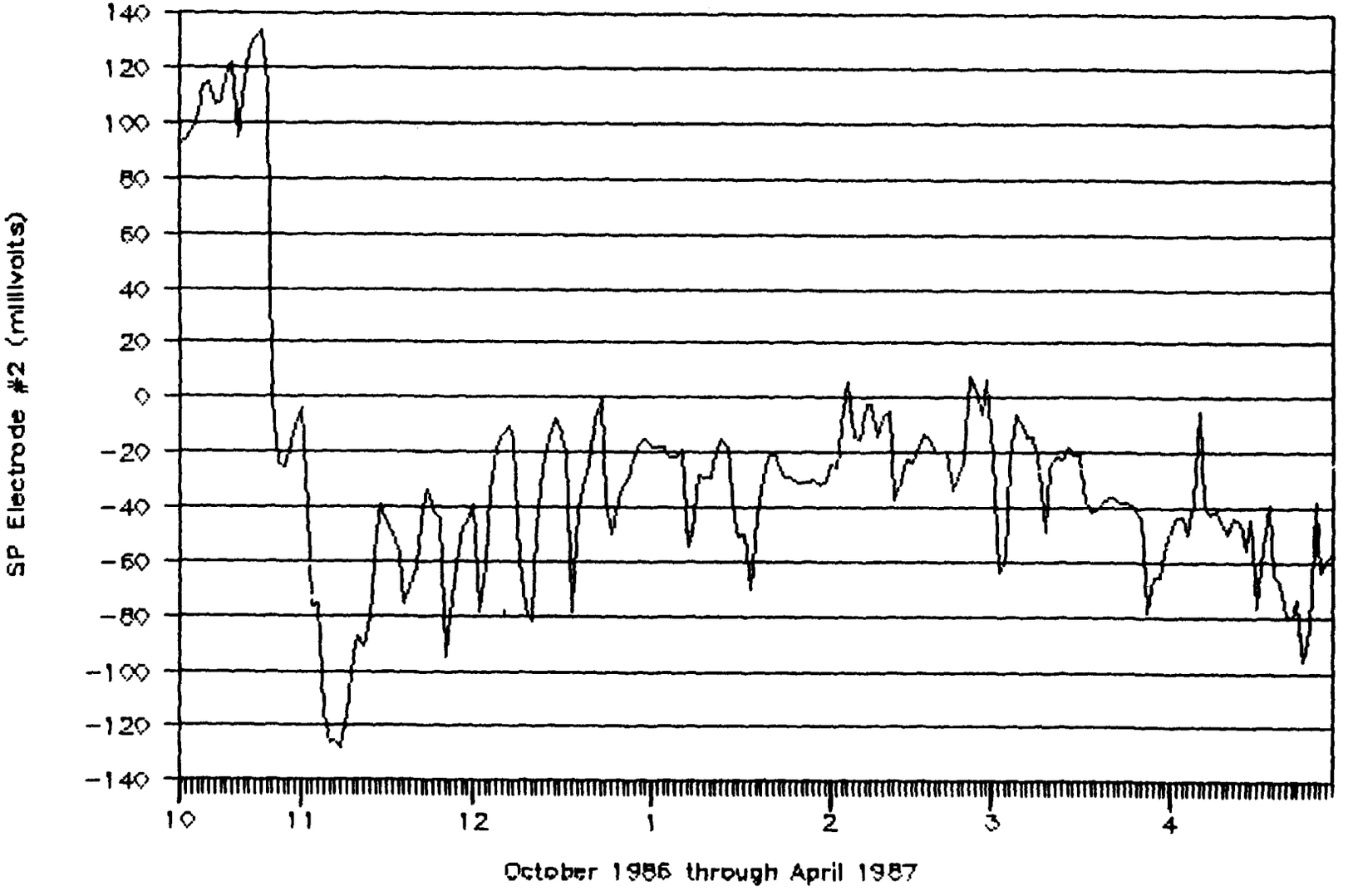

Figure 46. Daily average SP for electrode No. 2 at long-term monitoring site over 7-month period

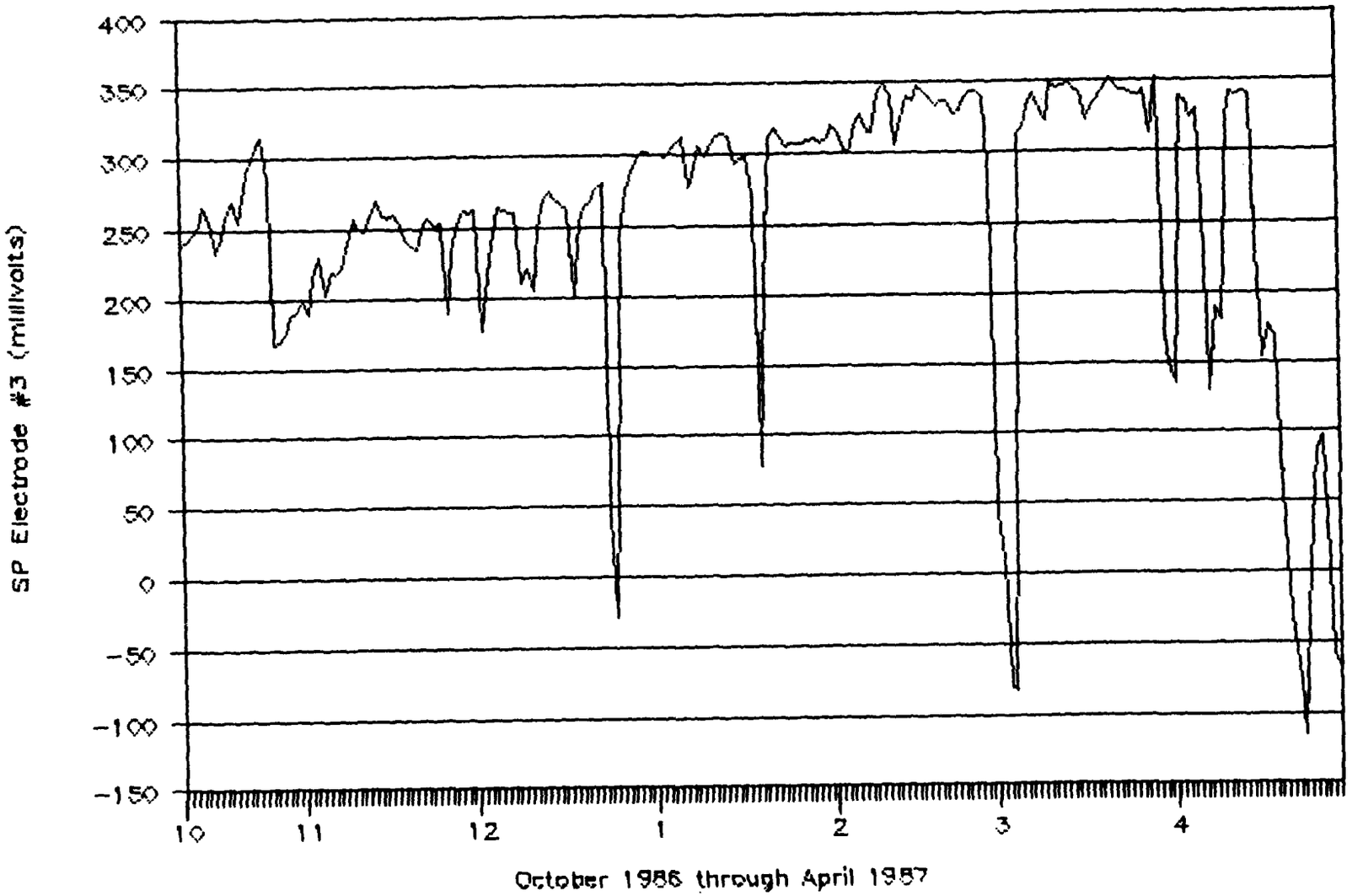

Figure 47. Daily average SP for electrode No. 3 at long-term monitoring site over 7-month period

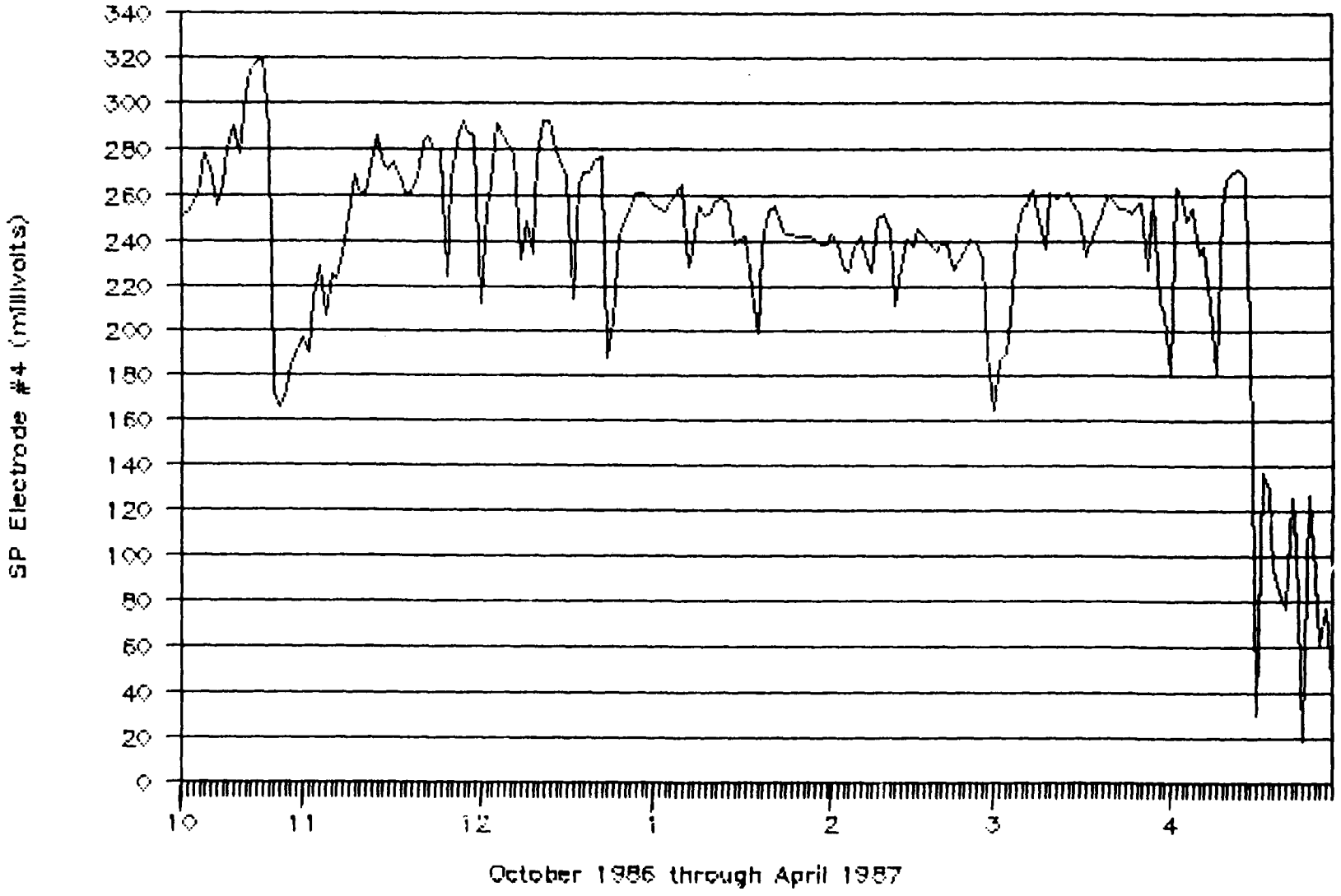

Figure 48. Daily average SP for electrode No. 4 at long-term monitoring site over 7-month period

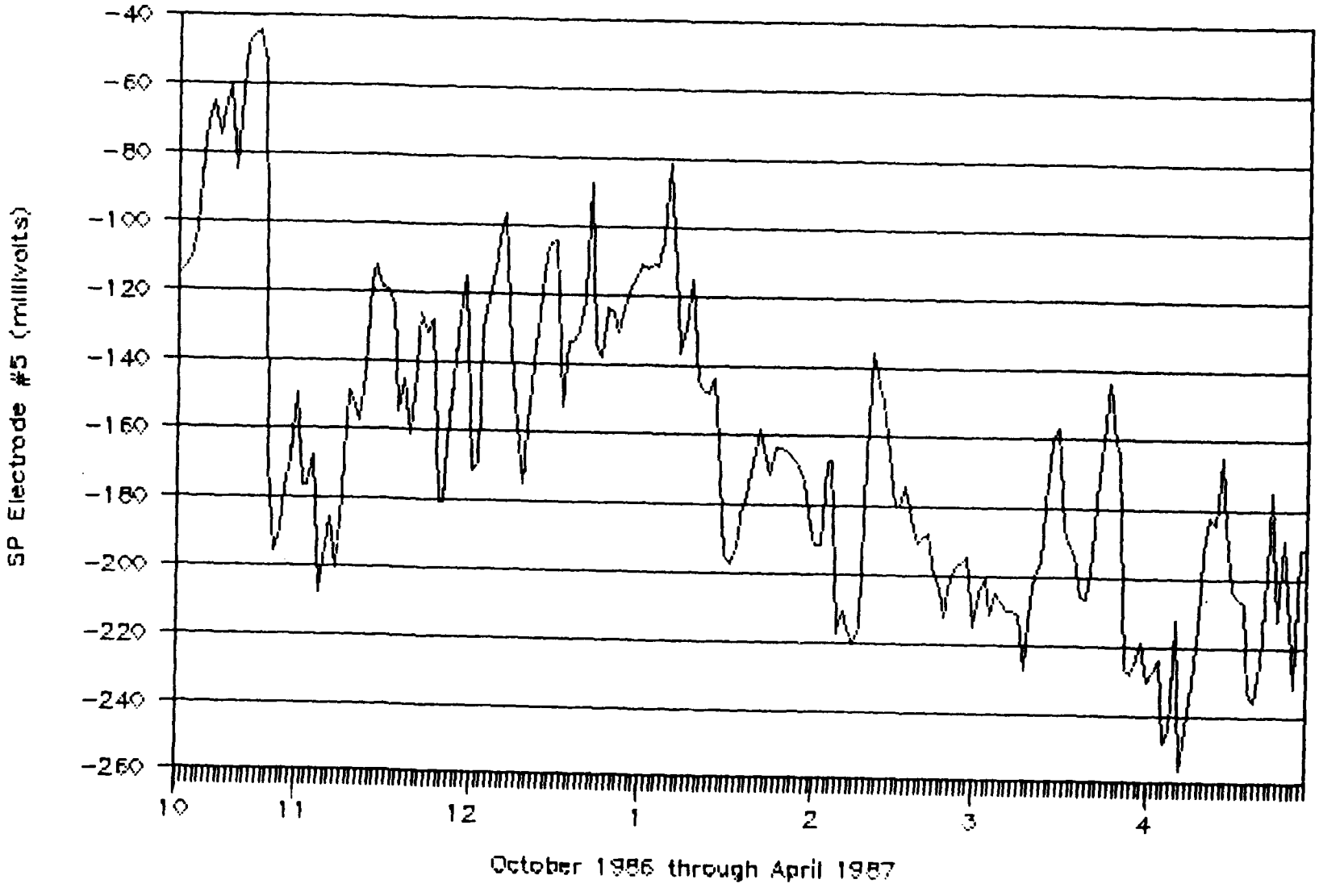

Figure 49. Daily average SP for electrode No. 5 at long-term monitoring site over 7-month period

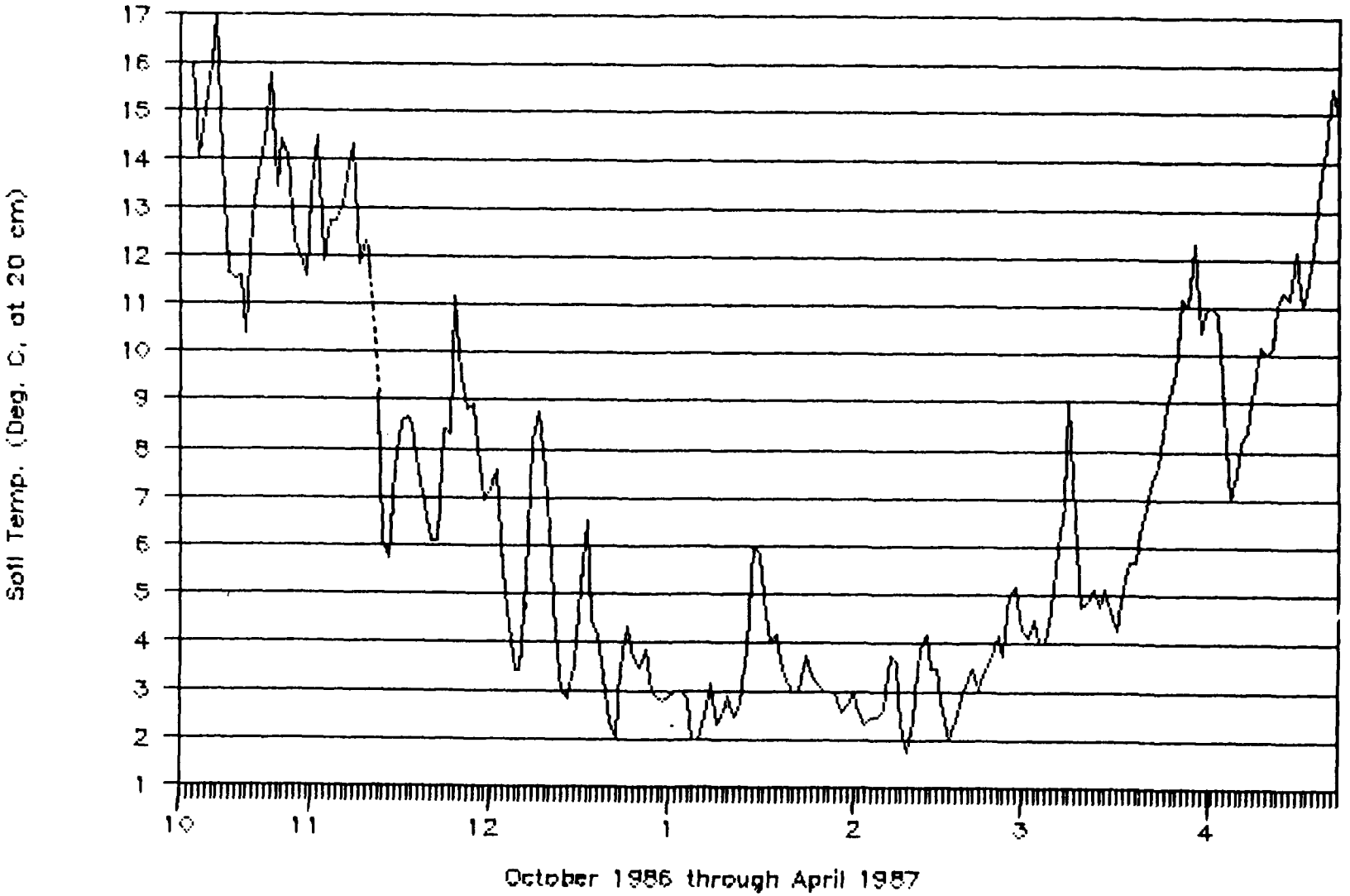

Figure 50. Soil temperature (degrees C) at depth of 20-cm at the long-term monitoring site for a period of 7 months. Data are daily averages from ADC record

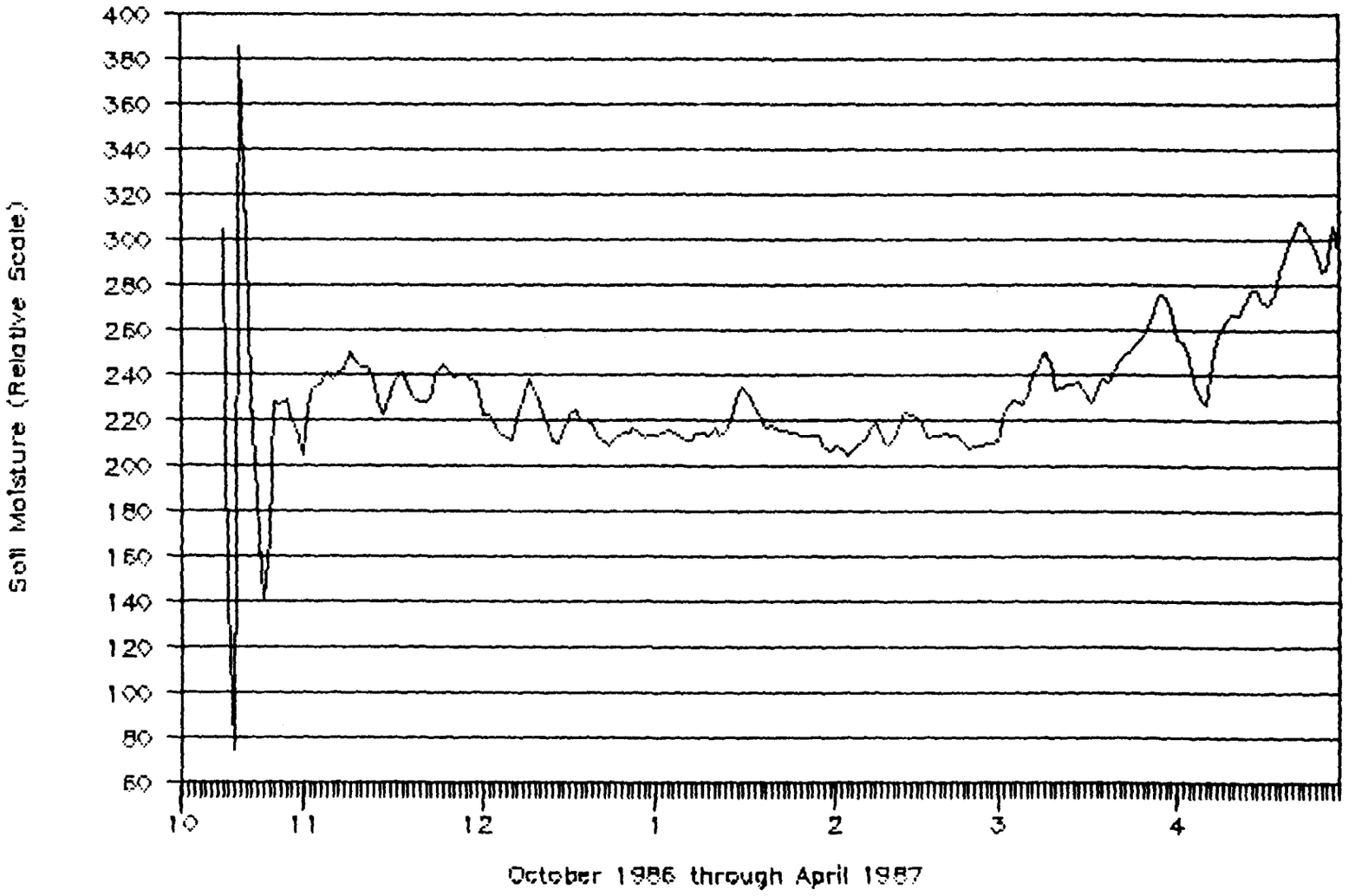

Figure 51. Daily average soil moisture at 20-cm depth at long-term monitoring site over 7-month period

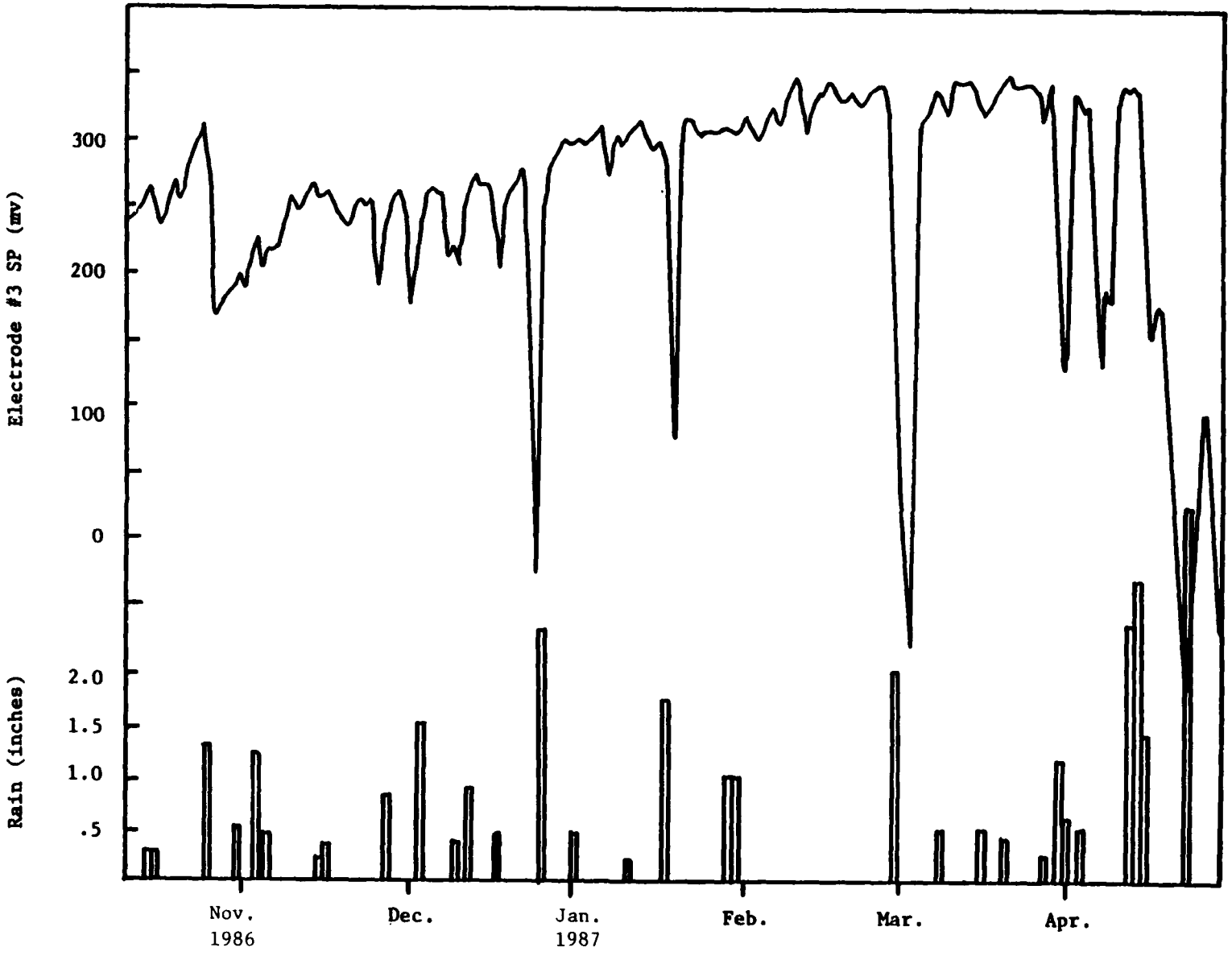

Figure 52. Relationship of rainfall to SP at electrode No. 3 (in bed of the intermittent stream) at long-term monitoring site. Sharp drops in SP occur when the stream was flowing

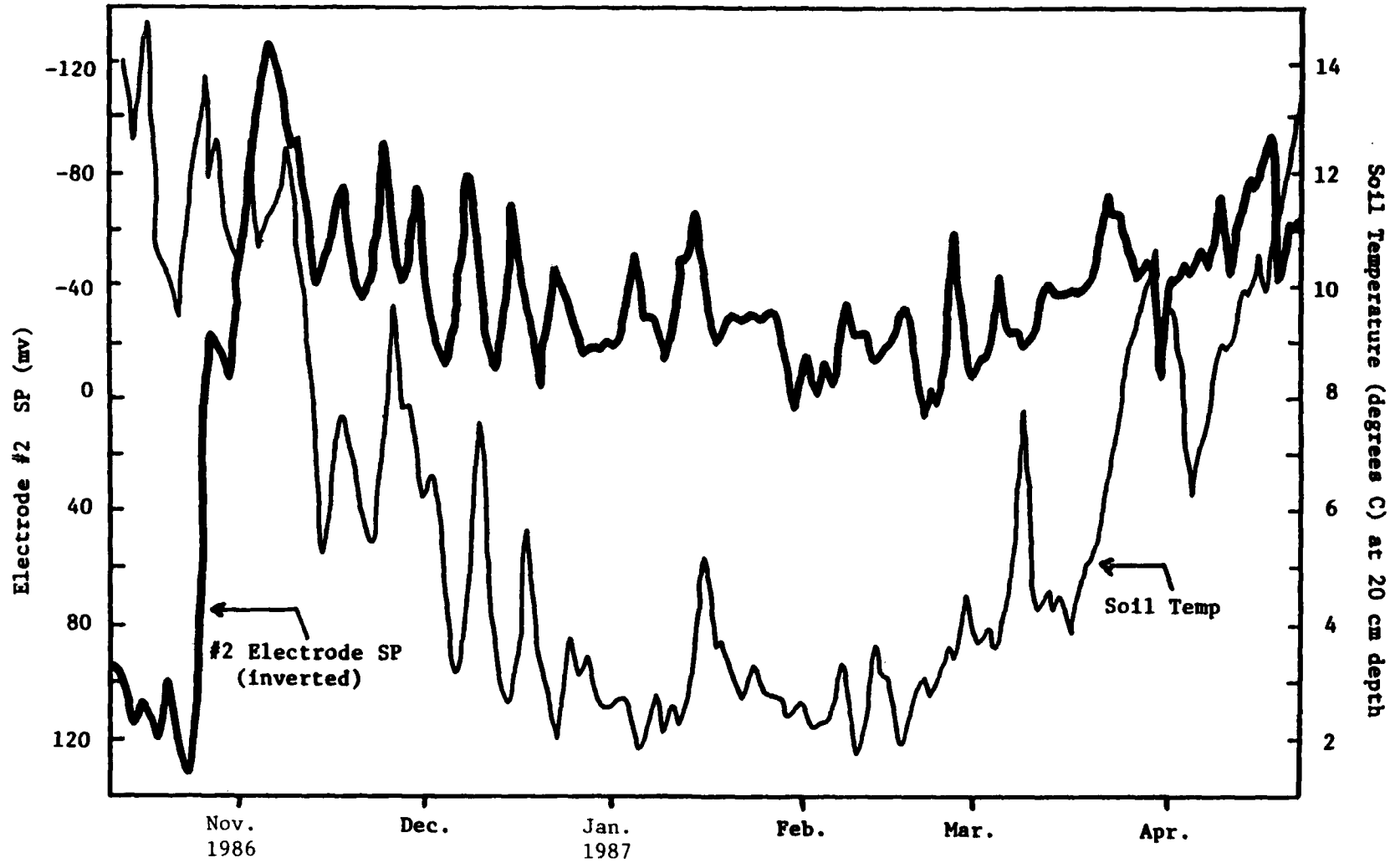

Figure 53. Correspondence of soil temperature and inverted SP record of electrode No. 2 at the long-term monitoring site

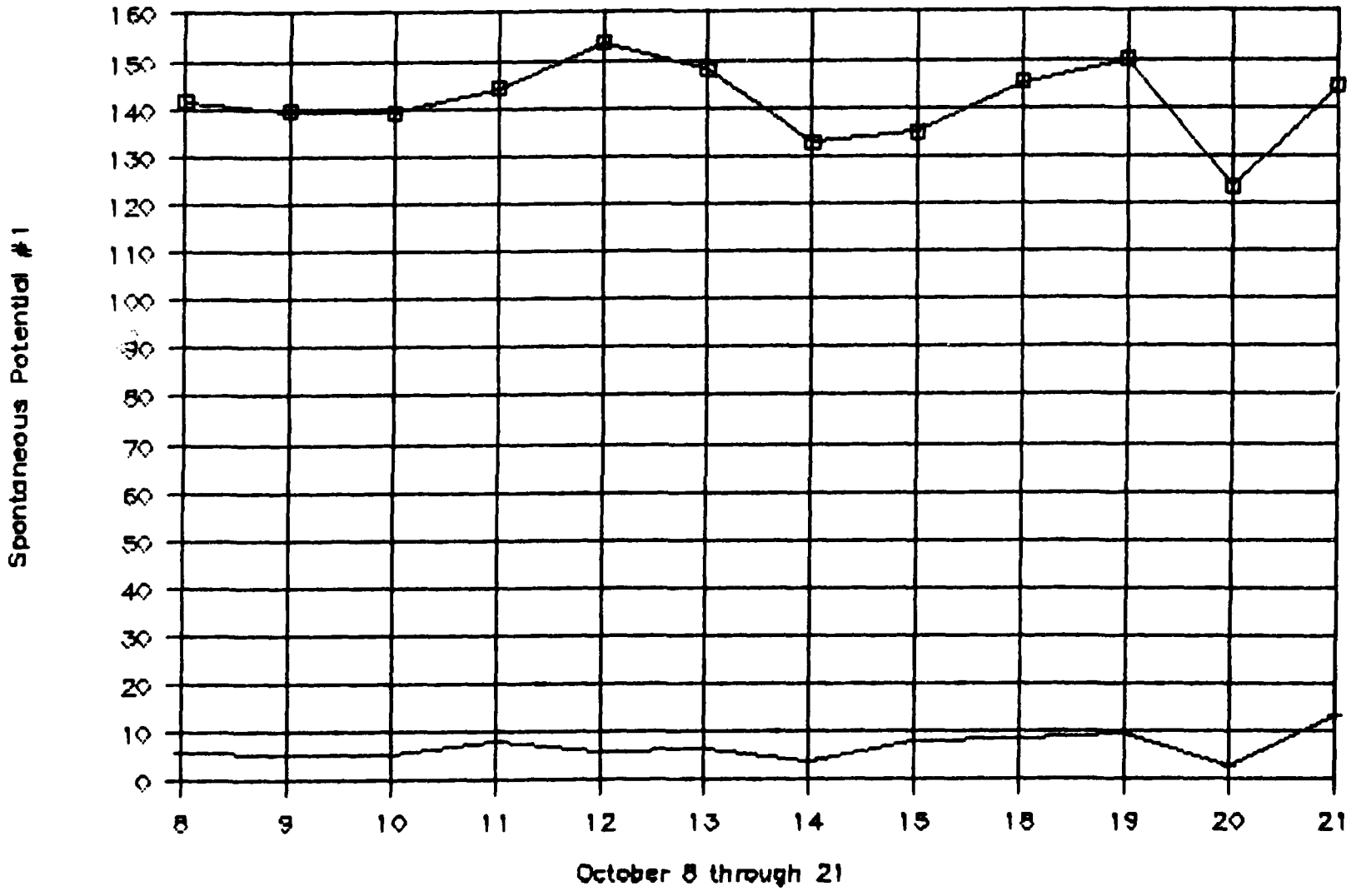

Figure 54. Daily average SP and standard deviation for electrode No. 1 at long-term monitoring site, 8-21 October 1986

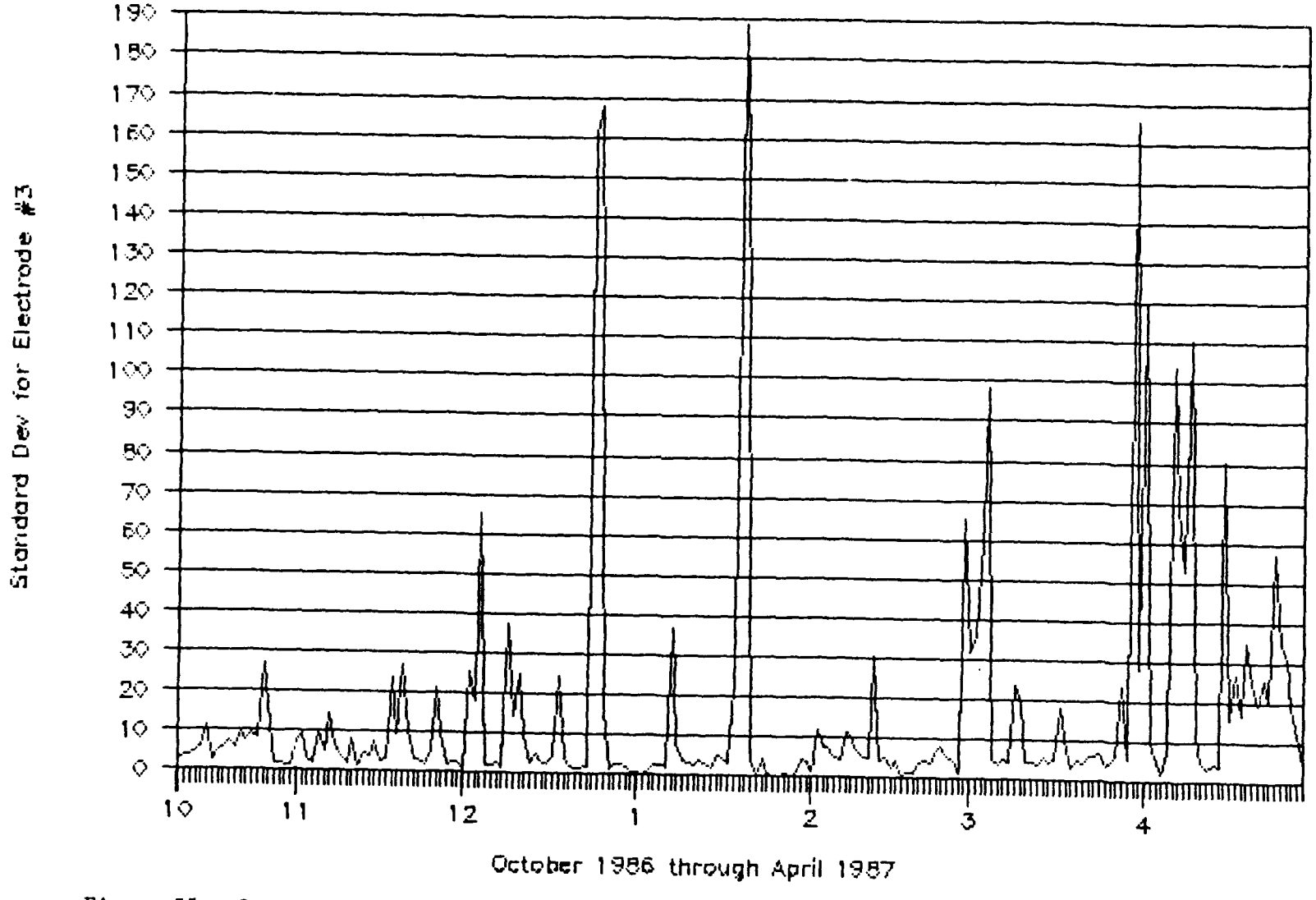

Figure 55. Standard deviation of daily average SP of electrode No. 3 over a 7-month period at the long-term monitoring site

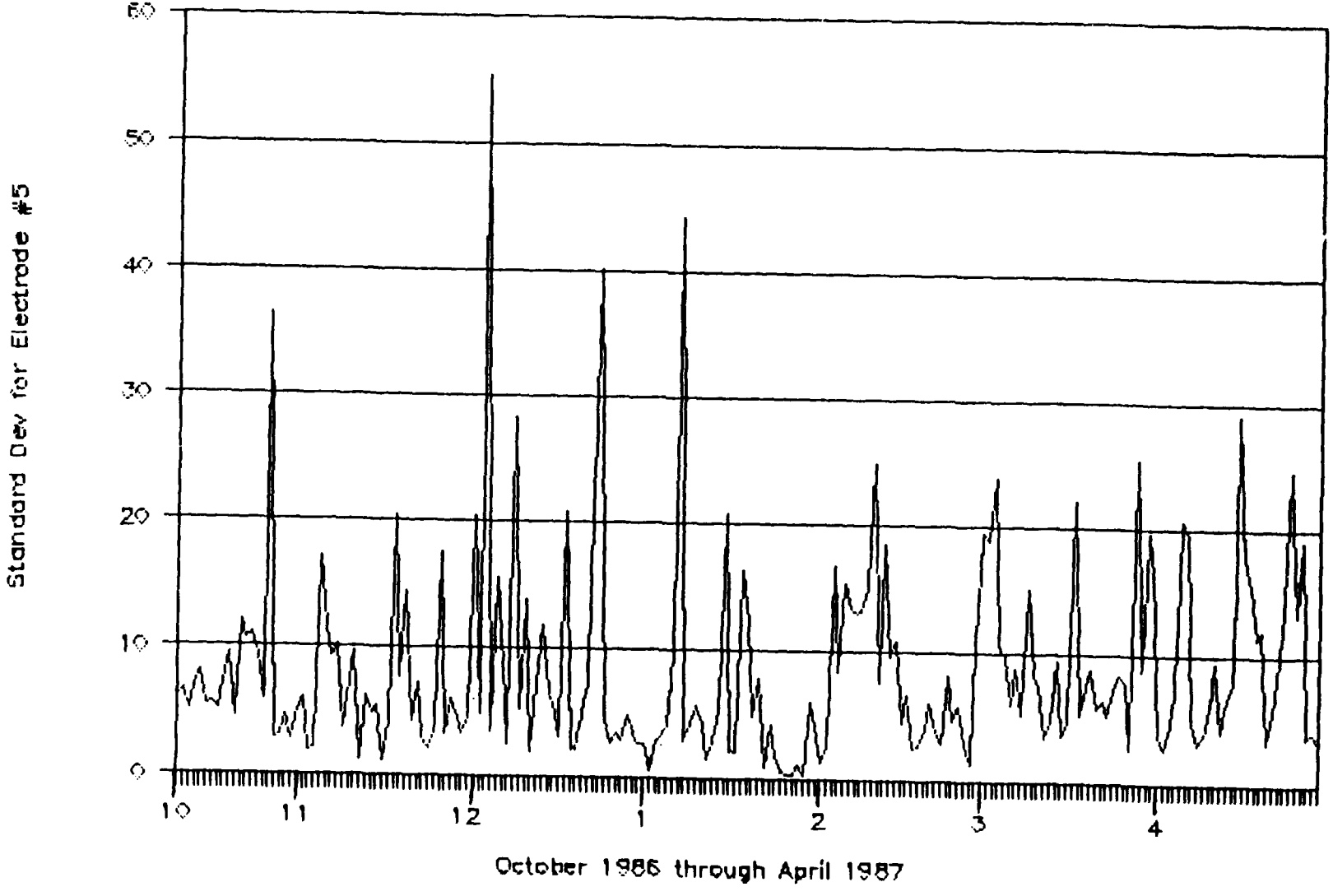

Figure 56. Standard deviation of daily average SP for electrode No. 5 over 7-month period at the long-term monitoring site